GENERAL RELATIVISTIC MHD

DEBORA LANČOVÁ

Silesian University In Opava, Czechia

(Starting January) CAMK, Agata Rozanska's group

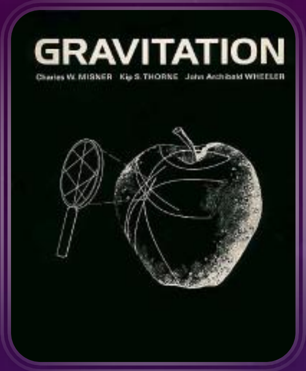

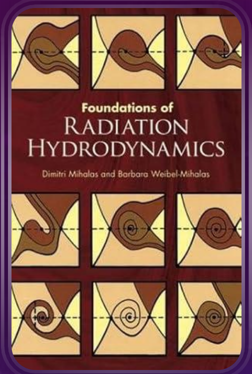

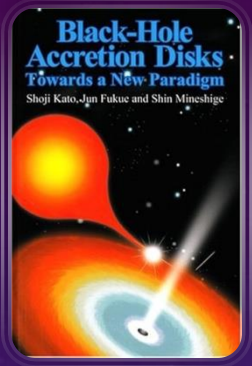

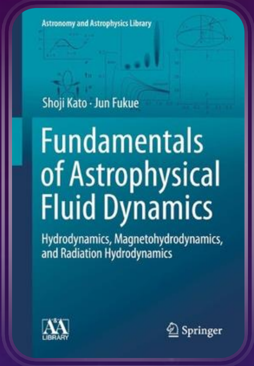

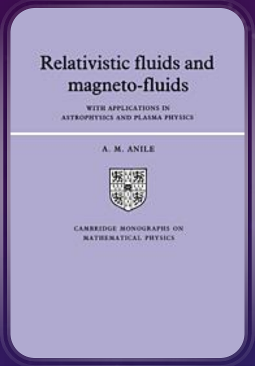

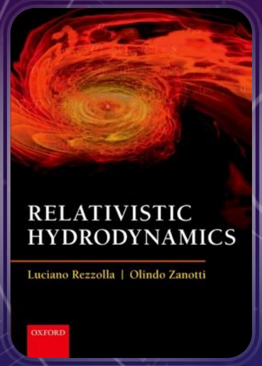

LITERATURE

- Kommissarov 1999 MNRAS
- BHAC paper – Porth 2017 CAaC
- Gammie 2003 APJ
- Tchekhovskoy 2011 MNRAS
- Toth 2000 JCP

… more to come

EXISTING CODES

- Athena++ (White+ 2016)
- HARM (Gammie+2003) and derivatives:
  - H-AMR, HARMPI, HARM_COOL
- BHAC (Porth+ 2017)
- Koral (Sądowski+ 2013 …)

- C/C++, highly paralelised (MPI)

WHY GR?

- It’s easier! At least the units are
- Accretion on compact objects *is* relativistic
  - Strong gravity, ISCO, event horizon
- Efficiency $\eta > 100\%$
- BH systems are producing a ridiculous amount of energy through accretion
- GRBs are most probably caused by highly-relativistic shock waves

PROBLEMS

- Dissipation contributes not only to the fluxes of conserved, but also to their space densities
- Mixed space and time derivatives
- Shocks have to be captured and evolved properly (Godunov-type shock-capturing schemes used)
- Time-scales are very short (for stellar-mass objects)

GEOMETRIZED UNITS

- Set fundamental constants to 1 (c = G = 1).
- Length, time, and mass share the same dimension
- Mass expressed as length

$$r_g = \frac{GM}{c^2} \qquad t_g = \frac{r_g}{c} = \frac{GM}{c^3}$$

	m	kg	s	K
m	1	$\frac{c^2}{G}$	$\frac{1}{c}$	$\frac{c^4}{Gk_B}$
kg	$\frac{G}{c^2}$	1	$\frac{G}{c^3}$	$\frac{c^2}{k_B}$
s	c	$\frac{c^3}{G}$	1	$\frac{c^5}{Gk_B}$
K	$\frac{Gk_B}{c^4}$	$\frac{k_B}{c^2}$	$\frac{Gk_B}{c^5}$	1

VERY BASIC INTRODUCTION TO GR

FOCUSING ON BLACK HOLES

GENERAL RELATIVITY

The curvature of spacetime is described by the metric tensor $g_{\mu\nu}$

Space-time interval (distance between 2 events in space and time)

$$ds^2 = g_{\mu\nu}\, dx^\mu dx^\nu$$

(using Einstein sum notation)

Einstein equation: Geometry of space-time = distribution of matter

$$G_{\mu\nu} + \Lambda g_{\mu\nu} = \frac{8\pi G}{c^4} T_{\mu\nu}$$

Einstein tensor

cosmological constant

metric tensor

energy-momentum tensor

$$G_{\mu\nu} = R_{\mu\nu} - \frac{1}{2} R g_{\mu\nu}$$

Ricci curvature tensor

Scalar curvature (Ricci Scalar)

$$R = R^{\mu}_{\mu}$$

$$R_{\mu\nu} = R^{\rho}_{\mu\rho\nu}$$

Rieman tensor

$$R^{\alpha}_{\beta\gamma\delta} = \Gamma^{\alpha}_{\beta\delta,\gamma} - \Gamma^{\alpha}_{\beta\gamma,\delta} + \Gamma^{\rho}_{\beta\delta}\Gamma^{\alpha}_{\rho\gamma} - \Gamma^{\rho}_{\beta\gamma}\Gamma^{\alpha}_{\rho\delta}$$

Christoffel symbols

$$\Gamma^{\mu}_{\alpha\beta} = \frac{1}{2} g^{\mu\nu}\left(-g_{\alpha\beta,\rho} + g_{\rho\alpha,\beta} + g_{\beta\rho,\alpha}\right)$$

Covariant derivation

$$A^{\mu}{}_{;\nu} = A^{\mu}{}_{,\nu} + \Gamma^{\mu}_{\alpha\nu} A^{\alpha}$$

$$A^{\mu}{}_{,\nu} = \frac{\partial A^{\mu}}{\partial x^{\nu}}$$

$$A^{\mu} = g_{\mu\nu} A_{\nu} \qquad A_{\mu} = g^{\mu\nu} A^{\nu}$$

$$g^{\mu\nu} g_{\mu\nu} = \delta^{\mu}_{\nu}$$

EINSTEIN (FIELD) EQUATION

- Set of differential equations for the metric tensor
- Cosmological constant usually omitted, important only on large scales
- Sign convention $(-,+,+,+)$
- Coordinates (x^t, x^i, x^j, x^k)
- In simulations:
  - Accretion discs – BH, sometimes NS, but complications with solid surface and high MF
    - Self-gravity ignored, change of M ignored – fixed static metric on background
  - Mergers – dynamic metric – EFE is solved together with the matter
    - Einstein toolkit ((Löffler+ 2012)
  - Cosmological – large scales
    - Includes cosmological constant
    - Tomasz Krajewski

METRICS FOR ACCRETION SIMULATIONS (M, a, Q)

- Schwarzschild: non-rotating, symmetric, static, not charged BH (1915)
- Kerr: rotating not charged BH, spacetime is dragger with the rotation (1963)
- Reissner-Nordström: non-rotating charged BH (1916-21)
- Kerr-Newman: rotating charged BH (1965)
- Hartle-Thorne: oblate rotating solid body, includes quadrupole moment (1968)

THE SAD STORY OF KARL SCHWARZSCHILD

- 1873-1916
- Two papers before the age of 16
- Director of the Göttingen observatory and the Postdam's Astronomical observatory
- volunteer for service in the German army when WWI started
- Worked on the EFE solution on front – wrote three papers, two on GR, one on quantum field theory
- Left the army due to serious illness in 1916, but passed away soon after

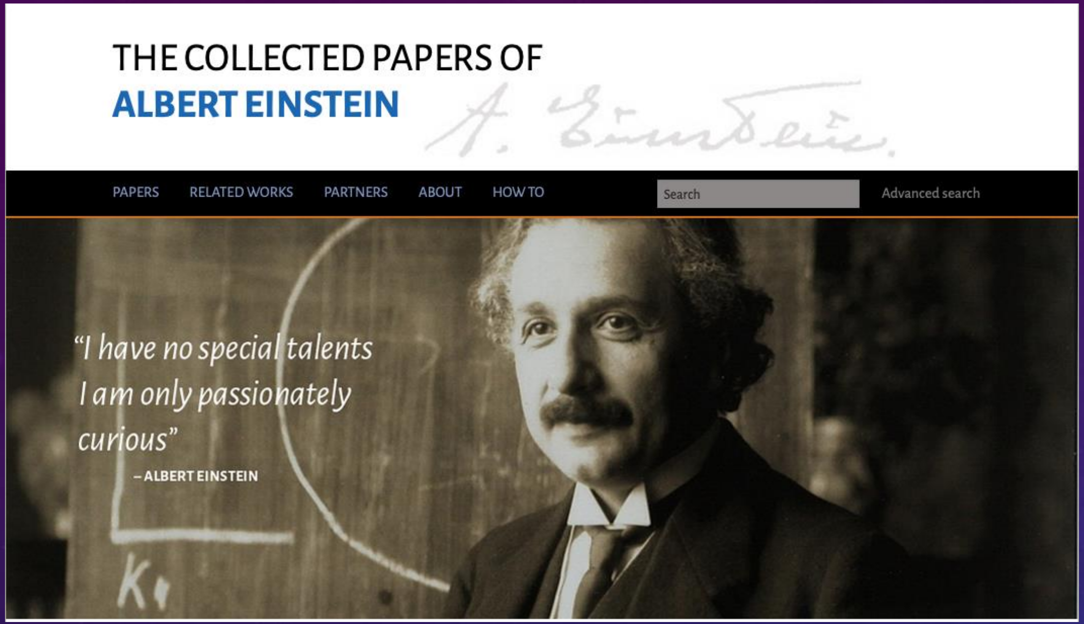

https://einsteinpapers.press.princeton.edu

169. From Karl Schwarzschild[1]

[at the Russian front,] 22 December 1915

Esteemed Mr. Einstein,

In order to become versed in your gravitation theory, I have been occupying myself more closely with the problem you posed in the paper on Mercury's perihelion[2] and solved to 1st-order approximation.[3] Initially, one factor made me very confused. I found for the coefficients $g_{n\nu}$ in first-order approximation, in addition to their solution, also the following second one:[4]

Thus the uniqueness of your problem is also in the best of order.[11]

It is a wonderful thing that the explanation for the Mercury anomaly emerges so convincingly from such an abstract idea.

As you see, the war is kindly disposed toward me, allowing me, despite fierce gunfire at a decidedly terrestrial distance, to take this walk into this your land of ideas.

"Dear Colleague!

I have reviewed your work with the greatest interest. I did not expect that one could formulate the strict solution to the problem so simply. The computational treatment of the subject pleases me greatly. Next Thursday, I will present the work to the Academy with some explanatory words.

Meanwhile, I received another letter from you last night, which I will also answer immediately."

181. To Karl Schwarzschild

[Berlin,] 9. I. 16.

Hoch geehrter Herr Kollege!

Ihre Arbeit habe ich mit grösstem Interesse durchgesehen.[1] Ich hätte nicht erwartet, dass man so einfach die strenge Lösung der Aufgabe formulieren könne. Die rechnerische Behandlung des Gegenstandes gefällt mir ausgezeichnet. Nächsten Donnerstag werde ich die Arbeit mit einigen erläuternden Worten der Akademie übergeben.[2]

SCHWARZSCHILD SOLUTION

- Describes gravitational field outside of a spherical, non-rotating body
- Schwarzschild coordinates (t, r, θ, ϕ)

$$ds^2 = -\left(1-\frac{2M}{r}\right)dt^2 + \left(1-\frac{2M}{r}\right)^{-1}dr^2 + r^2 d\theta^2 + \left(r^2\sin^2\theta\right)d\phi^2.$$

- 2 singularities, one on the horizon (coordinate), the second at r = 0 (physical)

$$r_s = 2\frac{GM}{c^2} = 2r_g$$

  - At r_s, g_tt = 0 – spacetime casually disconnected – can be crossed only one way
    - surface of infinite redshift (thus the “frozen star” name for black holes)

FALLING ONTO SCHWARZSCHILD BH

- The effective potential has maximum and minimum!
- Innermost Stable Circular Orbit
- Marginally Bound orbit
- Photon orbit

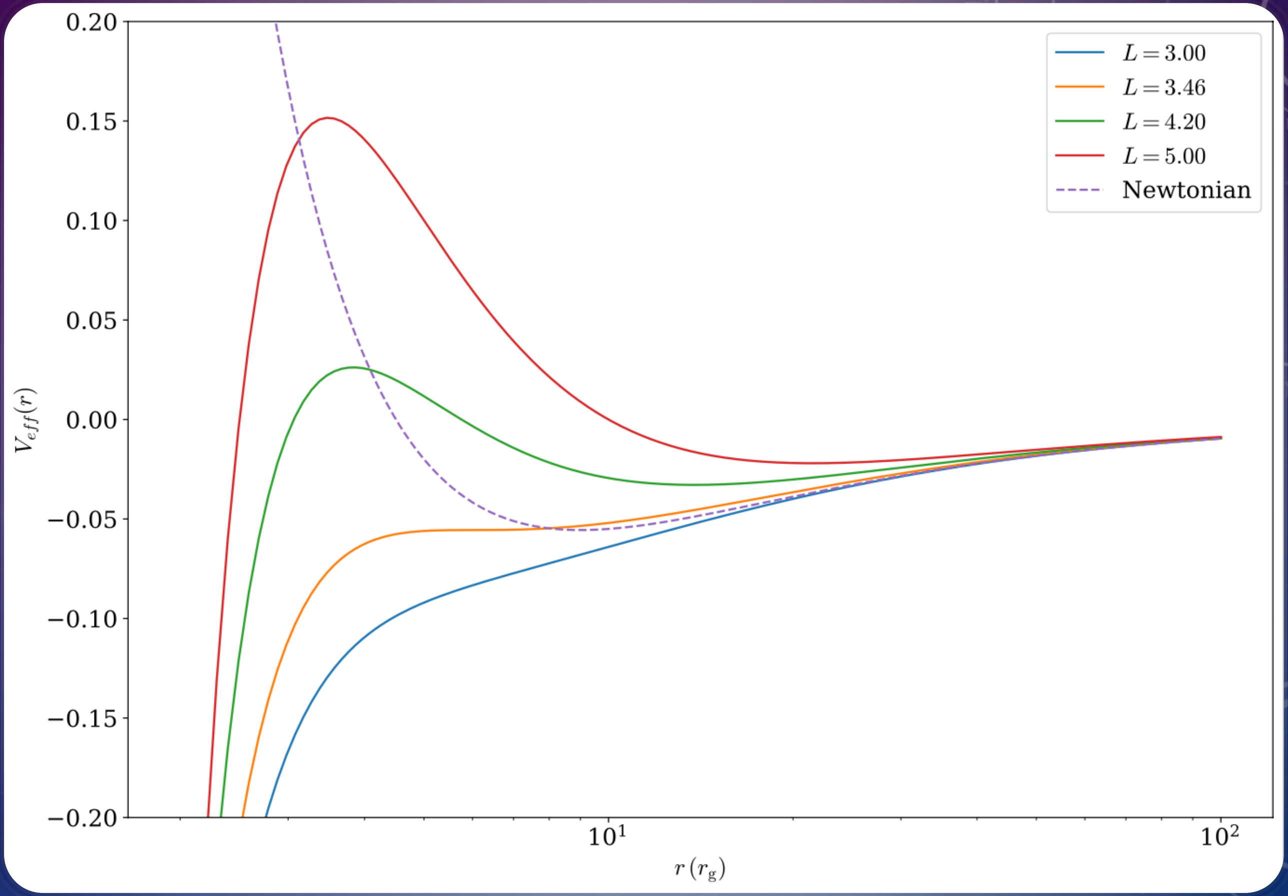

KERR SOLUTION

- Describes gravitational field outside of a rotating body with angular momentum J
- Dimension-less spin parameter $a = J/M^2$
- Boyer–Lindquist coordinates

$$ds^2 = -\left(1 - \frac{2Mr}{\Sigma}\right)dt^2 - \frac{4Mar}{\Sigma}\sin^2\theta\, dt\, d\phi + \frac{\Sigma}{\Delta}dr^2 + \Sigma d\theta^2 + \frac{A}{\Sigma}\sin^2\theta\, d\phi,$$

$$\Sigma = r^2 + a^2\cos^2\theta,$$
$$\Delta = r^2 - 2Mr + a^2,$$
$$A = \left(r^2 + a^2\right)^2 - a^2\Delta\sin^2\theta,$$

- Ring singularity in the centre
- Two horizons – inner and outer, ergosphere – surface of infinite redshift (g_tt = 0)

$$r_e^{\pm} = M \pm \sqrt{M^2 - a^2\cos^2\theta},$$
$$r_h^{\pm} = M \pm \sqrt{M^2 - a^2}.$$

- Ergoregion in between (no static observers, spacetime corotates with BH) – extends the outer horizon and drags the spacetime (frame-dragging)
- Reduces to Schwarzschild for a = 0

KERR SOLUTION II

- Frame dragging – ZAMO observers
  - appears as rotating with the BH for distant observers
- Ergosphere allows extraction of rotational energy – Blandford-Znajek process.
  - Jets launching with efficiency > 100 %
  - Confirmed in simulations (Tchekhovskoy+ 2011)

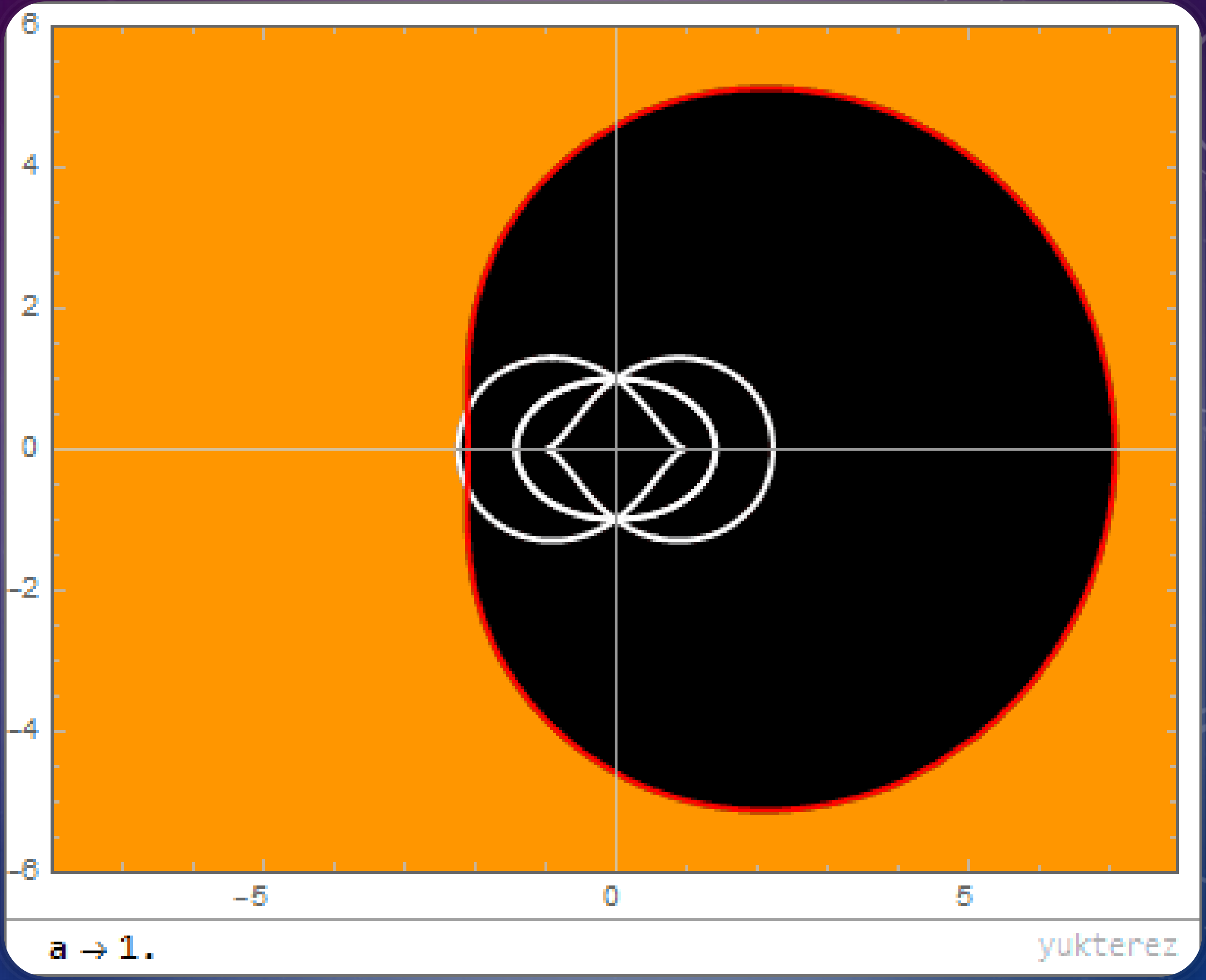

IMPORTANT RADII

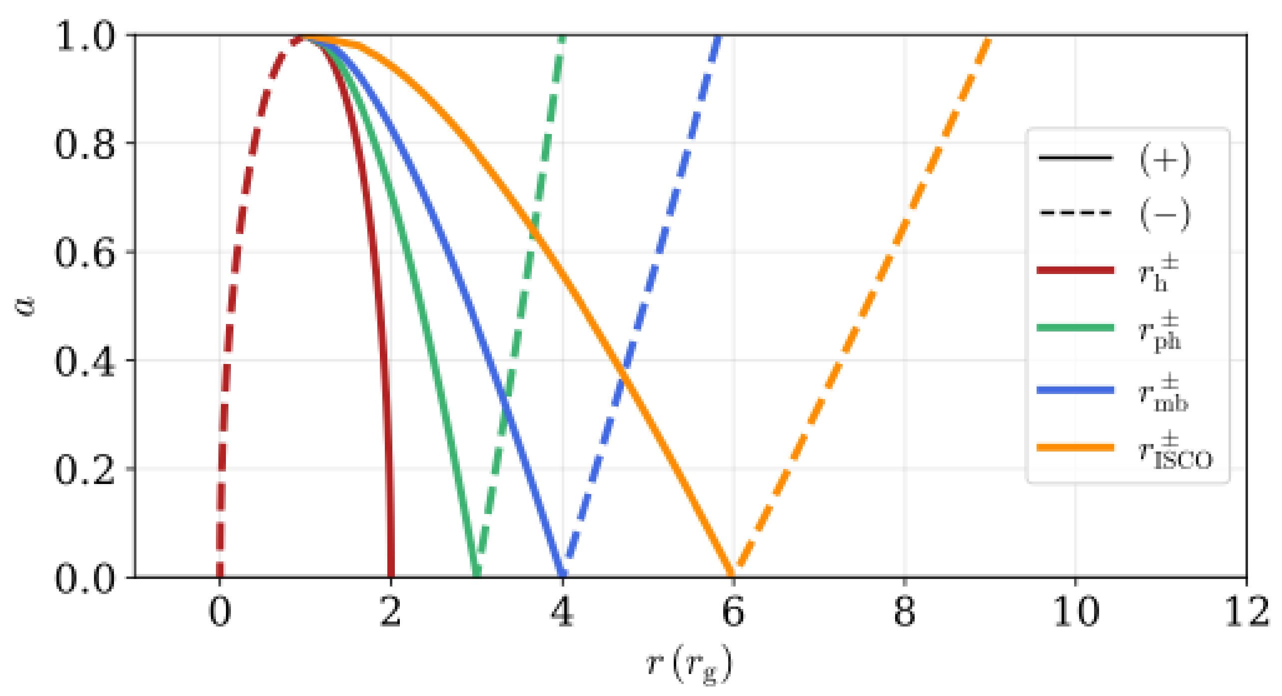

$$r_{\mathrm{ph}}^{\pm} = 2M\left\{1+\cos\left[\frac{2}{3}\cos^{-1}\left(\mp\frac{a}{M}\right)\right]\right\},$$

$$r_{\mathrm{mb}}^{\pm} = 2M \mp a + 2\sqrt{M\,(M\mp a)},$$

$$r_{\mathrm{ISCO}}^{\pm} = M\left[3+Z_2\mp\sqrt{(3-Z_1)\,(3+Z_1+2Z_2)}\right],$$

where

$$Z_1 = 1+\left(1-a^2\right)^{\frac{1}{3}}\left[(1+a)^{\frac{1}{3}}+(1-a)^{\frac{1}{3}}\right],$$

$$Z_2 = \sqrt{3a^2+Z_1^2}.$$

GRMHD

EQUATIONS AND METHODS

GRMHD

- Accretion disc material as a fluid (collisionless plasma)

  (Coulomb cooling scale) >> r_g
- Protons and electrons exchange energy efficiently
- Problematic for extremely low-density flows, such as ADAFs
- Somehow fixed with 2T simulations, where proton and electrons have different thermodynamics, 2 separated fluids
- Can explain problems with the EHT observations of Sgr A*

FRAMES

- Fluid
- Coordinate/lab
- ZAMO
- Orthonormal
- Co-rotating
- Co-moving

CONSERVATION LAWS

- Particle number/mass/density
- Energy – momentum
- Source-free Maxwell equation

MASS CONSERVATION

(non-rel)

$$\partial_t \rho = -\partial_i (\rho v_i)$$

(rel)

$$(\rho u_\mu)_{;\mu} = 0$$

$$\partial_t (\sqrt{-g}\, \rho u^t) = \partial_i (\sqrt{-g}\, \rho u^i)$$

metric determinant usually $r^2 \sin^2 \vartheta$ (volume element)

rest-mass density

in flat ST just γ

in flat ST γv^i

- Rest mass density
- Lab frame 4-velocity

ENERGY-MOMENTUM CONSERVATION

(non-rel) $\partial_t(\rho v_j) = \partial_i \Pi_{ij} - \rho \partial_j \phi$

$$\Pi_{ij} = \rho v_i v_j + (p + B^2/2)\delta_{ij} - B_i B_j$$

(rel)

$$(T^\mu{}_\nu)_{;\mu} = 0$$

$$\partial_t(\sqrt{-g}\, T^t{}_j) = -\partial_i(\sqrt{-g}\, T^i{}_j) + (\sqrt{-g}\, \Gamma^\mu_{j\nu} T^\nu{}_\mu)$$

$$T^\mu{}_\nu = (\rho + u_{int} + p_{gas} + b^2) u^\mu u^\nu + (p_{gas} + \frac{b^2}{2}) g^{\mu\nu} - b^\mu b^\nu$$

MAXWELL EQUATION

- Ideal MHD approximation
- Infinite conductivity – Lorentz force vanishes
- E is immediately carried away
- It does not hold for highly magnetized plasma

(non-rel)

$$\vec{E} + \frac{\vec{v} \times \vec{B}}{c} = 0$$

(rel)

$$\left(F^{*\mu\nu}\right)_{;\mu} = 0$$

MAGNETIC FIELD 4-VECTOR AND DIV B CONSTRAINT

$$F^{*\mu\nu} = b^\mu u^\nu - u^\mu b^\nu,$$

$$B^i = F^{*i0} = F^{*it} = b^i u^t - u^i b^t,$$

$$b^t = B^i u_i,$$

$$b^i = \frac{B^i + b^t u^i}{u^t}.$$

$\nabla \cdot B^i = 0$ constraint:

$F^{*00} = 0$ from $F^{*00} = b^0 u^0 - u^0 b^0$

$\Rightarrow \partial_t \left(\sqrt{-g}\, F^{*0i}\right) = -\partial_i \left(\sqrt{-g}\, F^{*ij}\right)$

$\partial_t \left(\sqrt{-g}\, B^i\right) = -\partial_i \left[\sqrt{-g}\left(b^i u^j - u^i b^j\right)\right]$

if $i = 0$

$\partial_t \left(\sqrt{-g}\, F^{*00}\right) = -\partial_i \left(\sqrt{-g}\, B^i\right)$

$\partial_t \sqrt{-g}\, F^{*00} + \sqrt{-g}\, \partial_t F^{*00} = -\partial_i \left(\sqrt{-g}\, B^i\right)$

Constrained-transport – Toth 2000

EQUATION OF STATE

$$p_{\text{gas}} = (\Gamma - 1)u_{\text{int}}$$

- Adiabatic polytropic EoS
- Gamma = 5/3 for gas pressure-dominated fluid
- Gamma = 4/3 for radiation pressure-dominated fluid

Part 4: Accretion discs in GR

GRMHD simulations

What is different?

- Inner edge – on ISCO
- Strong gravity effects on gravity potential and angular momentum
- Extremely high efficiency
- High temperatures
- Relativistic outflows

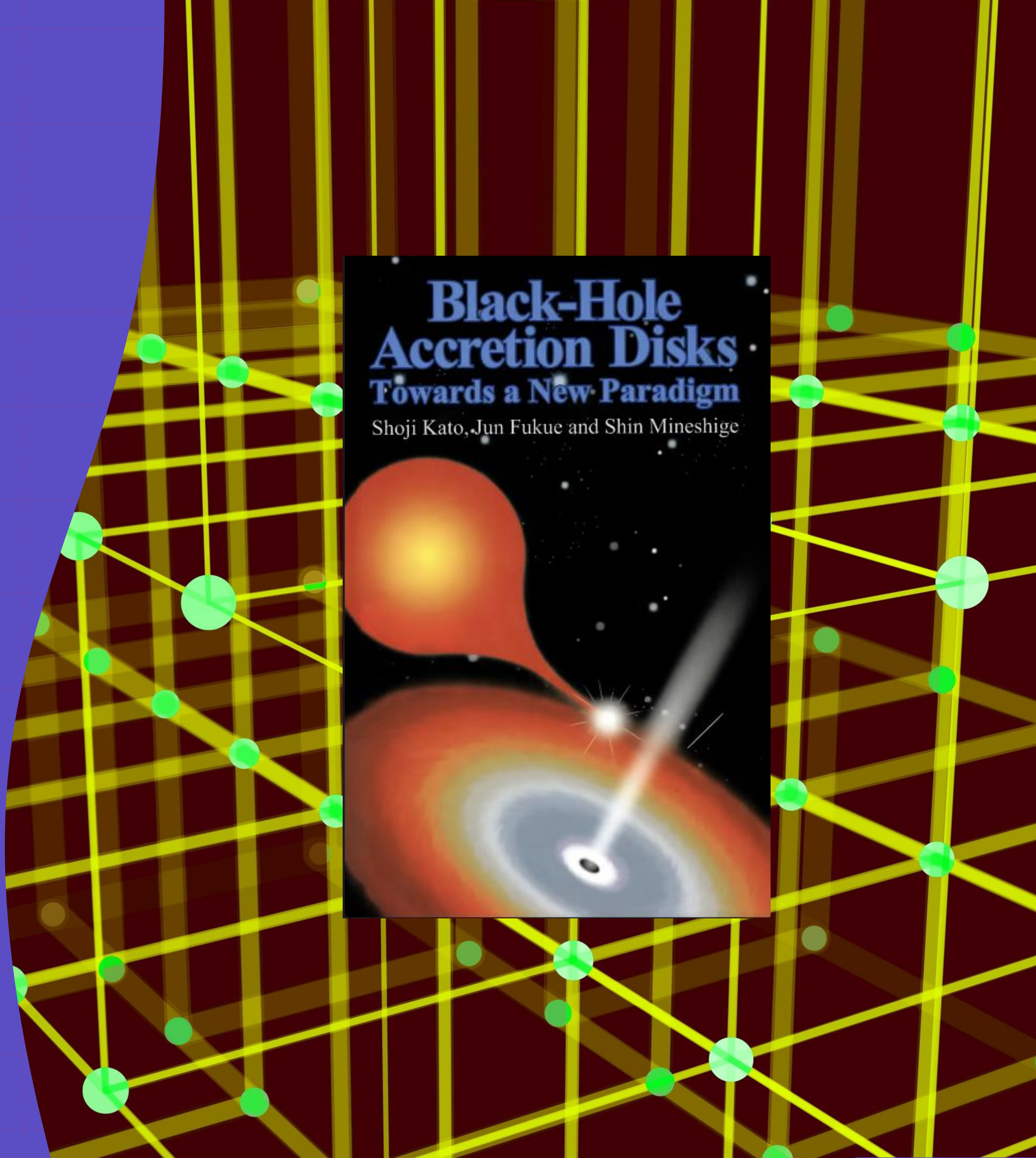

Angular momentum transport

- Magnetorotational instability (Balbus&Hawley 91, 98)
- Can be achieved in MHD sims, but the resolution has to be very high
- Quality parameter – Alfvén wave has to fit within one cell (Hawley+ 2013)

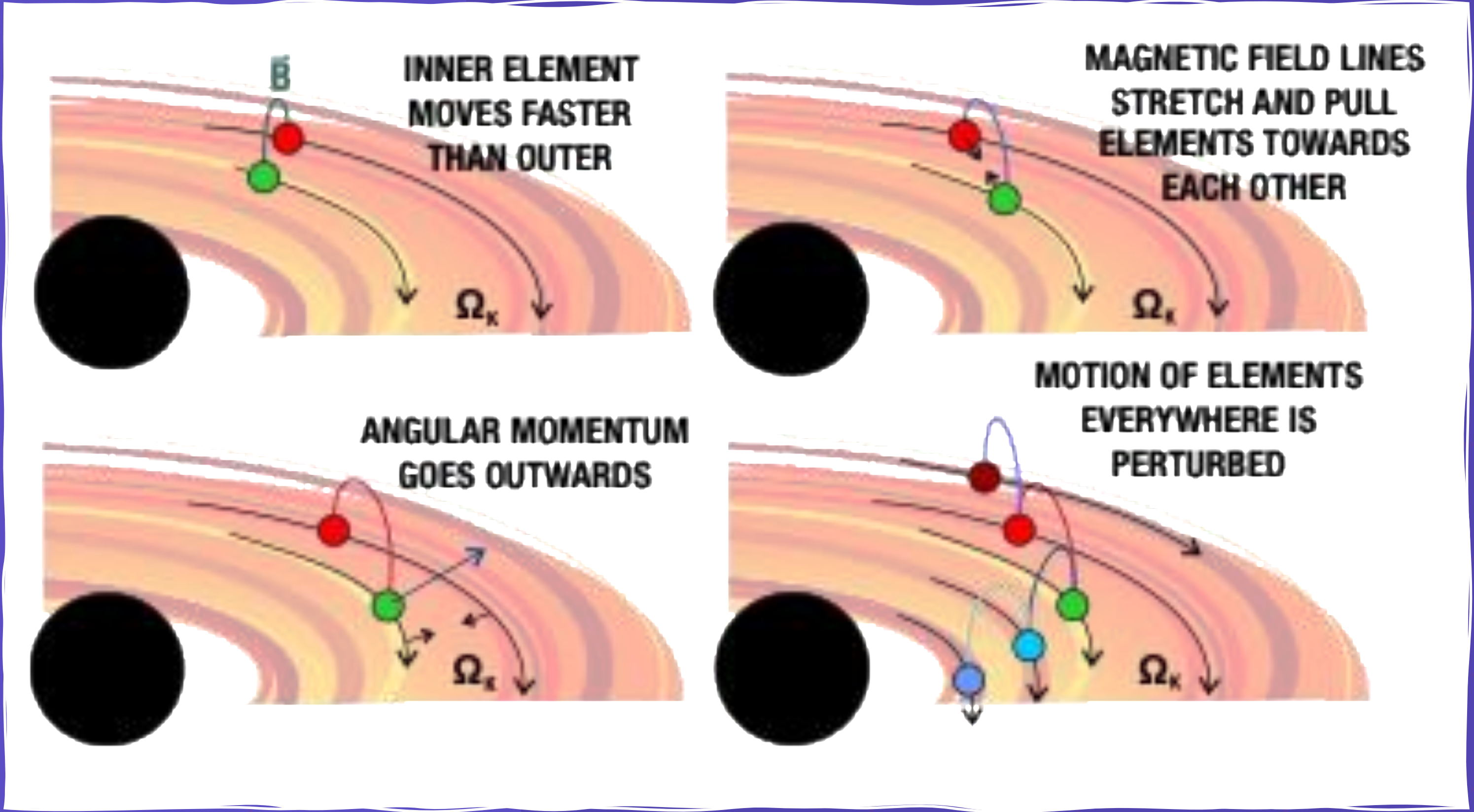

Accretion disc in BH system

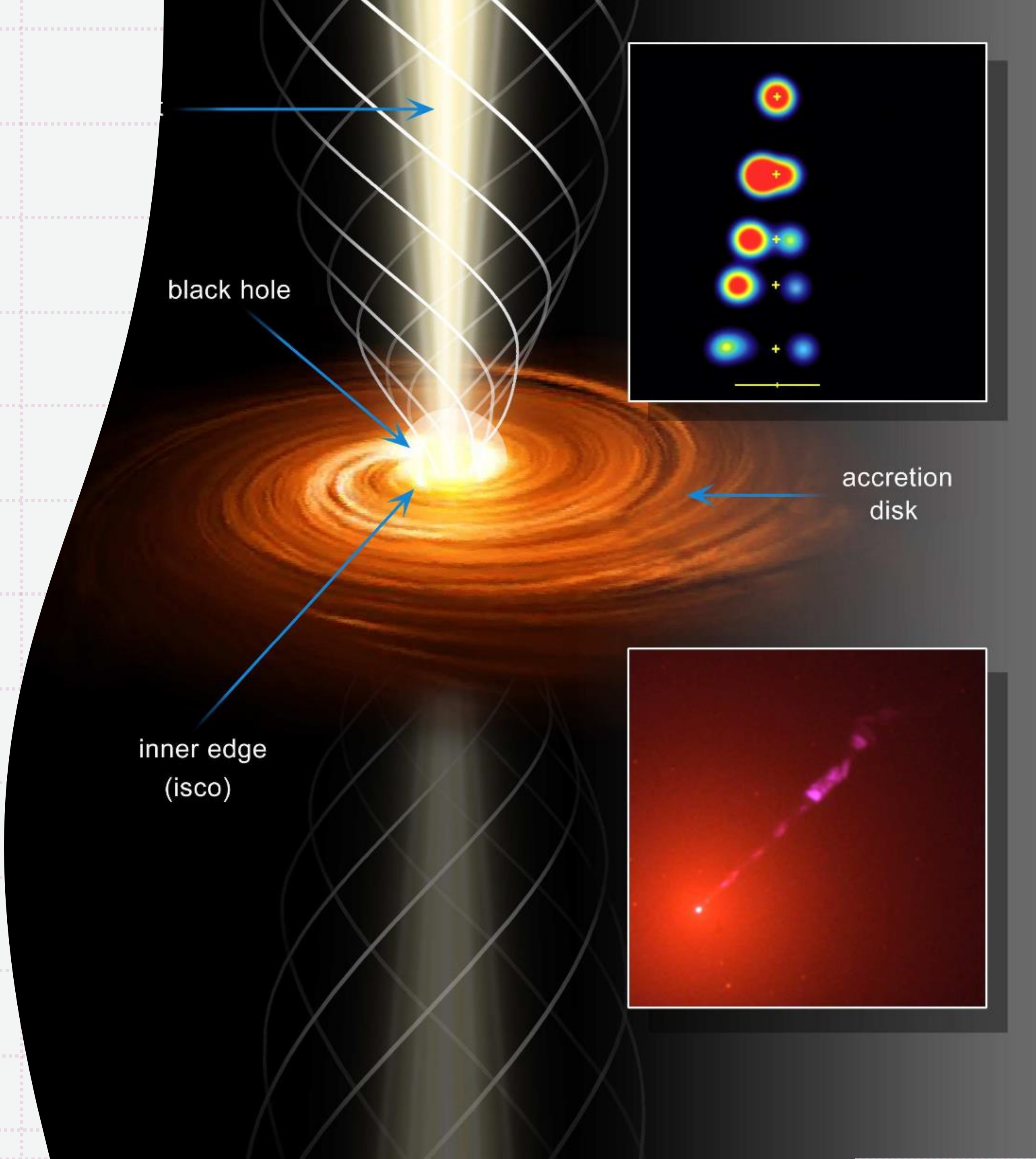

X-ray spectrum

- Stellar mass BH binaries are one of the most luminous objects in the sky
- Extreme efficiency of BH accretion – 0.05 for non-rotating, up to 0.42 for maximally rotating (not including other mechanisms of energy extraction)

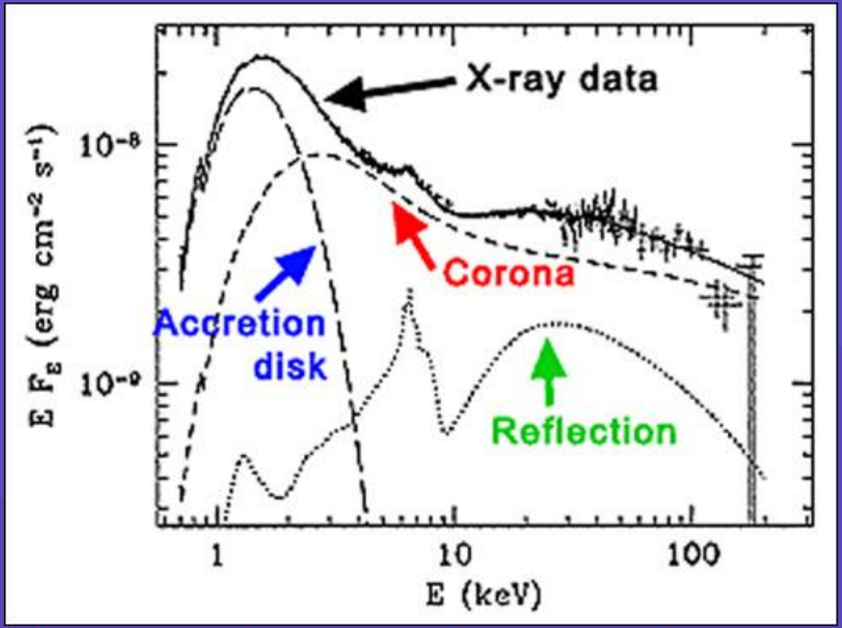

Gierliński+ 1999

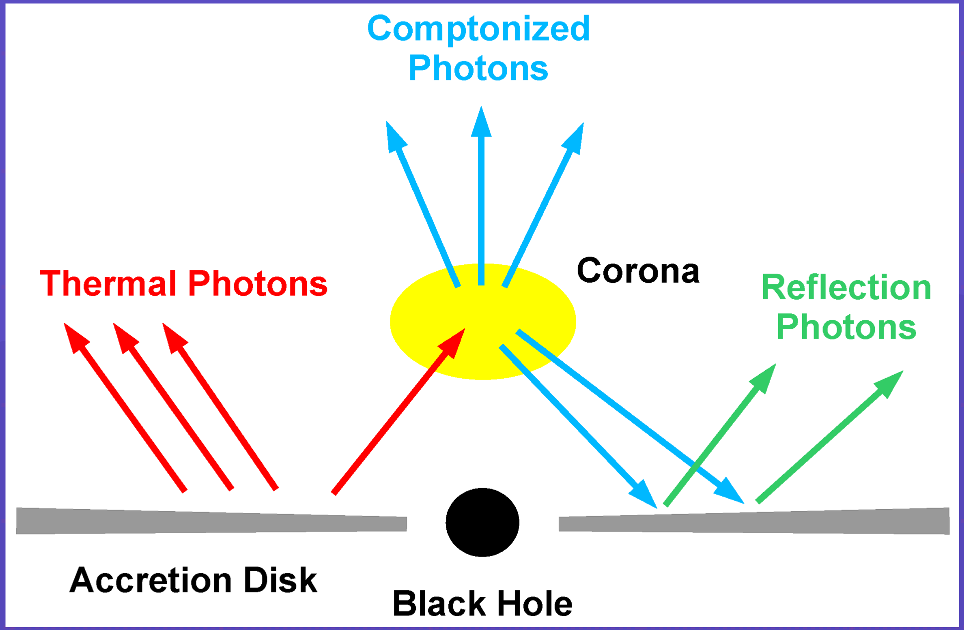

Bambi 2022

Standard thin disc

- Shakura&Sunyaev 1973, Novikov&Thorne 1973, Page&Thorne 1974
- Inner edge – integration constant for angular momentum conservation
- Geometrically thin, optically thick

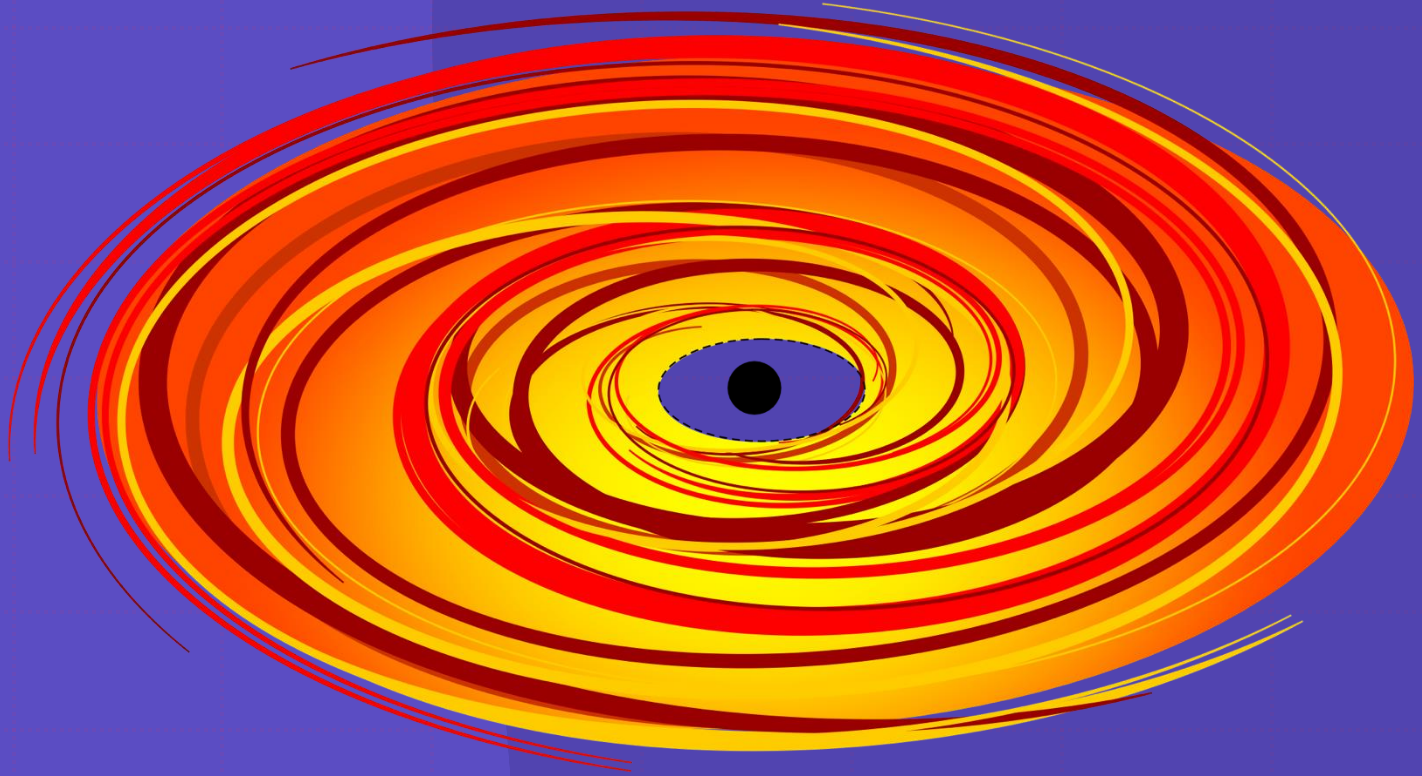

Thin disc in detail - Assumptions

Fully ionised H gas

Gravity determined by central object – no self-gravity

Disc is in the equatorial plane

Steady and axisymmetric

$$\frac{\delta}{\delta t} = \frac{\delta}{\delta \phi} = 0$$

Geometrically thin

$$H/r \ll 0$$

Keplerian rotation, dominant

$$v_\phi = \sqrt{\frac{GM}{r^3}} \gg v_r$$

Hydrostatic balance in vertical direction

Optically thick

α-prescription for viscosity

$$\alpha p = T_{r\phi}$$

Global MF ignored

Thin disc in detail - equations

- Mass conservation
- Momentum conservation
- Angular-momentum conservation
- Hydrostatic balance (one-zone approximation)
- Energy balance
- Equation of state
- Opacity
- Viscosity

$$\dot{M} = -2\pi r v_r \Sigma,$$

$$\Omega = \Omega_K \equiv \sqrt{\frac{GM}{r^3}} \quad \text{and} \quad v_\varphi = v_K \equiv \sqrt{\frac{GM}{r}},$$

$$\nu\Sigma = \frac{\dot{M}}{3\pi}\left(1 - \sqrt{\frac{r_{\rm in}}{r}}\right)$$

$$\frac{p}{H} = -\rho g_z(H),$$

$$p = p_{\rm gas} + p_{\rm rad} = \frac{2k_{\rm B}}{m_{\rm H}}\rho T_{\rm c} + \frac{aT_{\rm c}^4}{3},$$

$$Q^+_{\rm vis} = Q^-_{\rm rad},$$

$$\bar{\kappa} = \kappa_{\rm es} + \kappa_{\rm ff} = \kappa_{\rm es} + \kappa_0 \rho T_{\rm c}^{-3.5},$$

Thin disc - solution

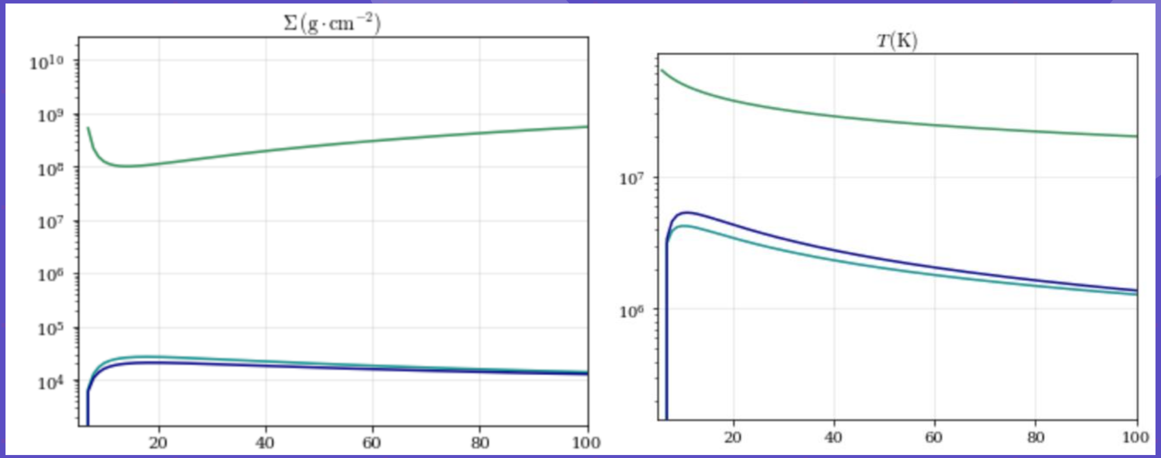

- 3 regions

$P_{GAS} < P_{RAD}$

$\kappa_{es} > \kappa_{ff}$

$P_{GAS} > P_{RAD}$

$\kappa_{es} > \kappa_{ff}$

$P_{GAS} > P_{RAD}$

$\kappa_{es} < \kappa_{ff}$

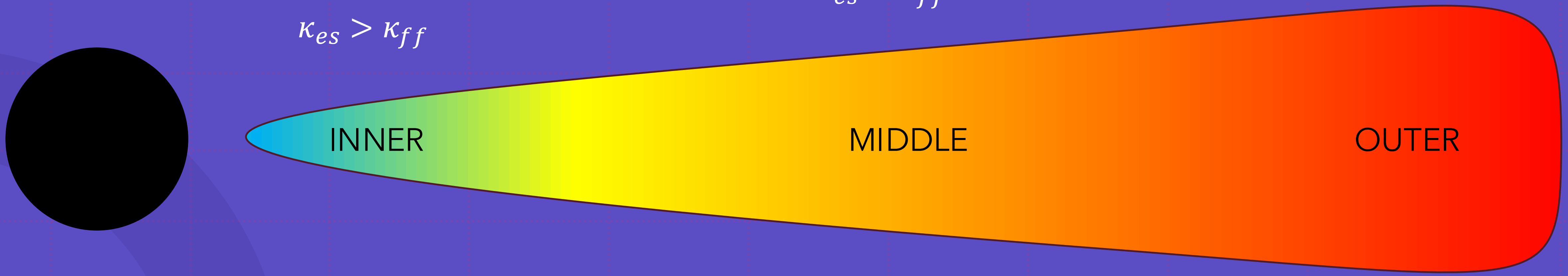

Observables

- Local LTE – locally radiates as BB
- Total spectrum = sum of BB from each radii
- **Multi-BB spectrum**

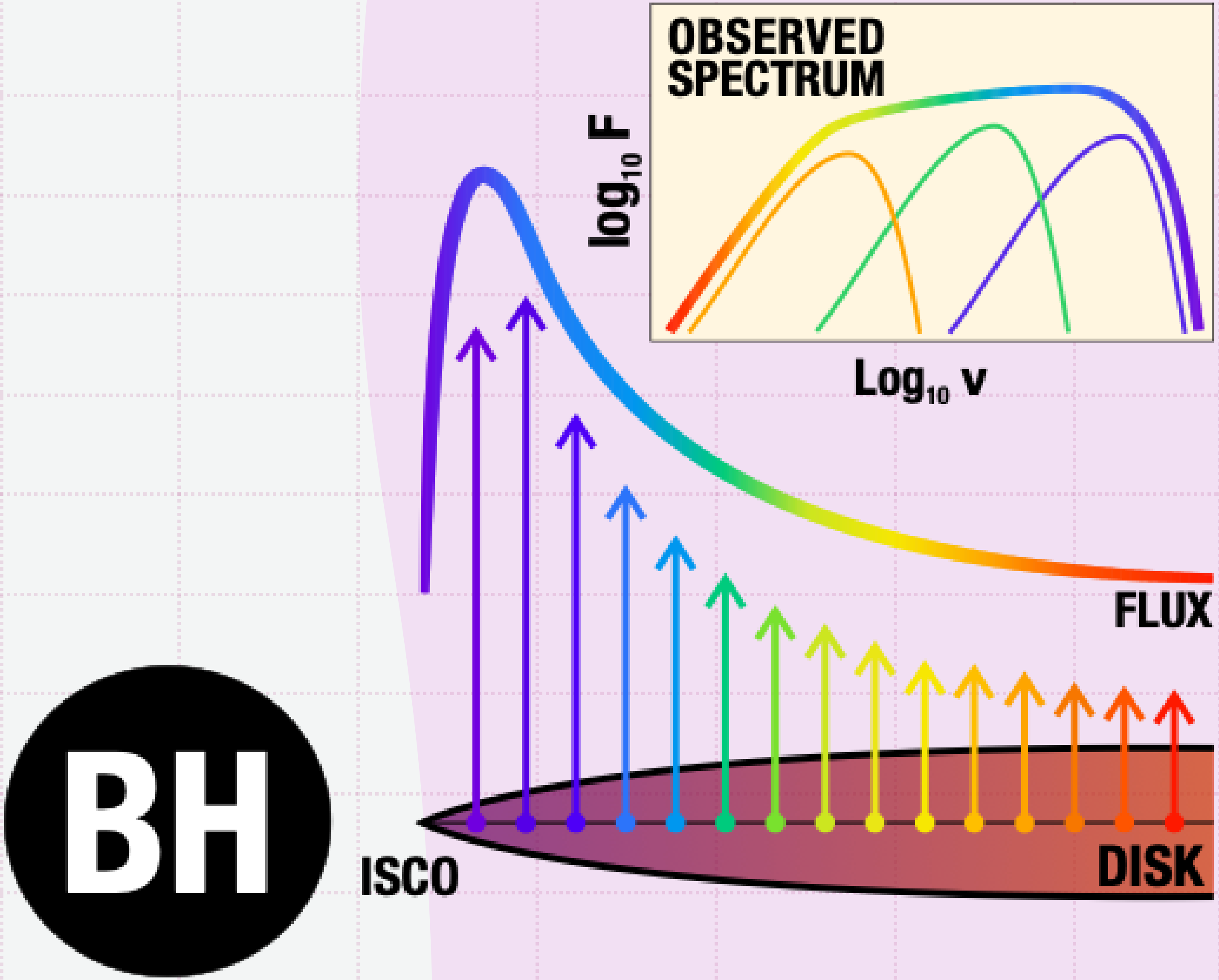

Inner edge

- Thin disc BB spectrum used to find the ISCO and thus the spin of the BH
- Does it really hold?

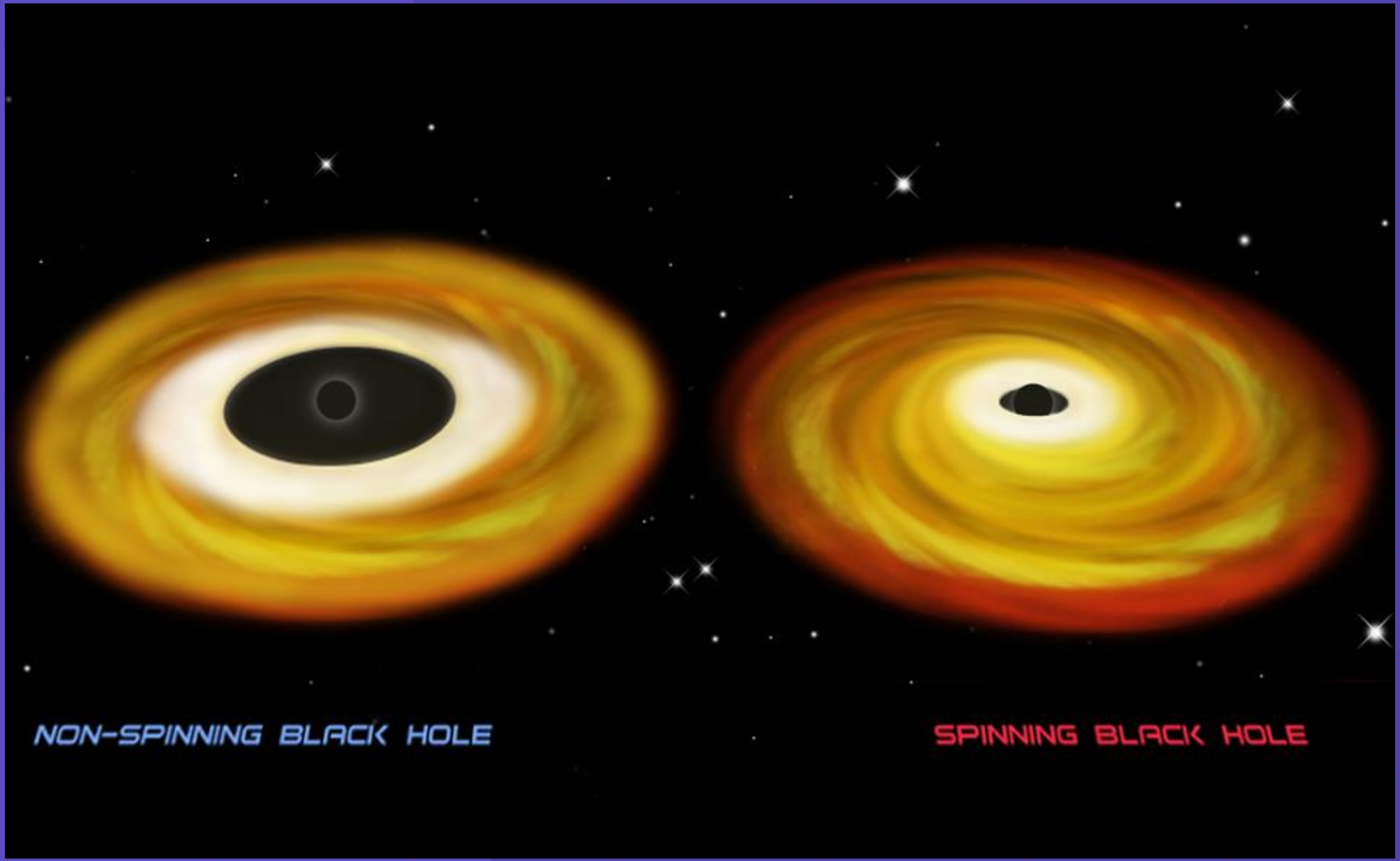

Spectral models

- Fails to fit spin when luminosity is changing
- Simulations shows the inner edge is closer

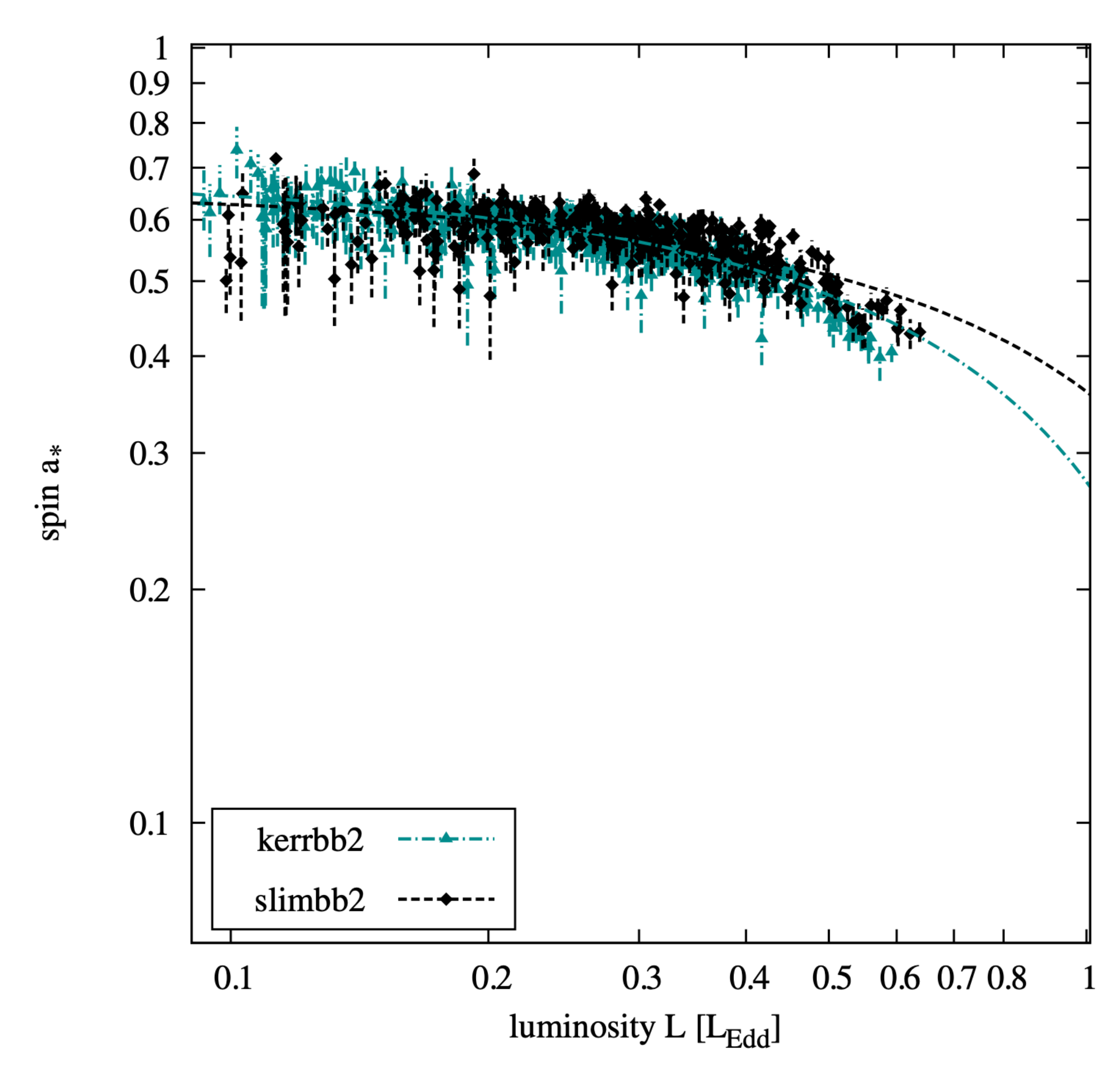

OBSERVATIONAL SIGNATURE

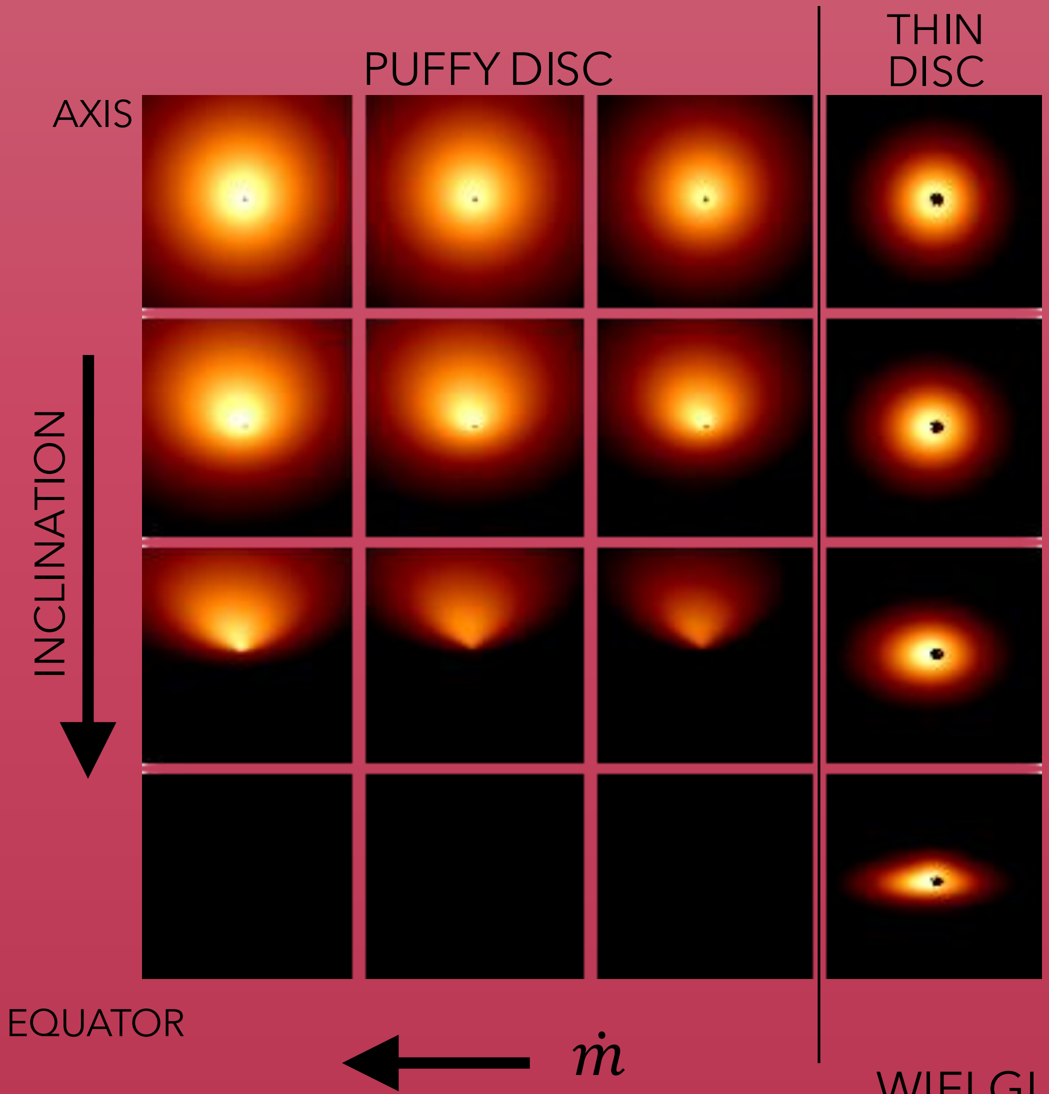

WIELGUS+ 2022

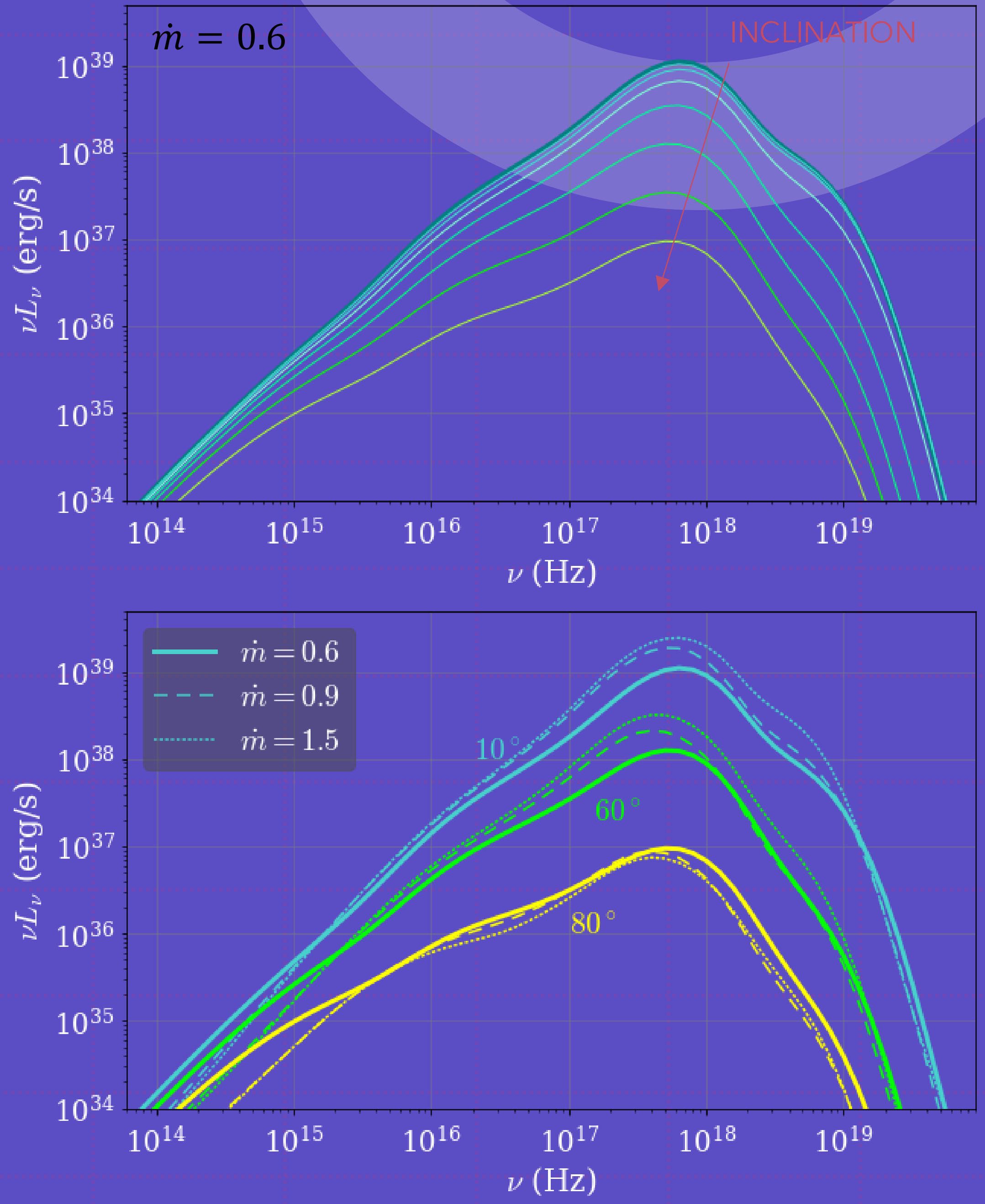

A toy to play

- https://github.com/dlancova/ThinDiskCode
- Calculates properties of a NT disc and many other GR-connected

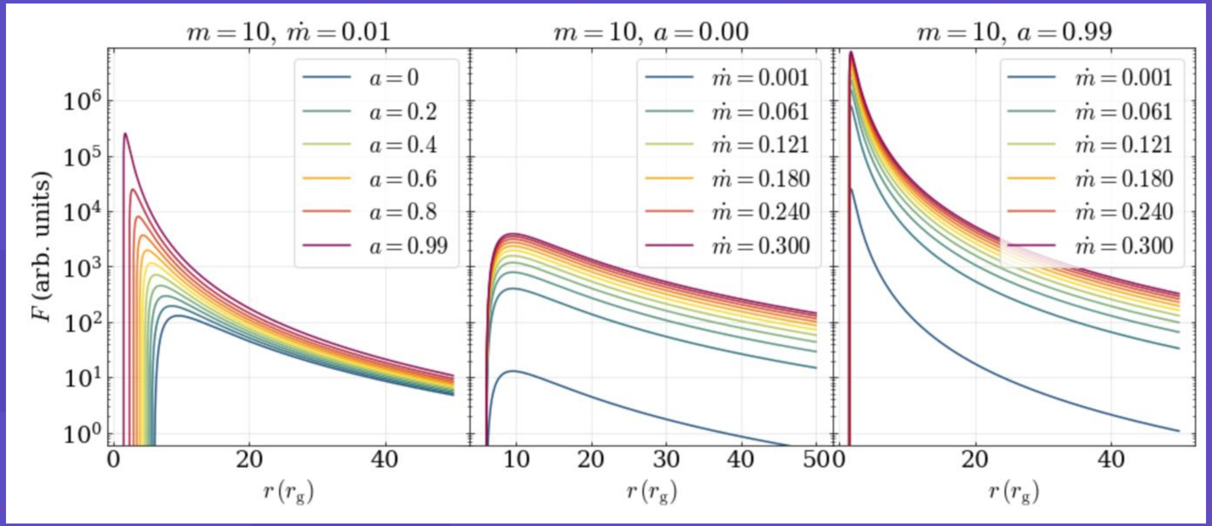

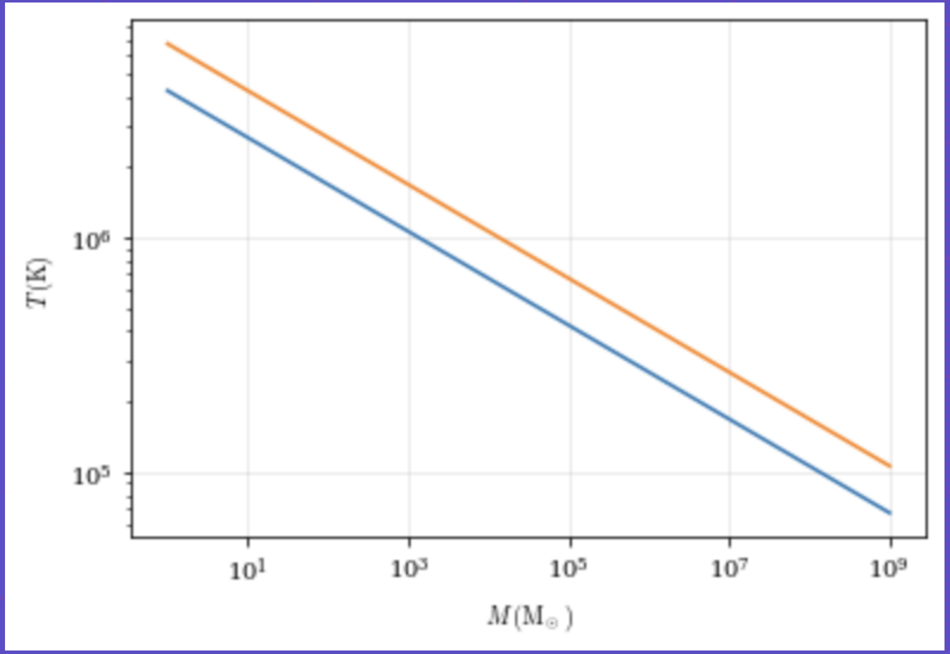

Instabilities

- The thin disc model is unstable when radiation pressure dominates
- But observations fit the model
- Searching for the stabilising mechanism

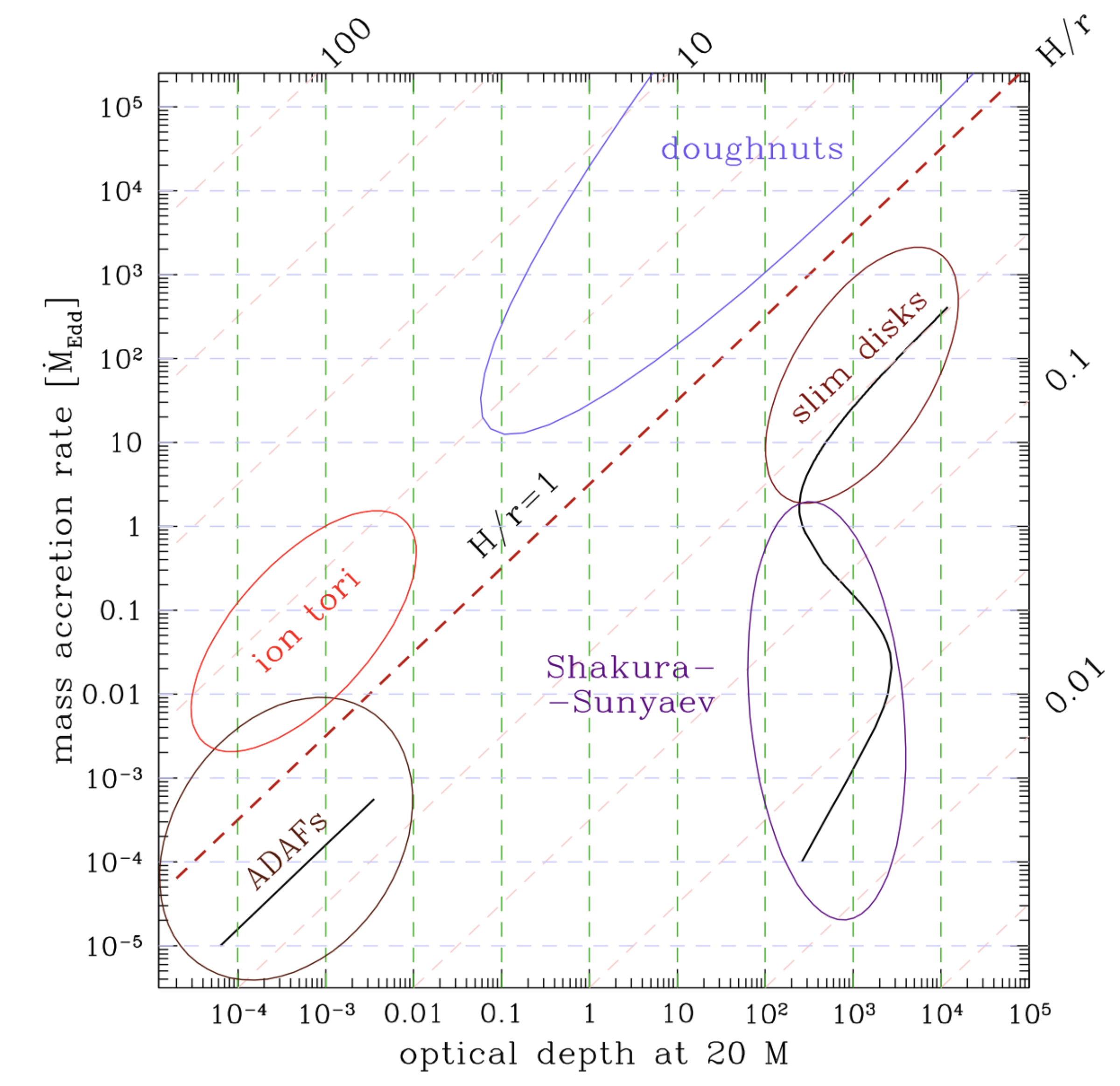

Sądowski 2011

Thermal instability

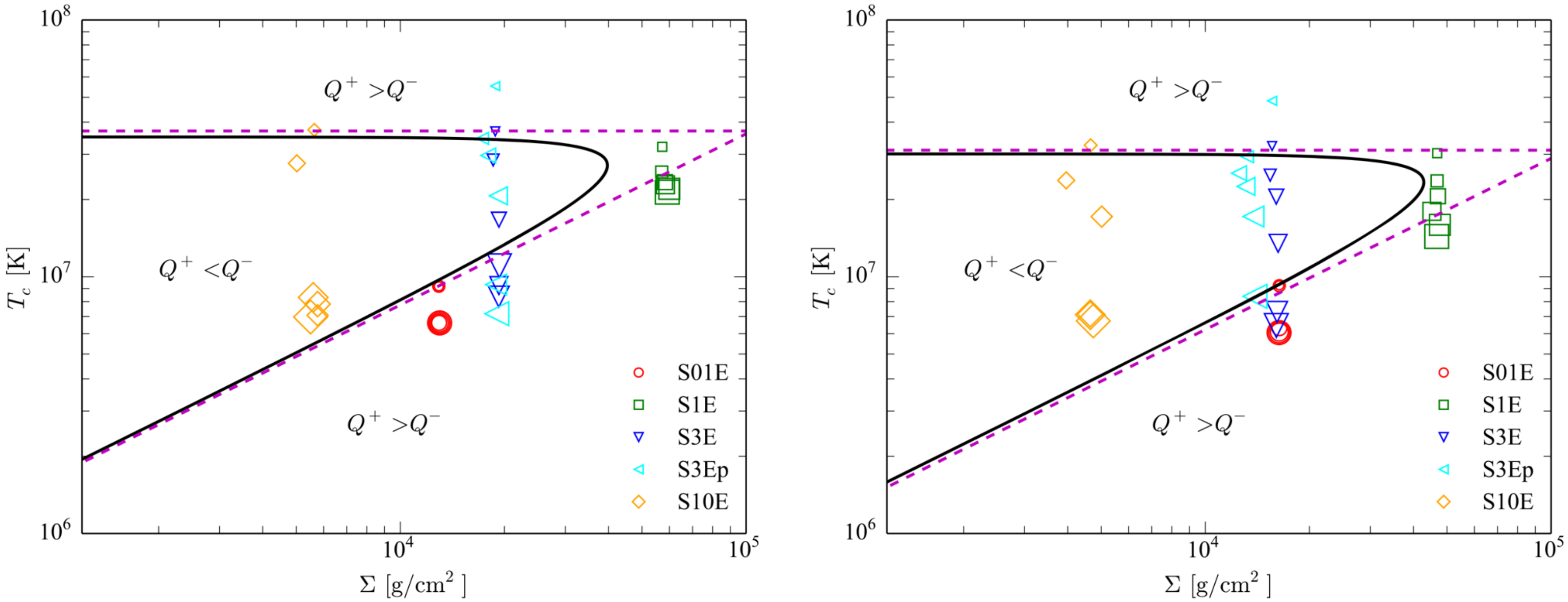

Figure 1. Thermal equilibrium (T_c–Σ) diagram for thin disks at $R = 10r_g$ (left panel) and $15r_g$ (right panel). The solid line is for the standard Shakura–Sunyaev model with $\alpha = 0.02$, with the asymptotic gas- (bottom) and radiation- (top) pressure-dominated branches shown by the dashed lines. The red circles show the evolution of simulation S01E, green squares the evolution of S1E, blue downward triangles the evolution of S3E, cyan leftward triangles the evolution of S3Ep, and yellow diamonds the evolution of S10E. Data from the simulations have been time-averaged over three ISCO orbital periods and radially averaged over intervals of 10 zones. Increasing point sizes correspond to time intervals centered at $t = 0$, 5000, 10,000, 15,000, 20,000, and 25,000 GM/c^3, respectively.

Fragile+ 2018

Modelling the observations

- Multiple types of discs exist together
- Different contributions to observed spectrum
- Microquasars' outbursts are the best tests to models

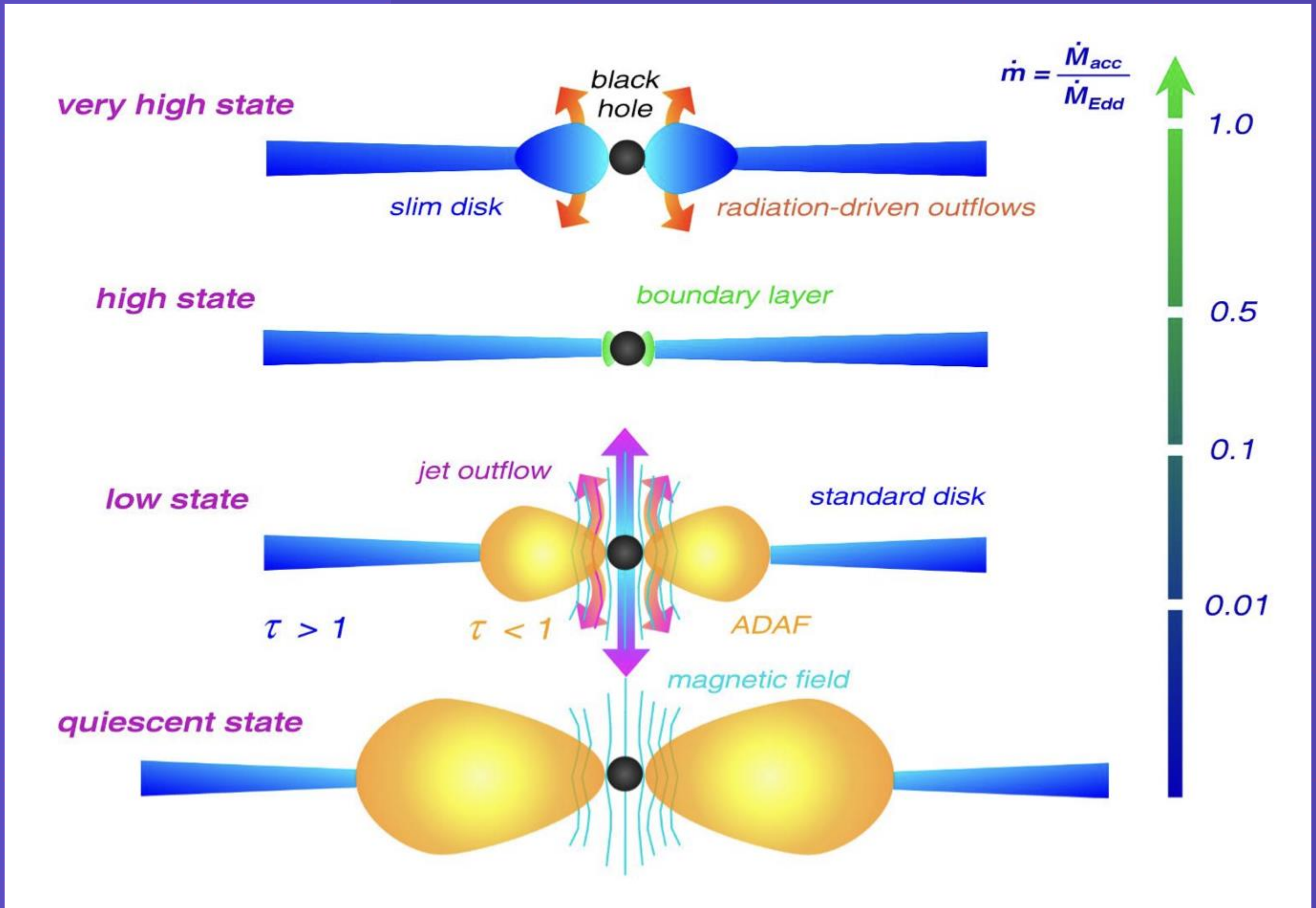

Müller 2004

Thin(-ish) disc simulations

- Radiation or artificial cooling function needed
- Extremely demanding – dense and thin region of the disc with small turbulence – needs huge resolution
- Simulations work for small $\dot{m}$ $(< 0.1\dot{m}_{Edd})$; for larger it extends in a vertical direction
- magnetically elevated discs – Sądowski 2016, Lančová+2019, Mishra+ 2020, Liska+ 2024, …

Existing simulations

	$\dot{m}/\dot{m}_{Edd}$	
Ohsuga+ 2011	0.01 (model B)	Radiative, super thin disk
Mishra+2016, Fragile+2018, Mishra+2019	0.01 - 0.1	Magnetically elevated disk, Thermally unstable, collapsing
Jiang+2019	0.07, 0.2	SMBH, stabilized by MF, not thin!
Kinch+2021	0.01, 0.1	No radiation, not thin, cooling function
Dexter+ 2021	$(0.2 - 1.57) \times 10^{-3}$	High $\dot{m}$ is colapsing Also, spectra!

Cooling functions

- Added “sink” term into energy conservation equations
- Set to work only within the disc – leads to results comparable to analytical models
- Shafee+ 2008, Noble & Krolik 2009, Nobre, Krolik & Hawley 2010 …

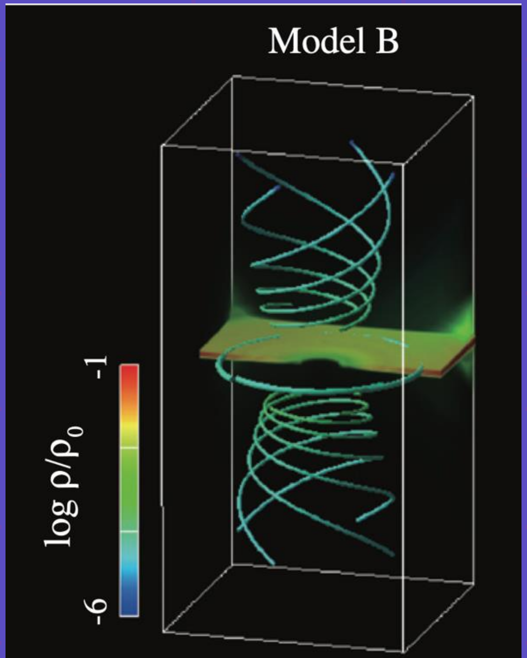

Ohsuge+ 2011

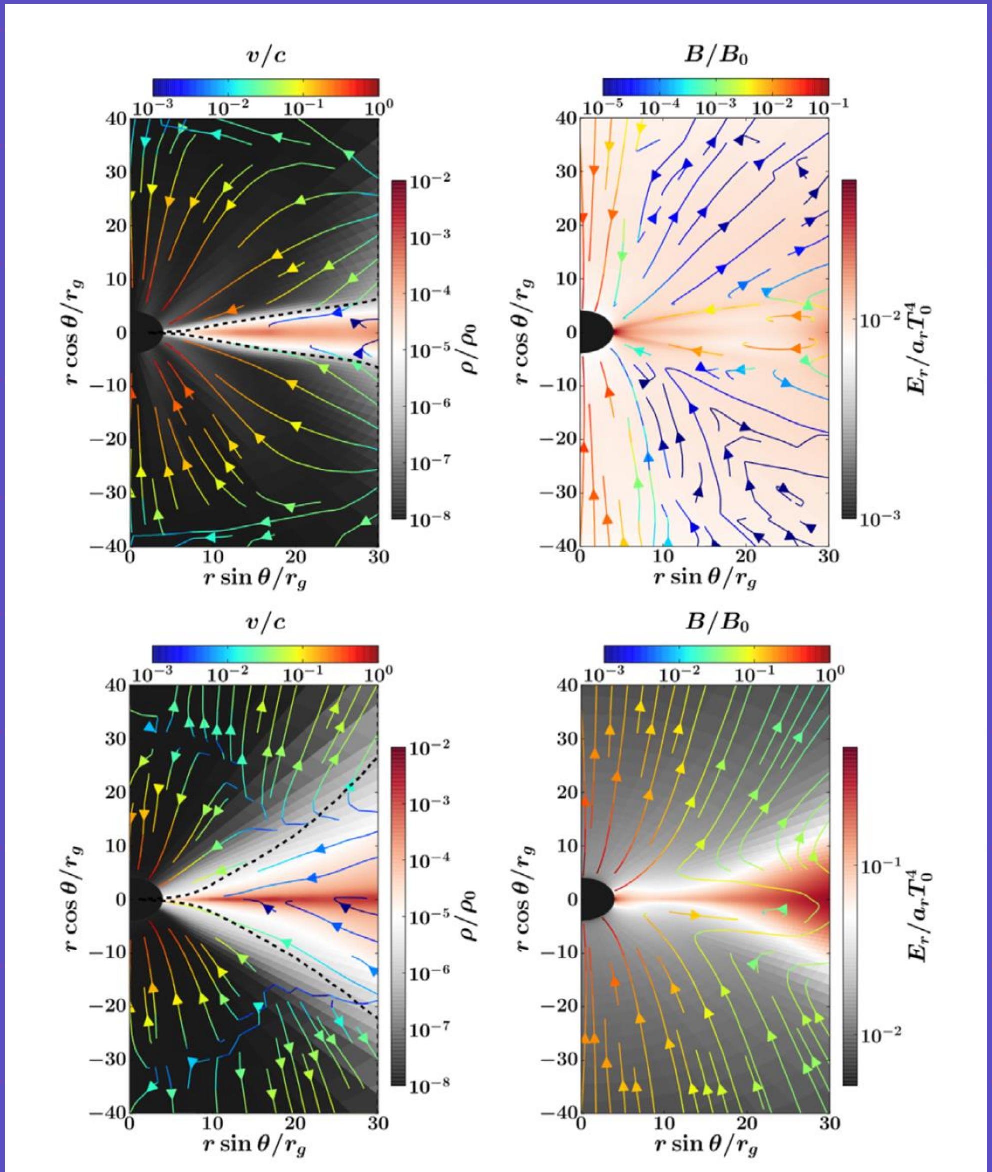

Jiang+ 2019

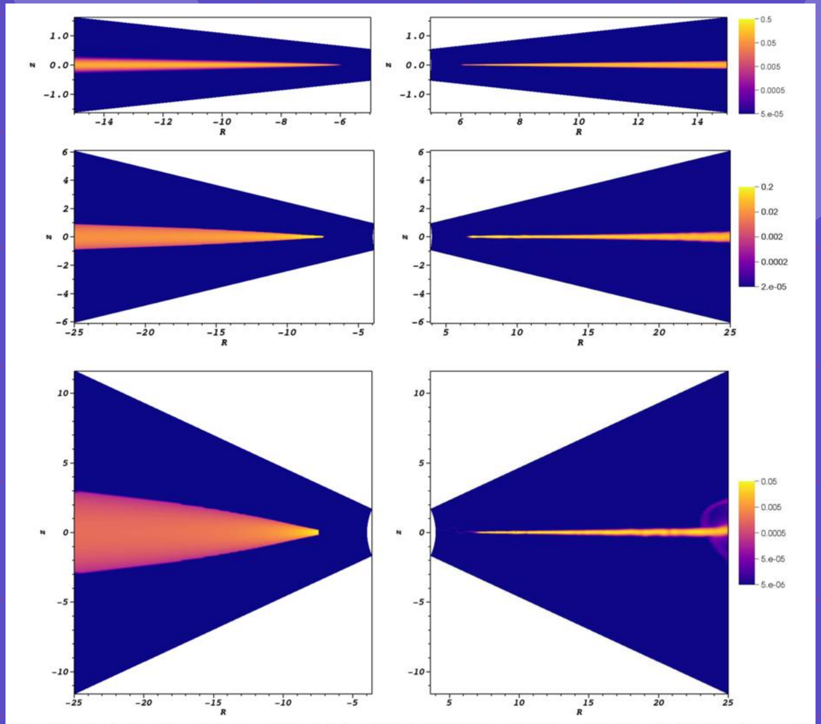

Figure 2. Pseudo-color plots of mass density (cgs units) for simulations S01E (top), S3E (middle), and S10E (bottom). The left- and right-hand panels correspond, respectively, to $t = 0$ and $t = 27{,}475\ GM/c^3$. Note the vertical collapse of simulations S3E and S10E.

Fragile+ 2018

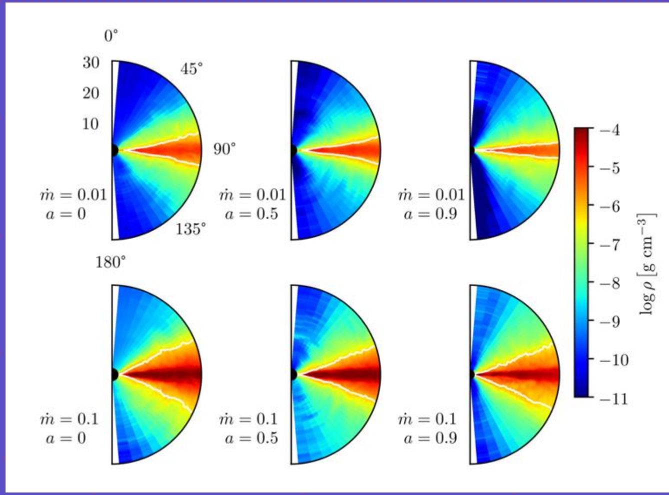

Kinch+ 2018

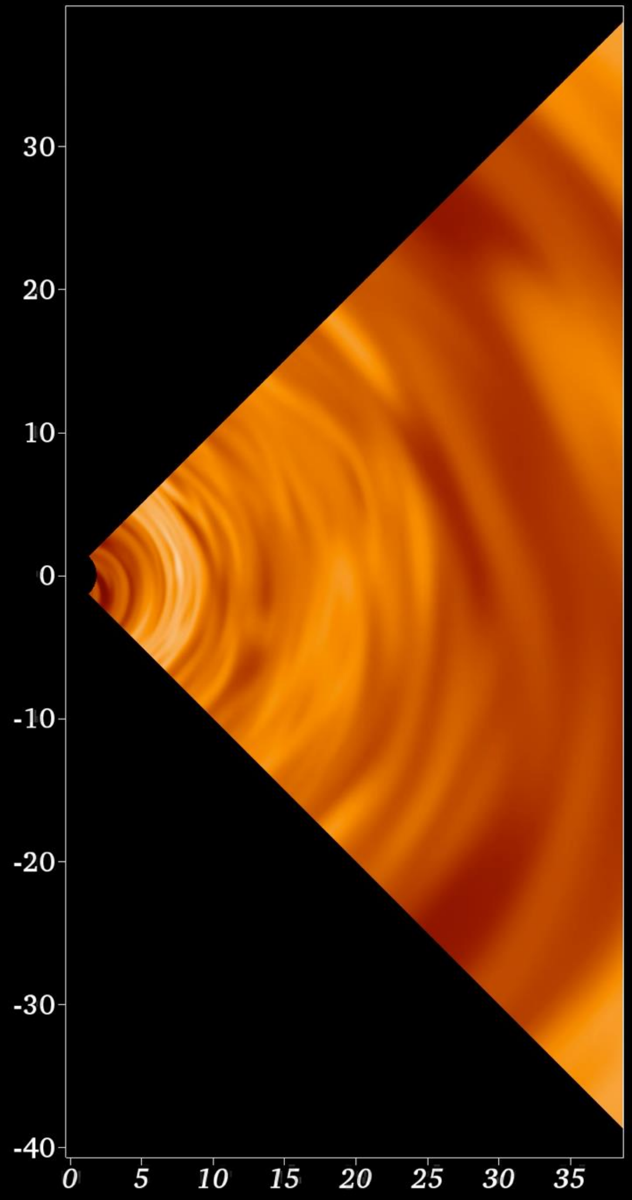
30
20
10
0
-10
-20
-30
-40
0
5
10
15
20
25
30
35

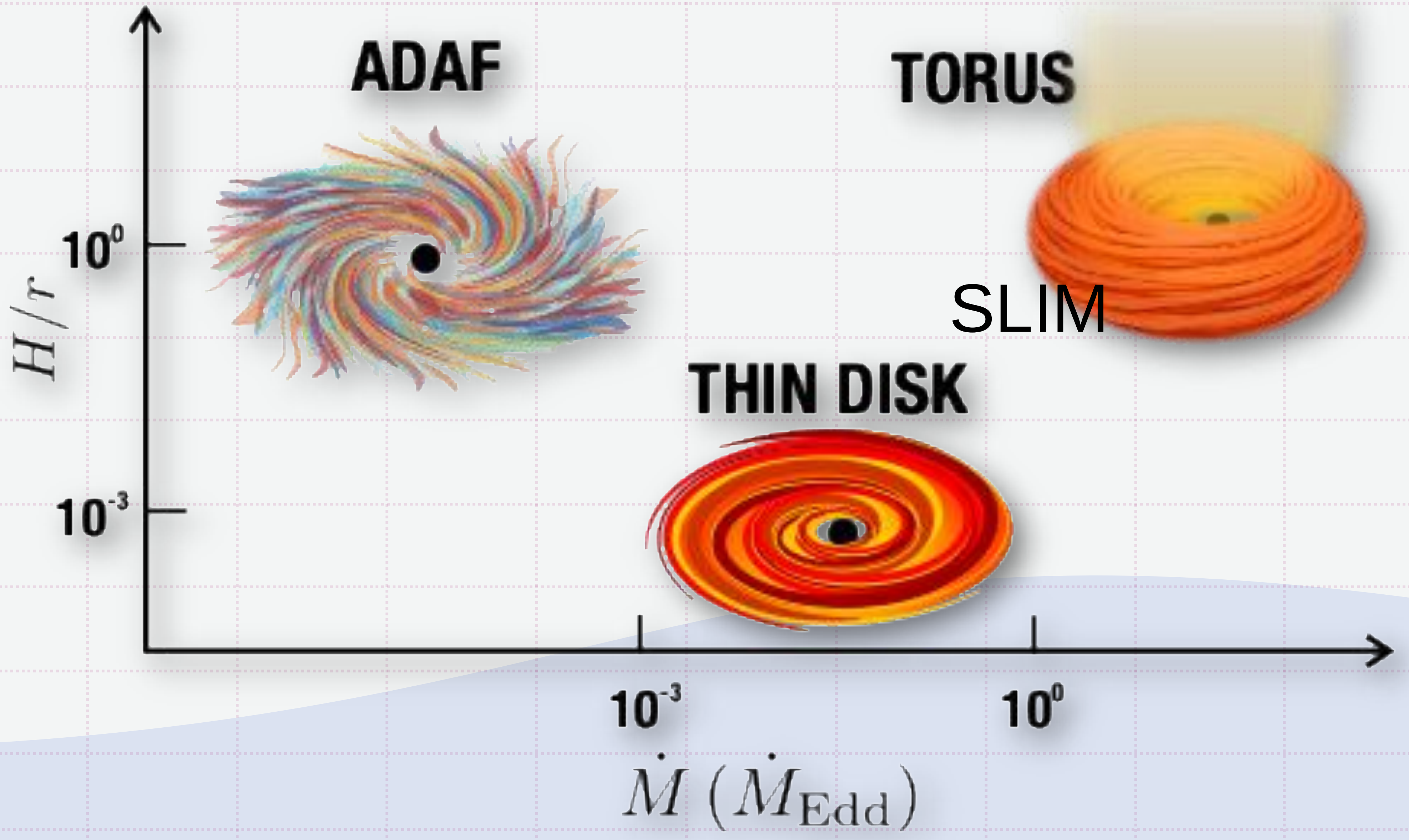

ADAF
TORUS
SLIM
THIN DISK
10^0
10^{-3}
H/r
10^{-3}
10^0
$\dot{M}\ (\dot{M}_{\rm Edd})$

SLIM discs

- Abramowicz, Lasota, Czerny & Szuskiewicz 1988
- Extension of thin disc for $\dot{M} \sim \dot{M}_{Edd}$
- Vertically integrated, but includes more physics than TD
- Trans-sonic solution, advection cooling,

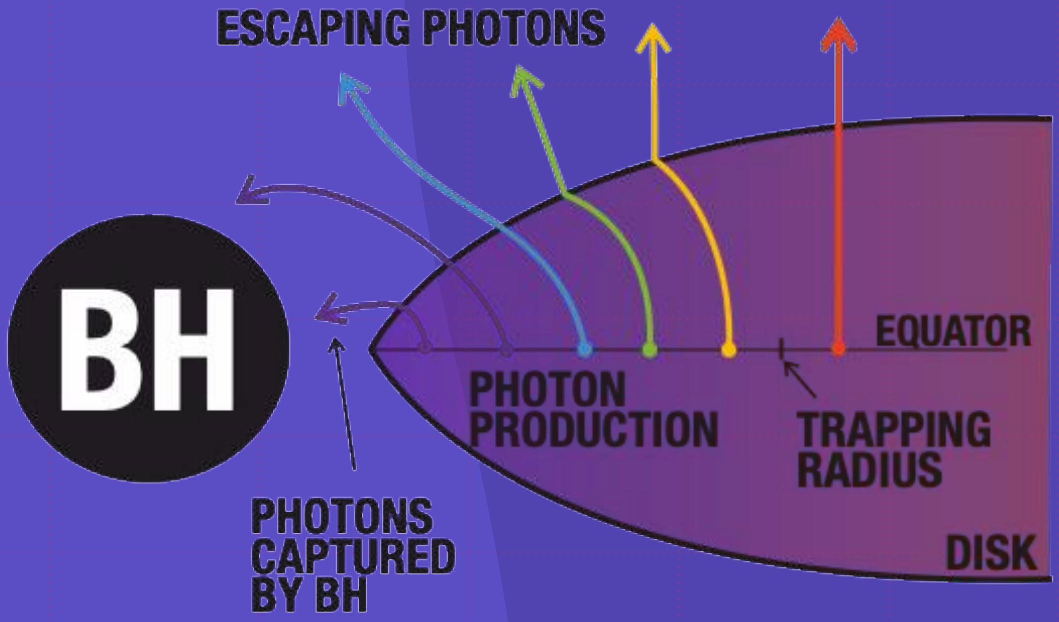

Photon trapping

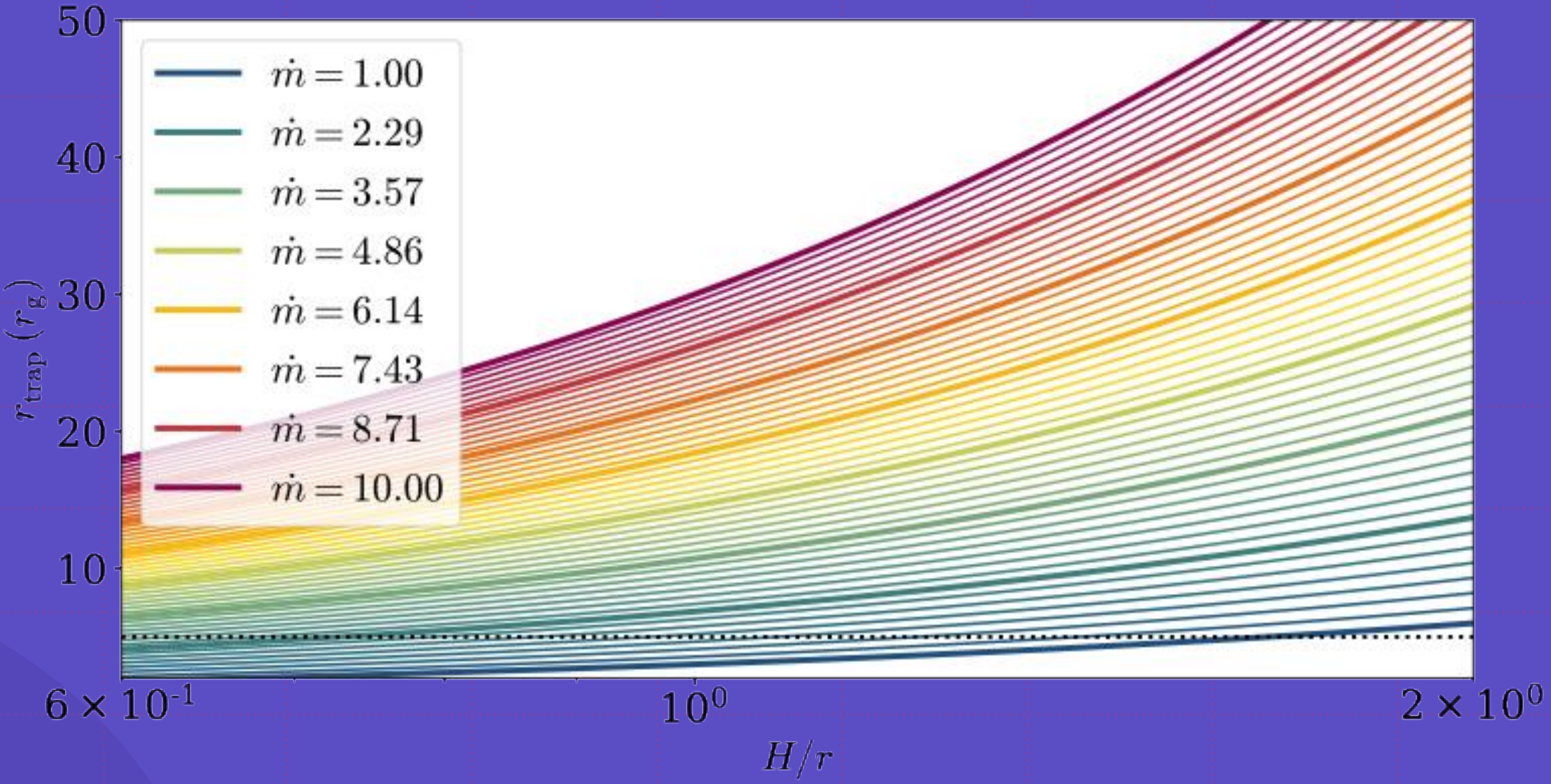

Polish dougnuts or thick discs in general

- Jaroszynski, Abramowicz&Paczynski 1980
- Constant angular momentum within the disc (von Zeipel theorem) – makes equations integrable
- Function for potencial, pressure, density, … distribution in r, θ

Marginaly overflowing torus – cusp torus

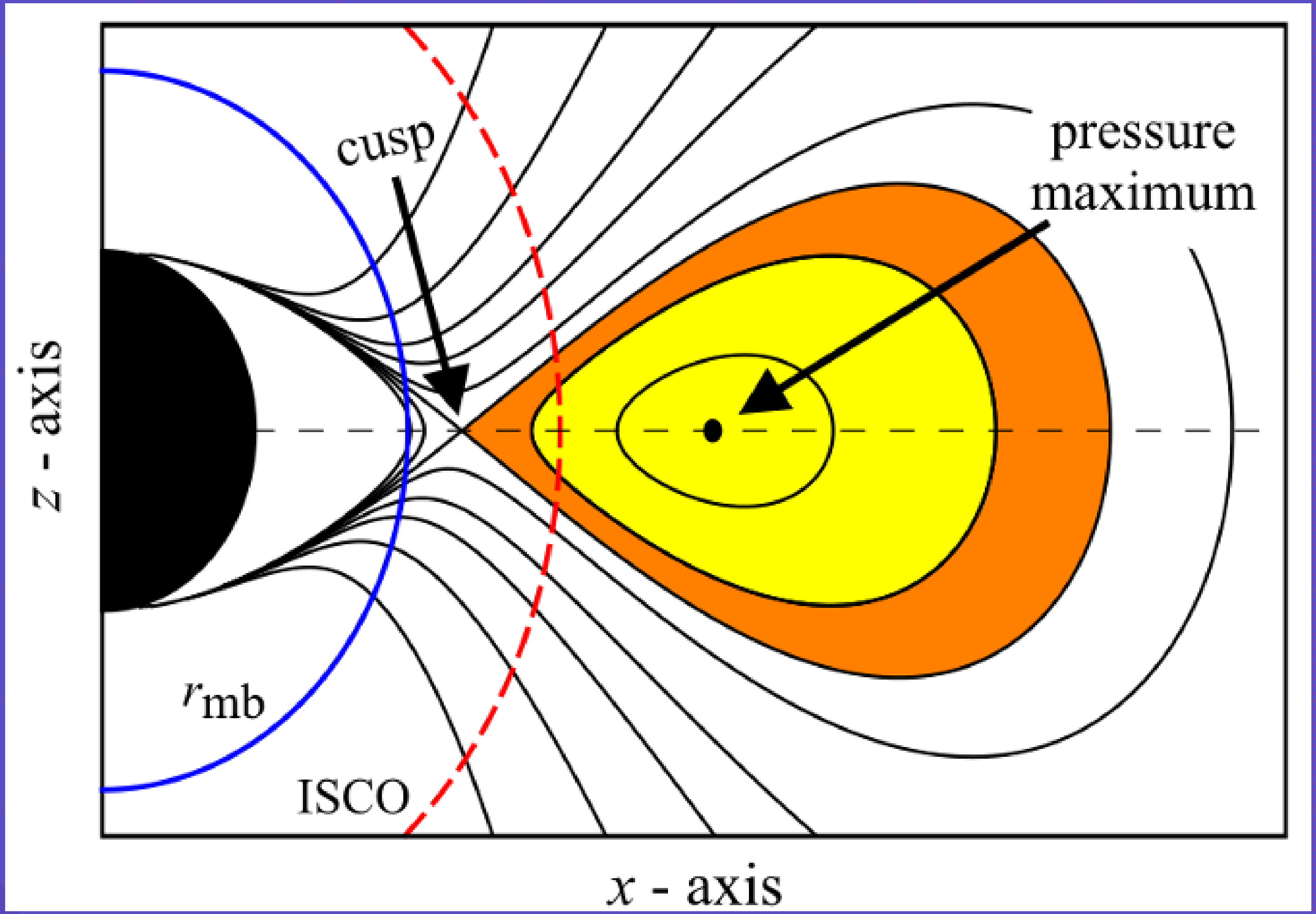

Kotrlová+ 2020

Polish doughnuts

- Radiation-pressure supported thick disc
- Narrow funnels along the rotational axis – radiation escapes
- Collimated – super-Eddington luminosity
- Low efficiency – high mass-accretion rate

ADAFs, Hot flows

- Advection-dominated Accretion flow
- Narayn&Yi 1994, 1995
- Advective cooling dominates
- Extremely low efficiency
- Very low $\dot{m}$
- Very hot – close to virial temperature
- Optically thin, geometrically thick
- Non-thermal spectra (Comptonisation), power-law
- Inefficient Coulomb cooling – different proton and electron temperature

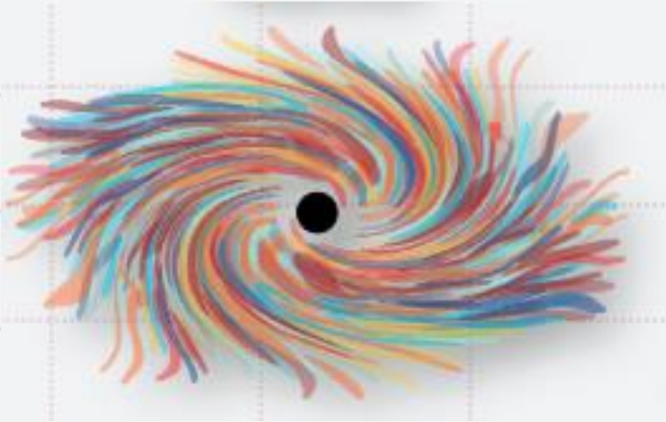

ADAF simulations

- Relatively easy – no need of radiation
- Komissarov 1999, Gammie, McKinney&Tóth 2003, Liska 2018
- 2T is better – Ressler 2015, Sądowski 2017, Ryan 2017, Chael 2018
- High magnetisation – ideal MHD may broke
- Force-free formalism (Chael+ 2024), PIC ?

Going MAD

- Magnetically Arrested Disc
- Narayan, Igumenshchev & Abramowicz 2003 ->
- BH "wants" matter, doesn't "want" the MF – do all discs go MAD eventually?
- Reconnection – energy eruptions?
- MAD supports jet formation and BZ mechanism – jets with total $\eta > 1$
- MAD limit:

$$\phi_{\rm BH} = \frac{\Phi_B}{\sqrt{\dot{M} c r_g^2}} \gtrsim 50$$

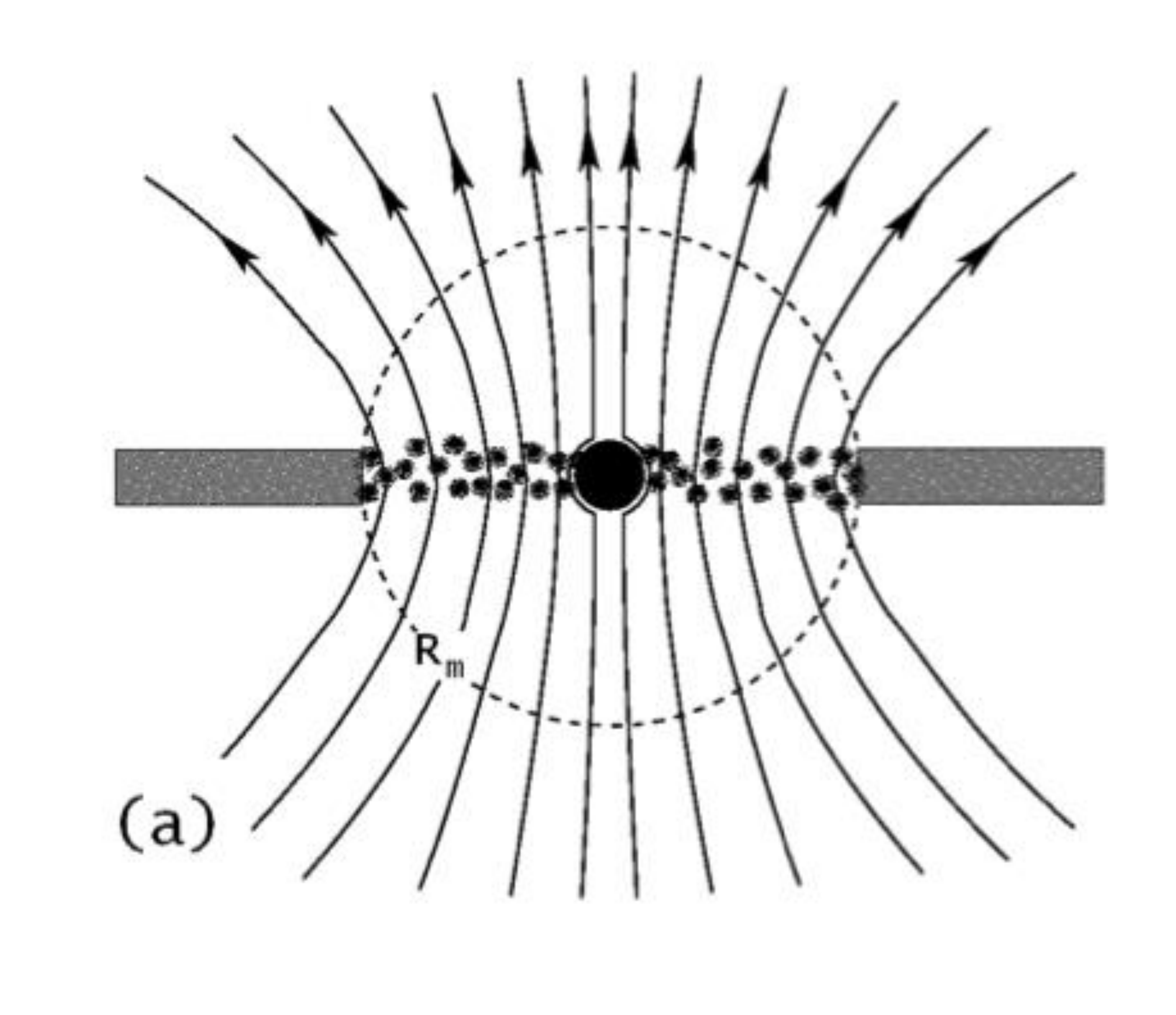

MAD simulations

- Tchekhovskoy+ 2011
- Tchekhovskoy&McKinney 2012 ->
- Liska+ 2020
- Curd&Narayan 2023
- PIC – Vos+ 2024
- Large variability of $\dot{m}$

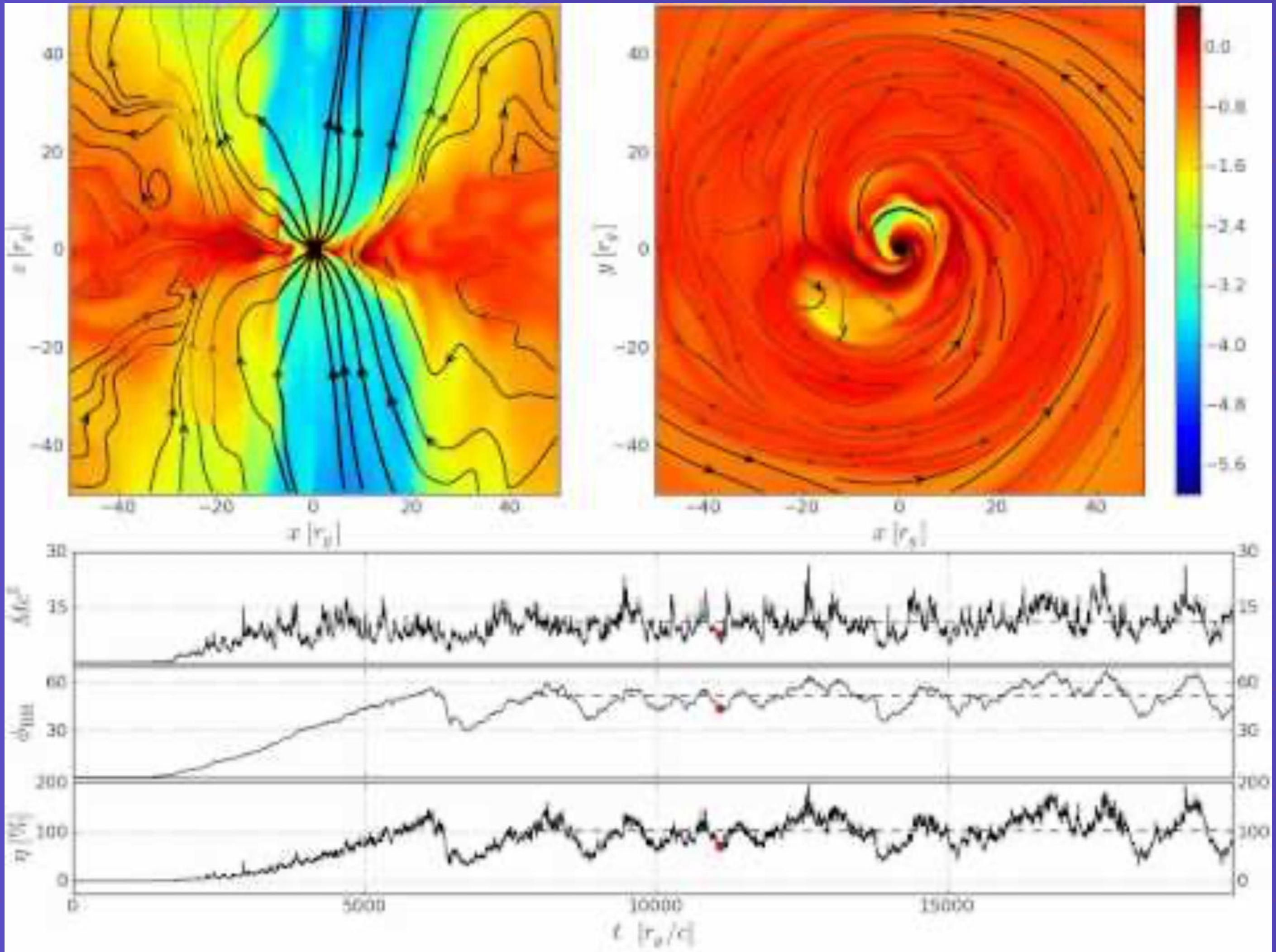

Staying SANE?

- Standard And Normal Evolution (really)
- Poloidal magnetic flux below the MAD limit
- Still highly magnetised
- Weak jets, low efficiency
- Low variability
- Narayan+ 2012, McKinney+ 2012, White+ 2020

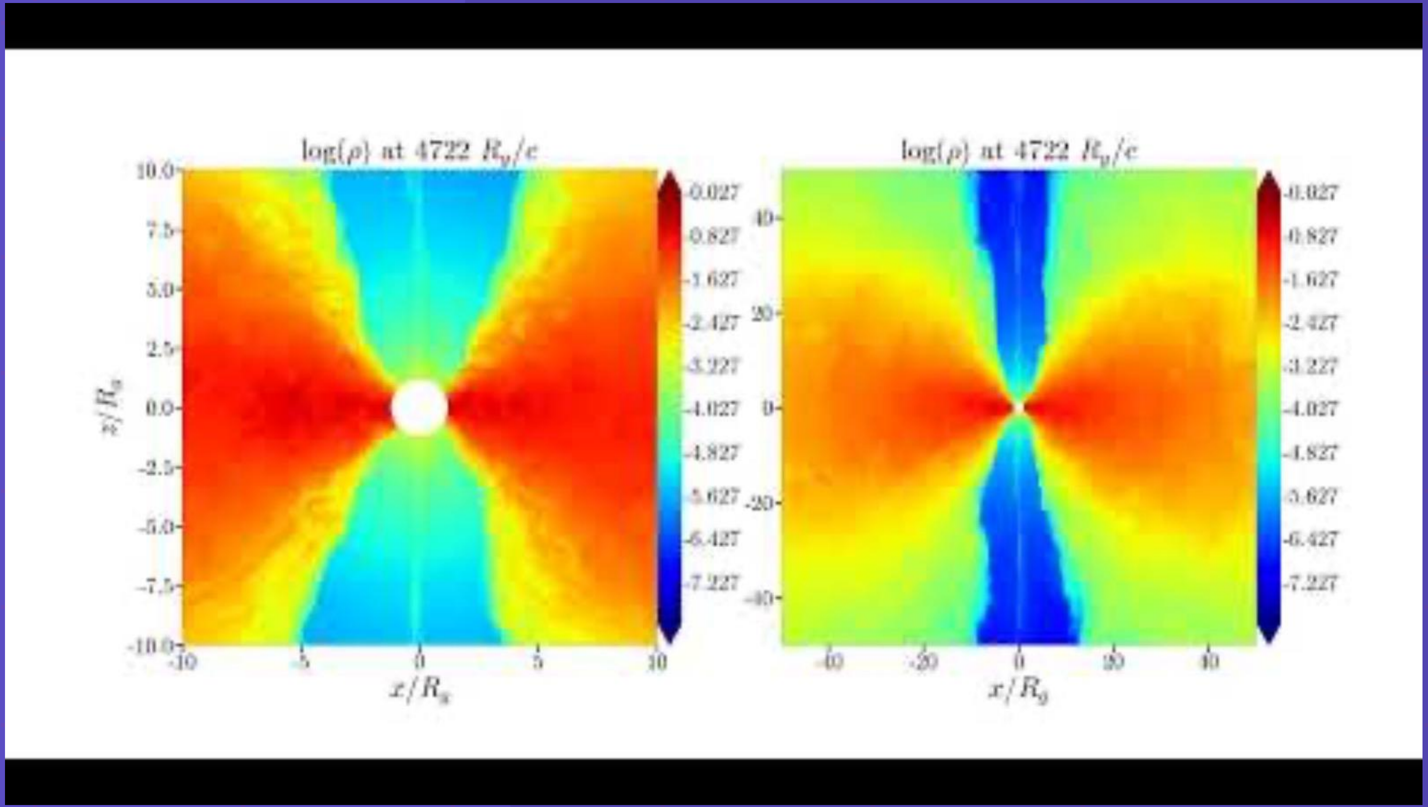

Porth+ 2019 (H-AMR code)

RELATIVISTIC JETS

GRMHD simulations of accretion disks

WHY STUDY JETS

Very luminous systems

Highly collimated, very fast outflow

AGN jets, microquasars, GRBs

Extreme collimation - even on kpc scale, extremely stable

Mirabel 2003 (rewiev), Tchekhovskoy 2011

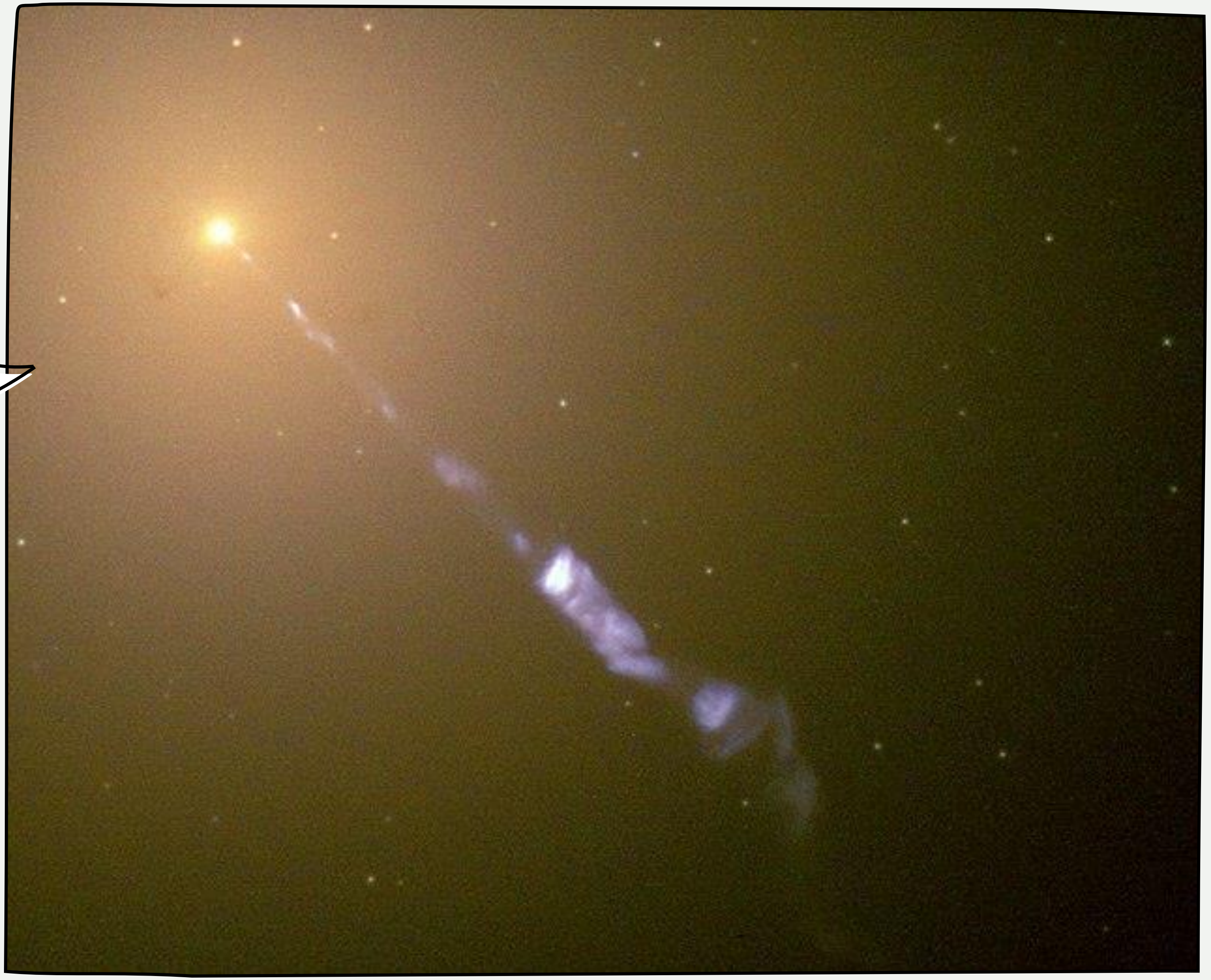

LARGE AND SMALL SCALES

Quasars

Quasi-stellar (radio) source

High redshift, fast variability, extreme luminosity -> SMBH scale

We know over 200 000 now

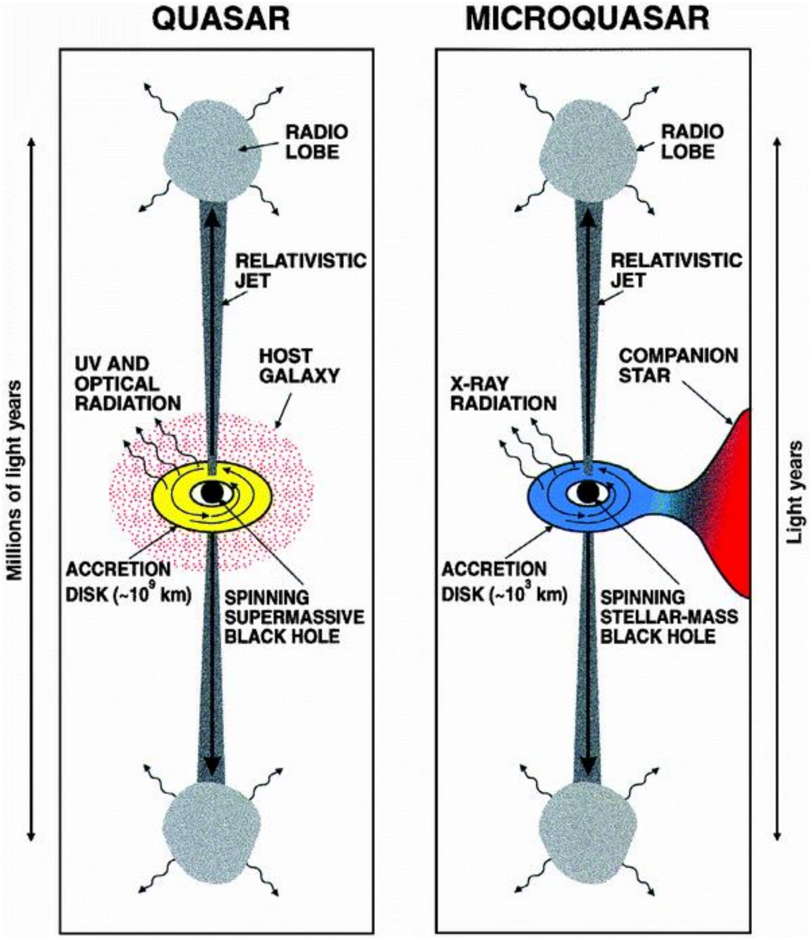

Mirabel+ 1998

Microquasars

Stellar-mass BH

Outbursts - AGN may have them to (changing-look AGN)

Strong radio jets

Mirabel+1992

LARGE AND SMALL SCALES

Quasars

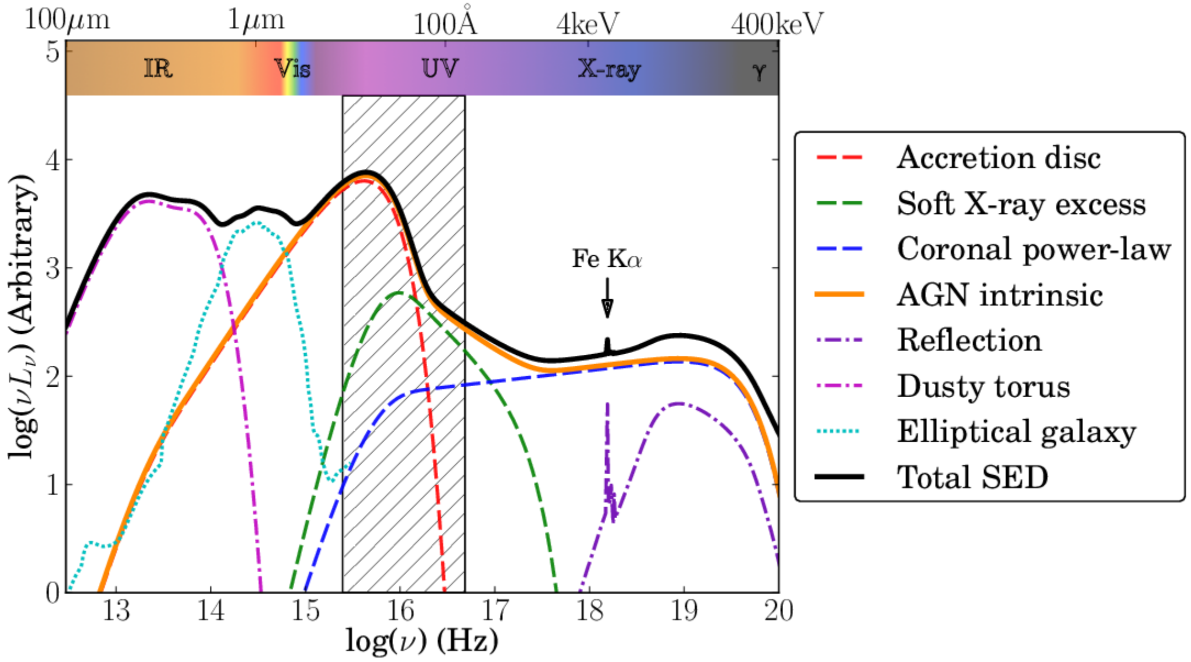

Collison+ 2016

Microquasars

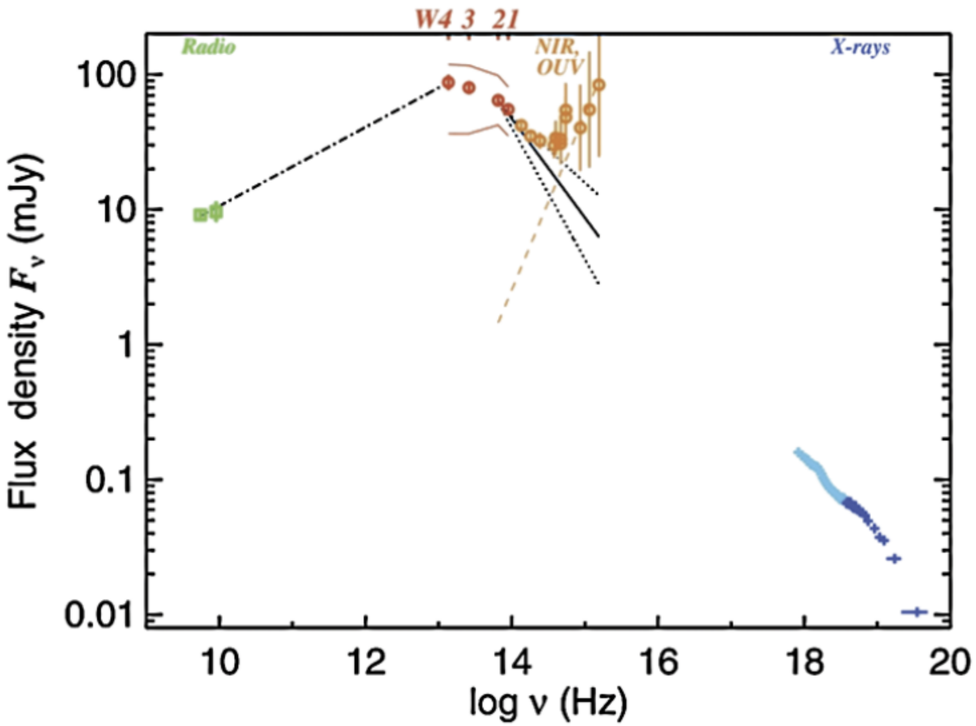

Ghadi+ 2011

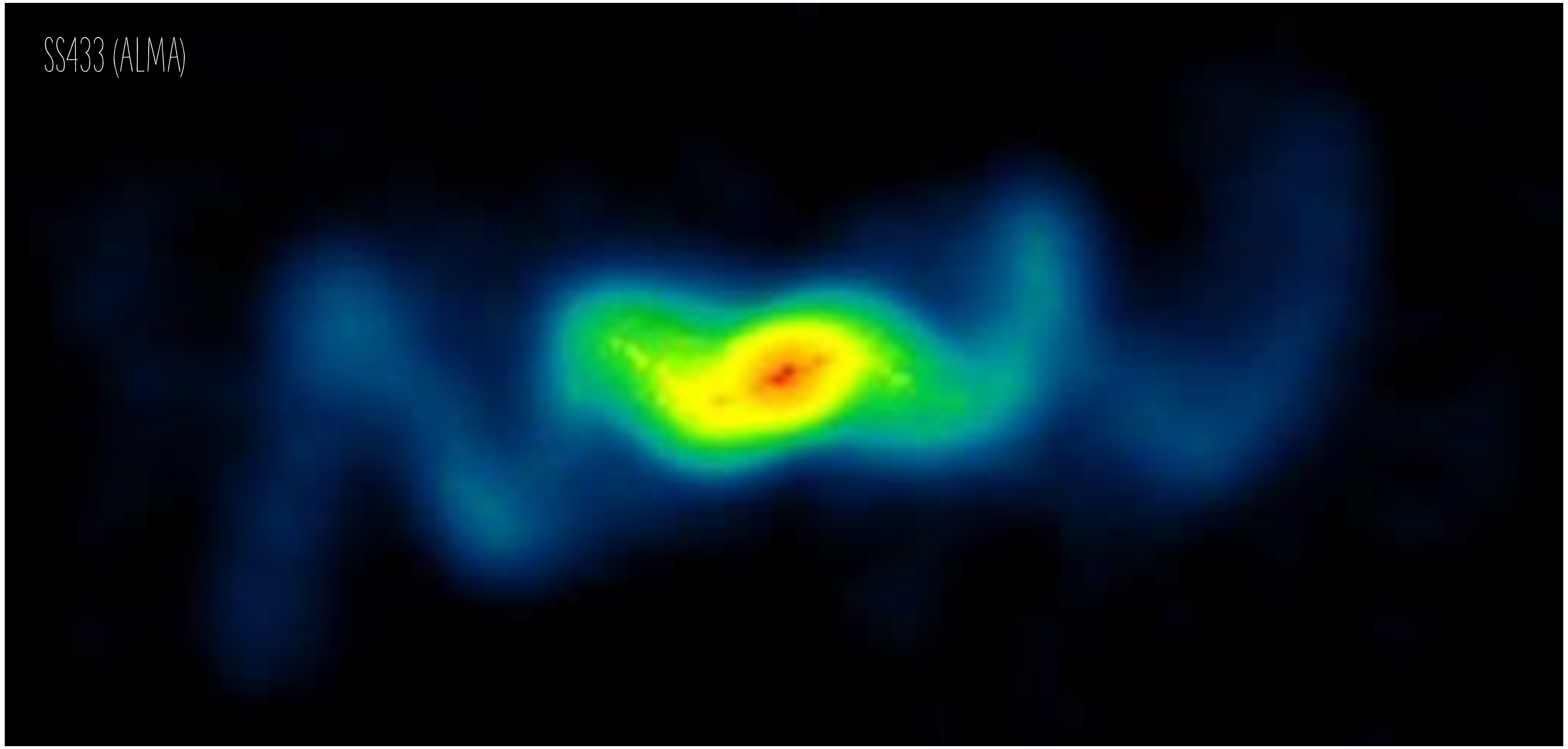
SS433 (ALMA)

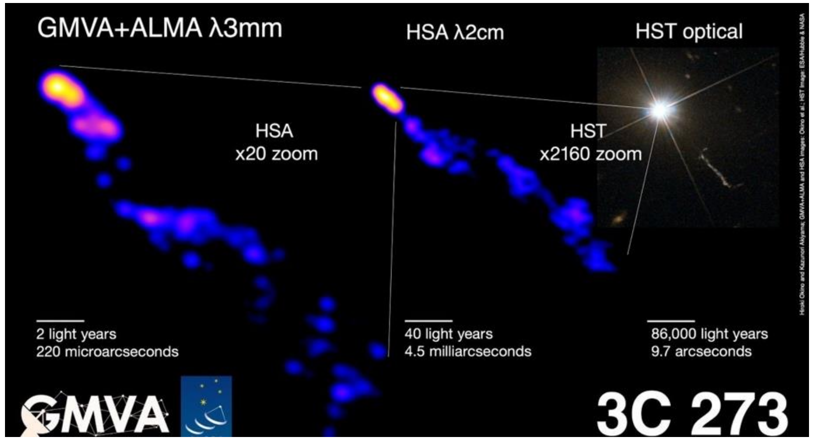
GMVA+ALMA λ3mm
HSA λ2cm
HST optical
HSA
x20 zoom
HST
x2160 zoom
2 light years
220 microarcseconds
40 light years
4.5 milliarcseconds
86,000 light years
9.7 arcseconds
GMVA
3C 273

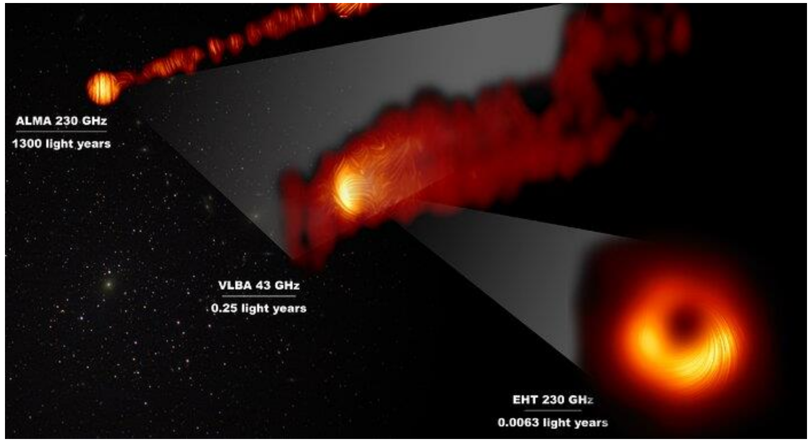
ALMA 230 GHz
1300 light years
VLBA 43 GHz
0.25 light years
EHT 230 GHz
0.0063 light years


13 bil. Years old quasar (JWST)

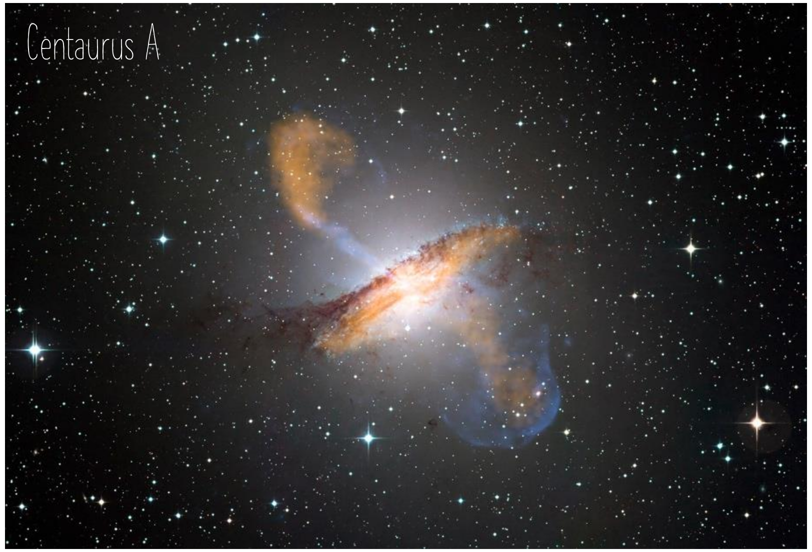
Centaurus A


PKS 1127-145 (Chandra)

ROTATING BLACK HOLE – THE KERR METRIC

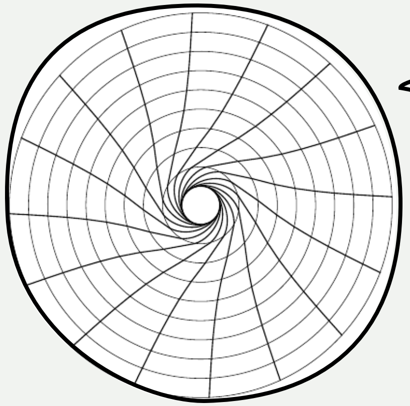

Energy can be extracted from BH, if it rotates

(Penrose–)Blandford–Znayek mechanism

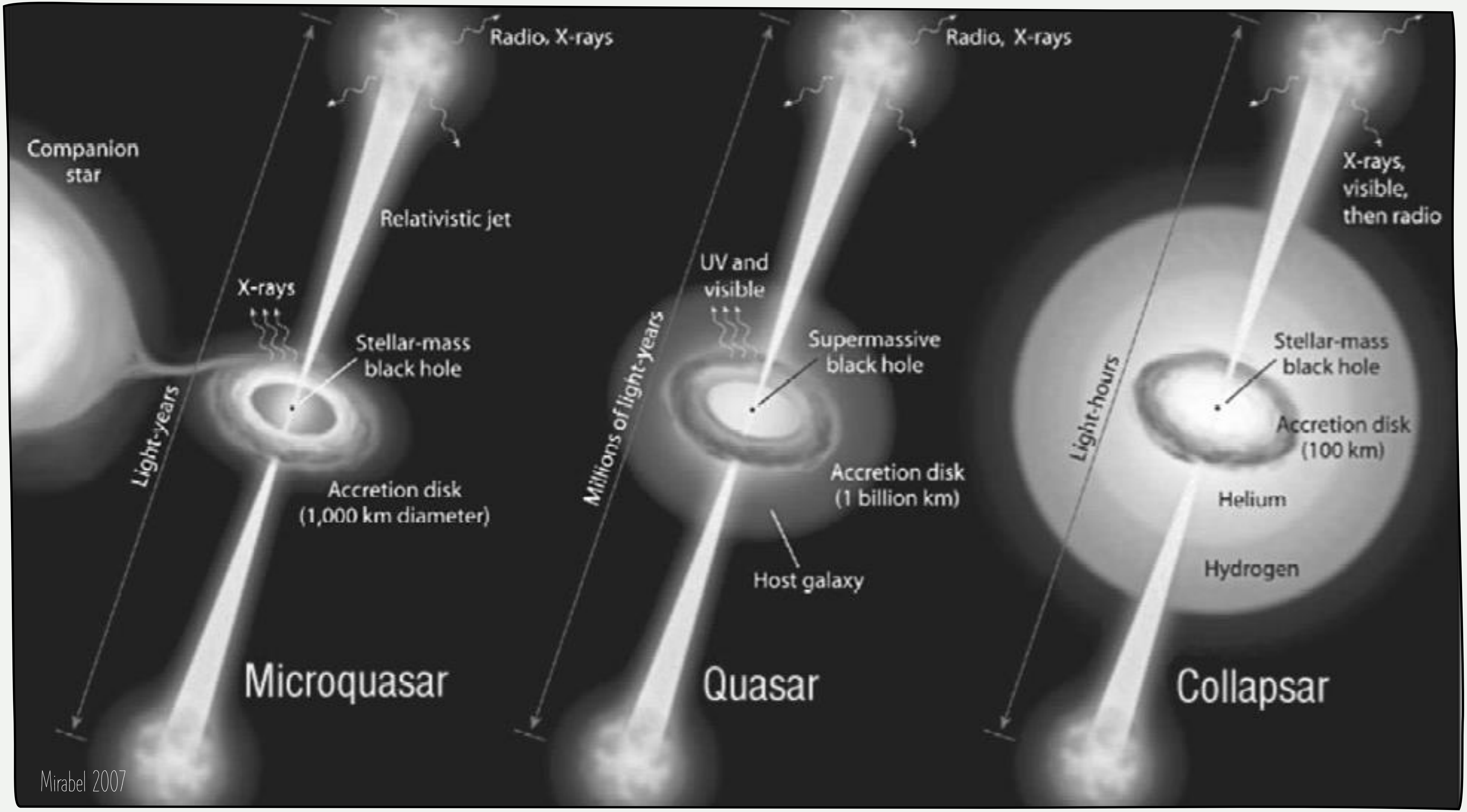

Mirabel 2007

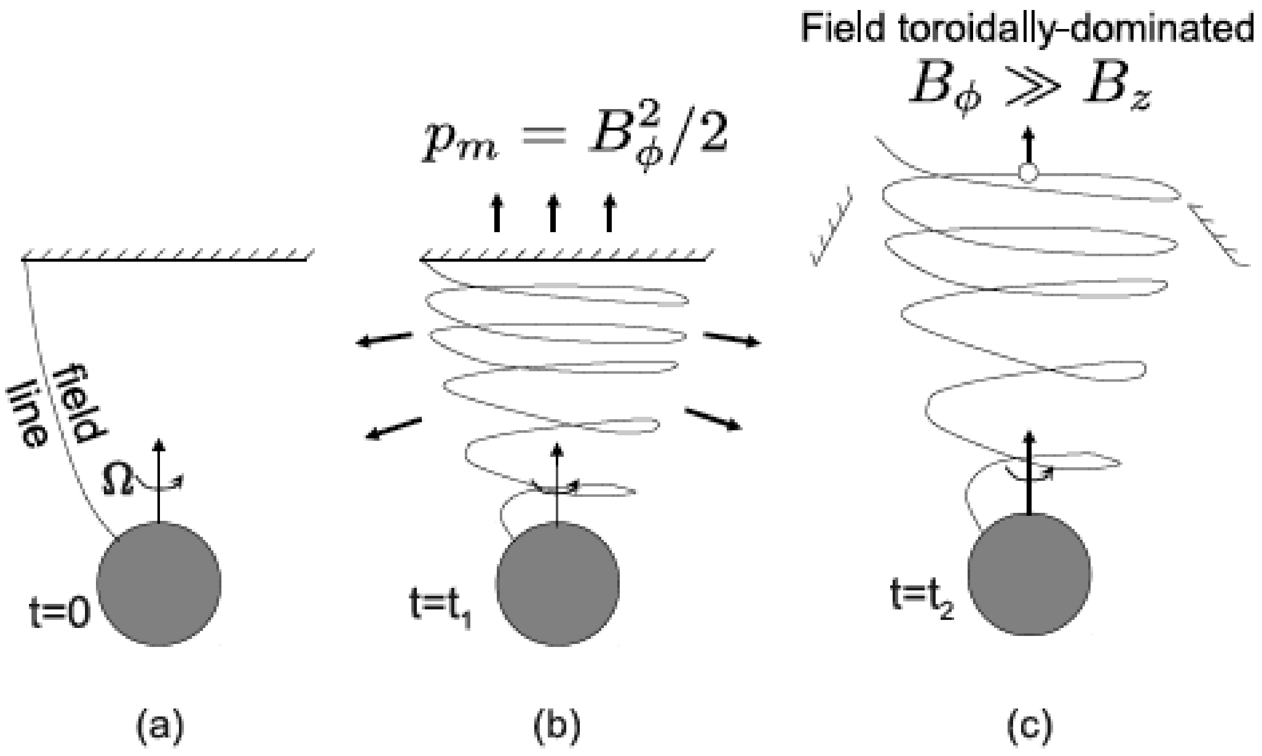

Alexander Tchekhovskoy

JET LAUNCHING

Accretion brings poloidal MF

BH doesn't eat the MF

BH rotation twists the fieldlines

Toroidal field becomes dominant

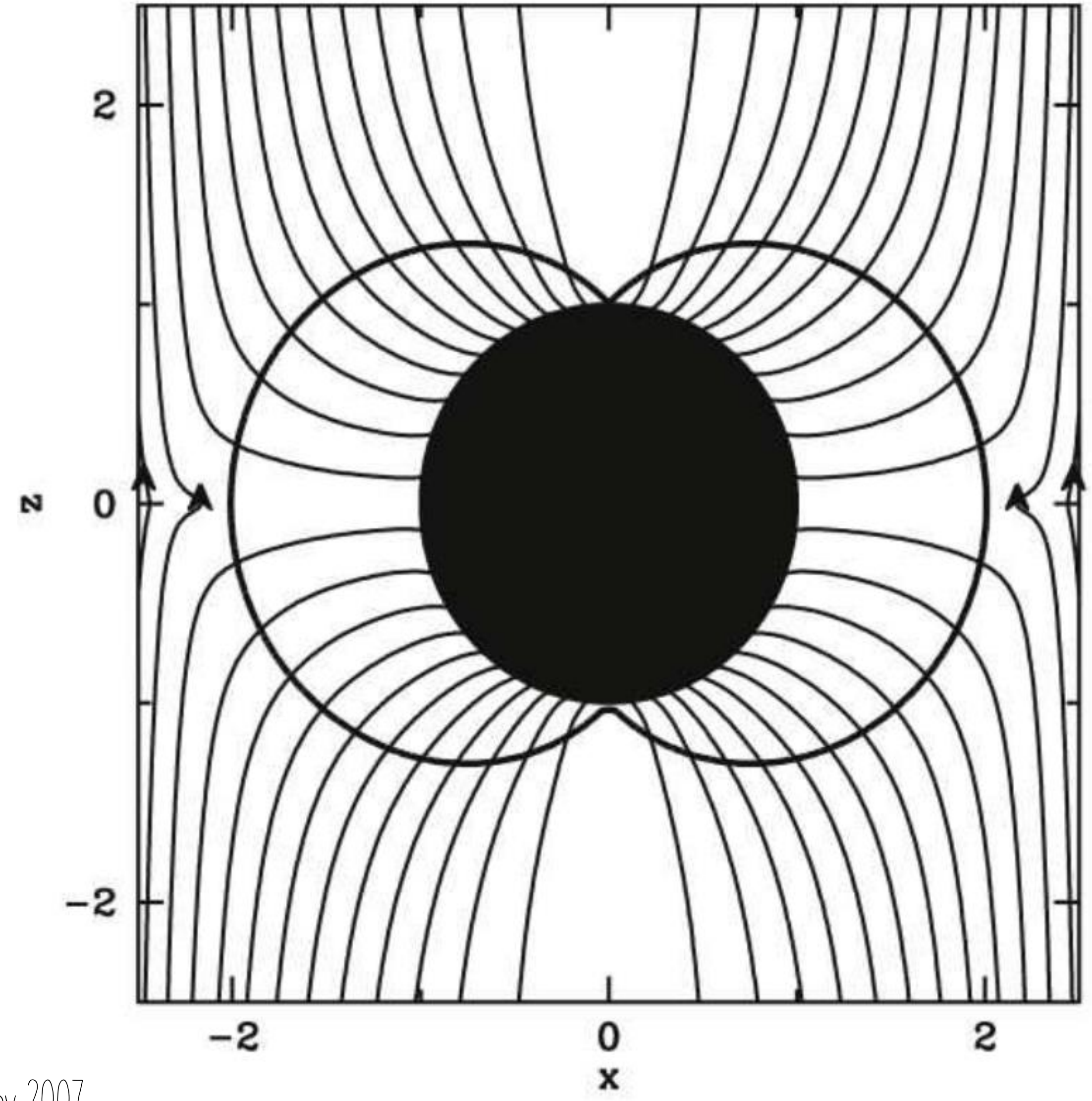

Komissarov 2007

THE BLANDFORD-ZNAYEK MECHANISM

Blandford&Znayek 1977, MNRAS

Extraction of spin energy via a torque provided by MF lines that thread the ergosphere

OTHER MECHANISMS

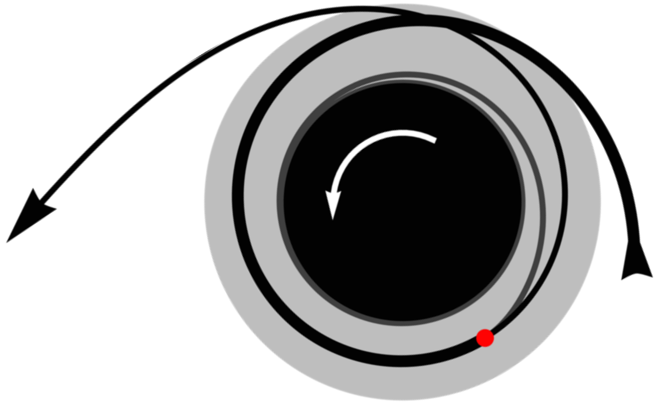

Blandford-Payne Mechanism

Disk-driven magnetic winds

Energy extracted from the disk

Mildly relativistic disk winds or outflows

More important for jet launching

Penrose process

Splitting of particles inside ergosphere - allows one part to escape and carry away BH rotational energy

Purely geometrical

Low efficiency

CONDITIONS FOR JET FORMATION

Spinning black hole

Accretion disk – preferably thick

Strong poloidal magnetic field

Tchekhovskoy 2011 – first GRMHD simulation with efficiency > 100 %

BZ power

$$P_{BZ} = \frac{\kappa \Omega_H^2 \Phi_{BH}^2 f(\Omega_H)}{4\pi c}$$

κ – constant depanding on MF topology ($\kappa = 0.052$ split monopole)

$\Omega_H = \frac{ac}{2r_H}$ – angular frequency of horizon

Φ_{BH}–magnetic flux threading BH horizon

$f(\Omega_H)$ – correction for high spin

ACCRETION DISC

In BZ, disc is "only" a source of MF

However, can they really supply enough flux?

MAD supports jets better - strong poloidal field

MF lines more organised

Can produced X-ray flares (observed)

Fits observations better

GRMHD SIMULATIONS OF JETTED SYSTEM

MAD VS SANE

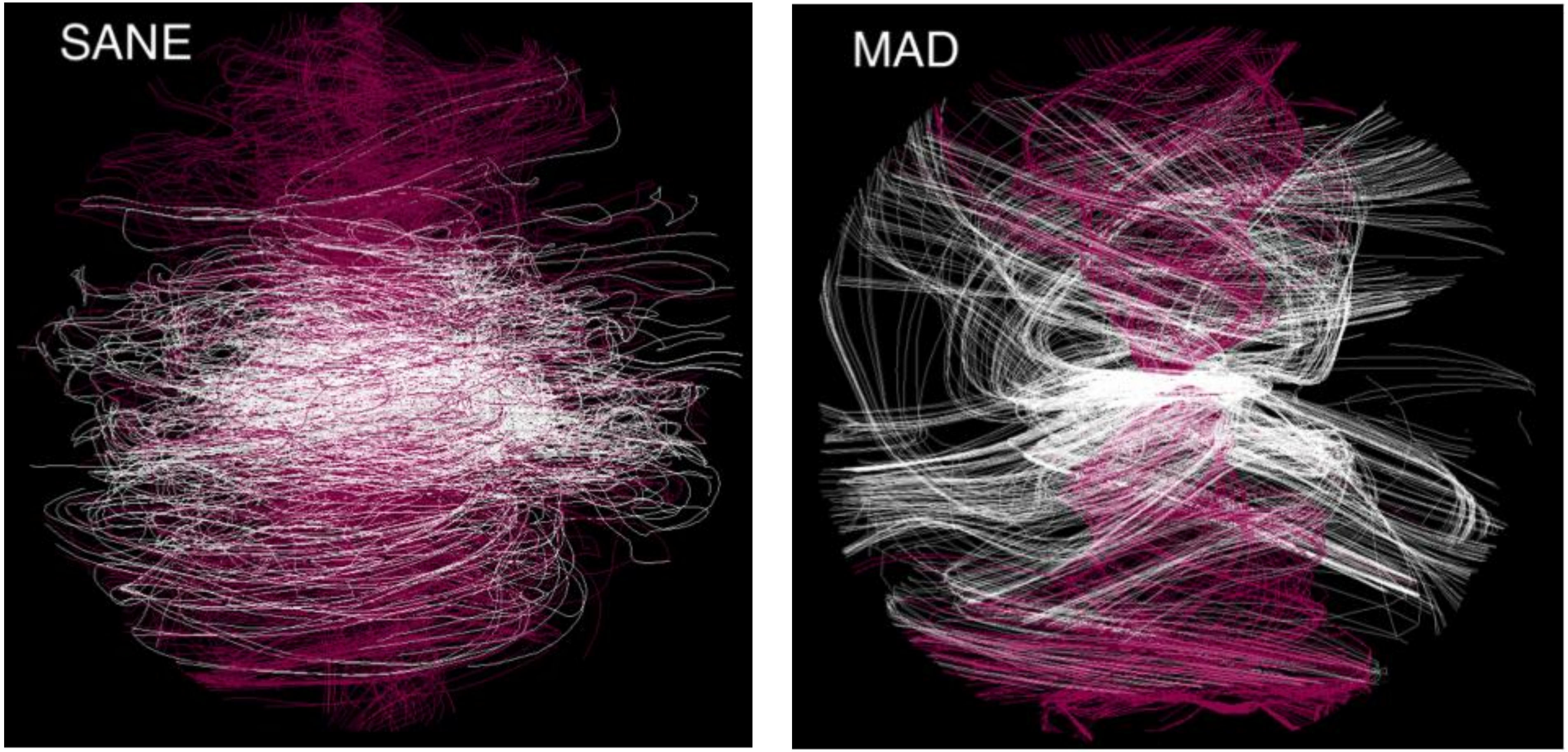

Foucart+ 2015

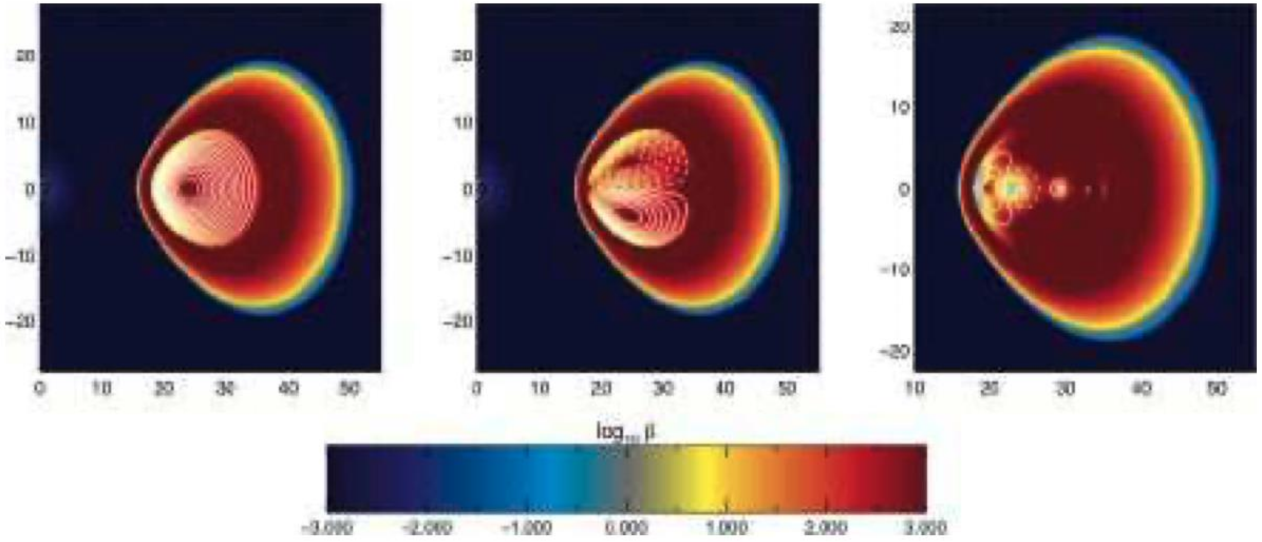

Beckwith+ 2008

INITIAL PARAMETERS

Initial MF topology doesn't matter much

Multiple loops lead to fast formation of MAD, but can recconnect

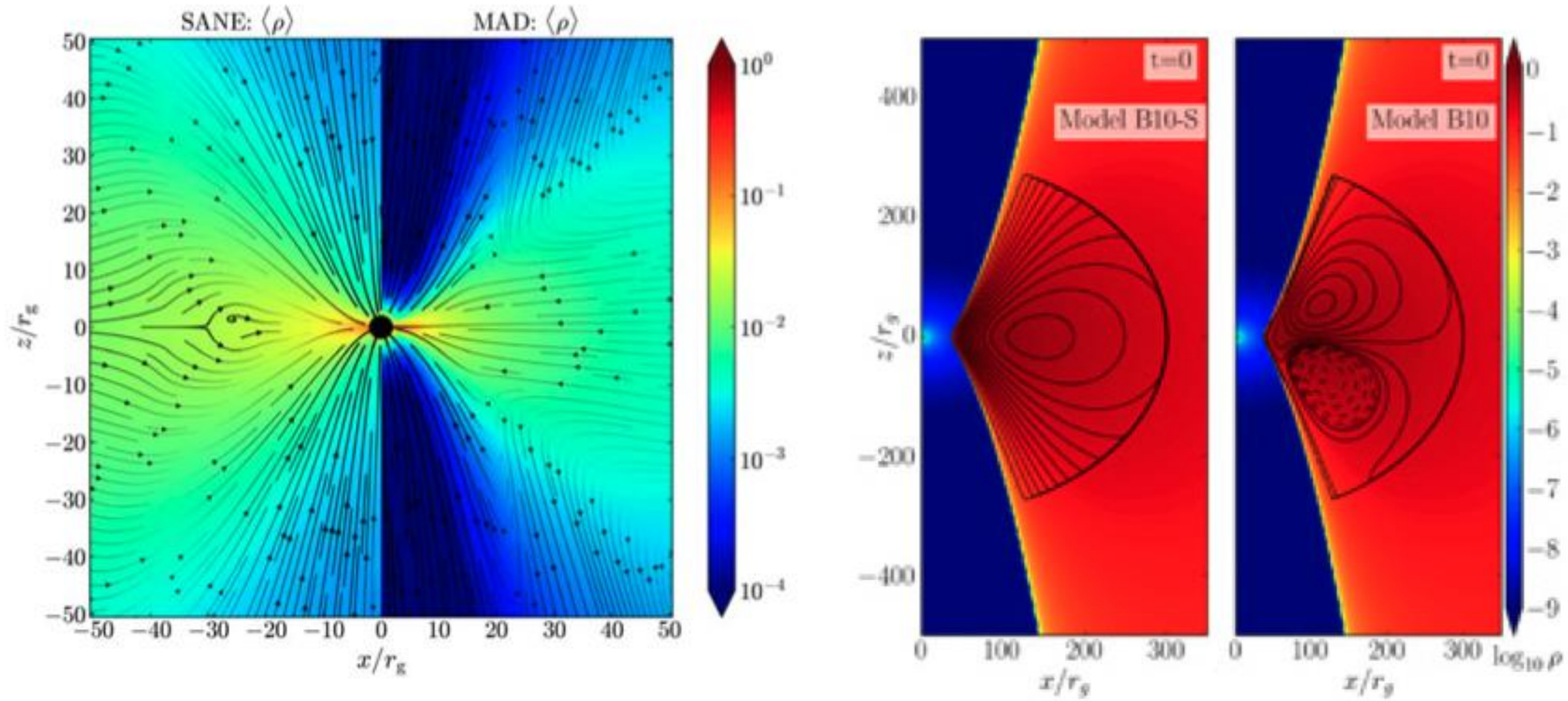

Chatterjee+ 2019

GRID & RESOLUTION CHALLENGES

Need to resolve both the disc (MRI leading to accretion of MF) and the polar regions

Ressler+ 2017 - smart coordinate system

disc + jet "patches"

Cylindrification (Tchekhovskoy+ 2011) - "stretching" of polar cells in r

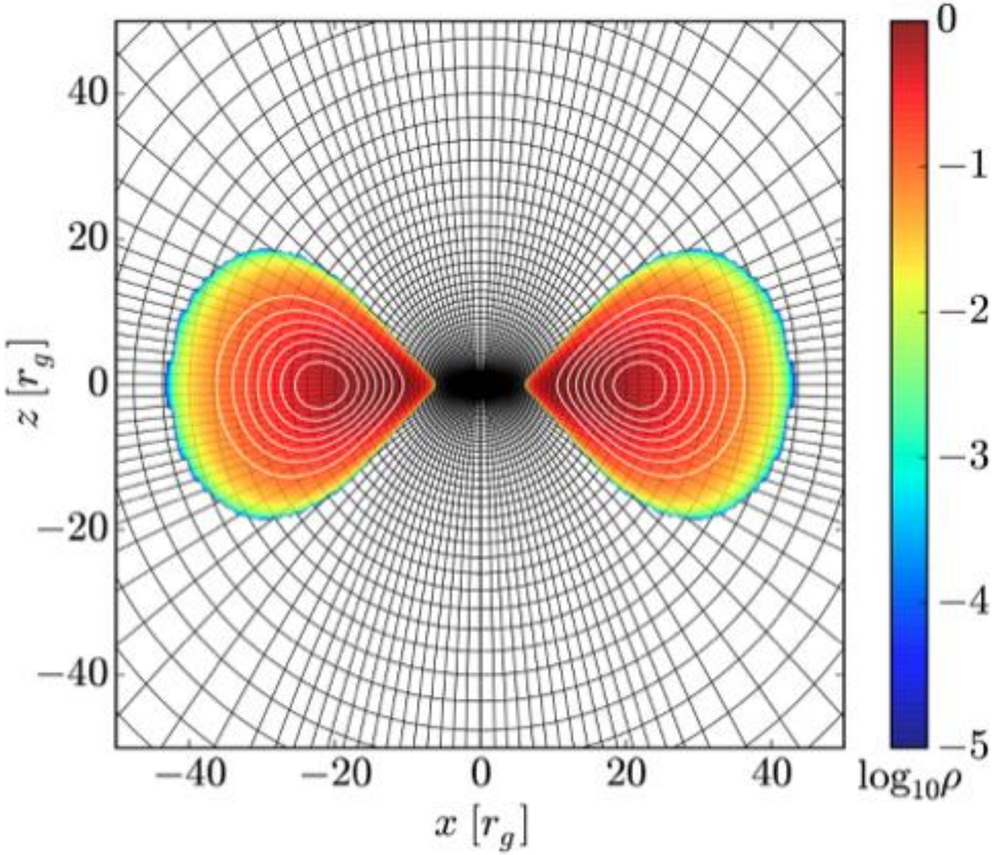

Ressler+ 2017

PROBLEM OF FLOORS

Jets are empty and magnetized - MHD may fail for $\boldsymbol{\sigma = \frac{b^2}{\rho^2} \gtrsim 100}$

Imposed floors can change the results - injection of mass into highly magnetised area

lower Lorentz factor

Hybrid approach – better understanding of jet formation and background physics and better agreement with observations

HIGH MAGNETISATION SIMULATIONS

PIC

Particle-in-cell

Extremely computationally expensive

Extreme resolution

Non-ideal MHD, reconnection, particle creation

Can cover only small area – base of jet, BH ergosphere

Parfrey+ 2019, Crinquand+ 2022, Vos+ 2024

GRFFE

GR force-free electrodynamics

Combination of GRMHD where σ is low and force-free where it is high

Much faster, covers the whole torus-jet domain

Chael+ 2024

$$\nabla_\mu T^{\mu\nu}_{\rm EM} = 0,$$

$$\nabla_\mu {}^{\star}F^{\mu\nu} = 0.$$

PIC

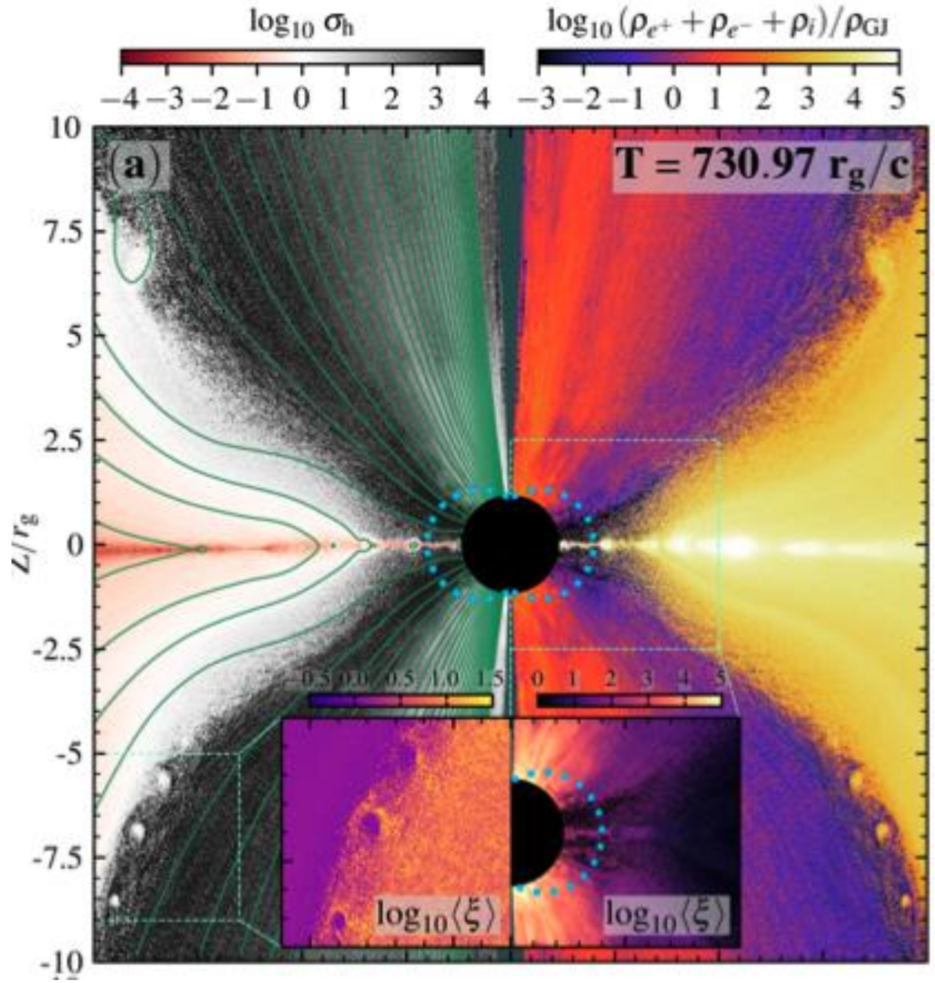

Hybrid GRMHD + GRFFE

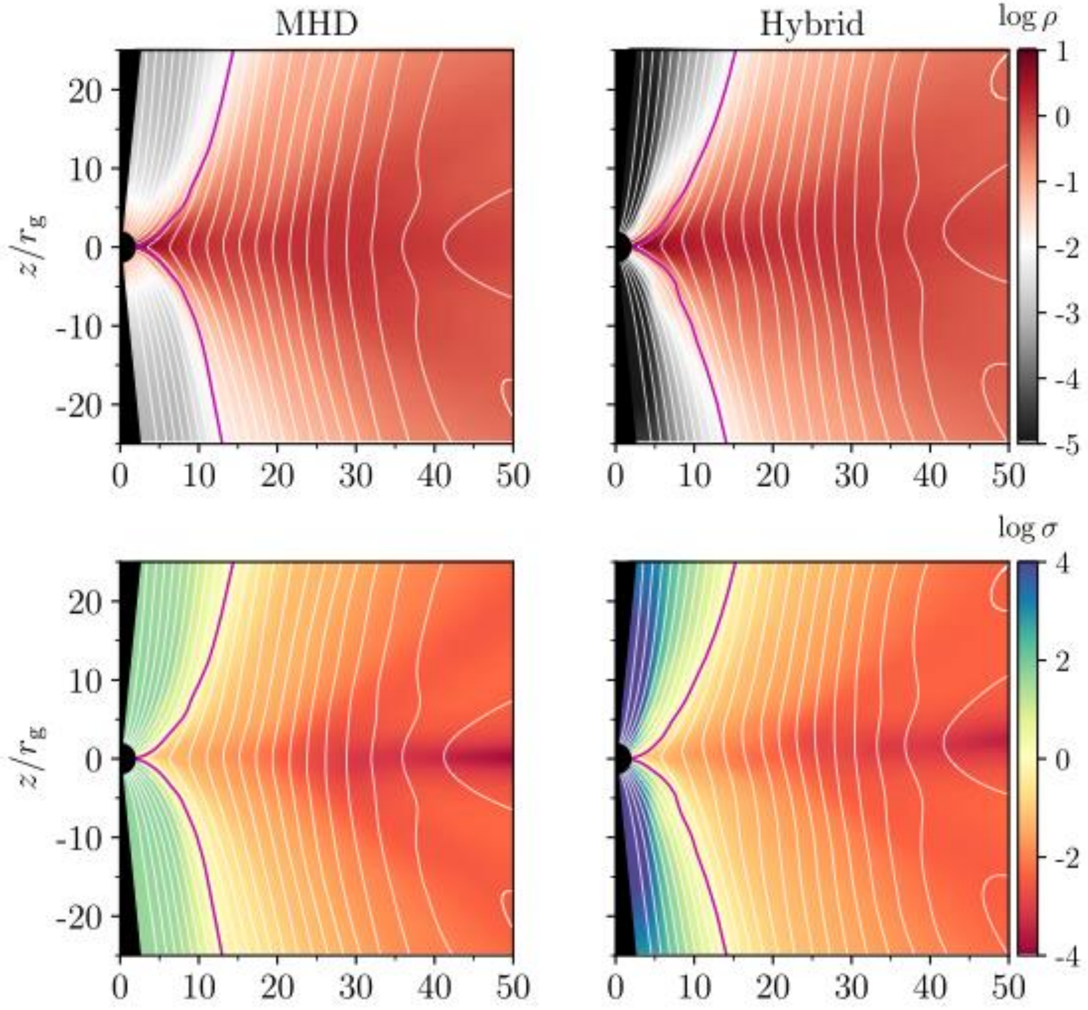

Vos+ 2024

Chael+ 2024

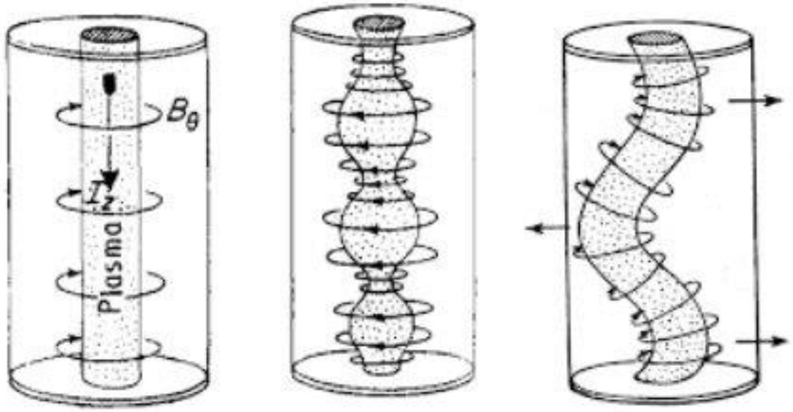

Equilibrium Sausage instability Kink instability

STABILITY & INSTABILITIES

Kink Instability – in plasma collum where poloidal field dominates

leads to jet bending and warping

Sausage instability – strangle the jet

Leads to dissipation of energy – acceleration

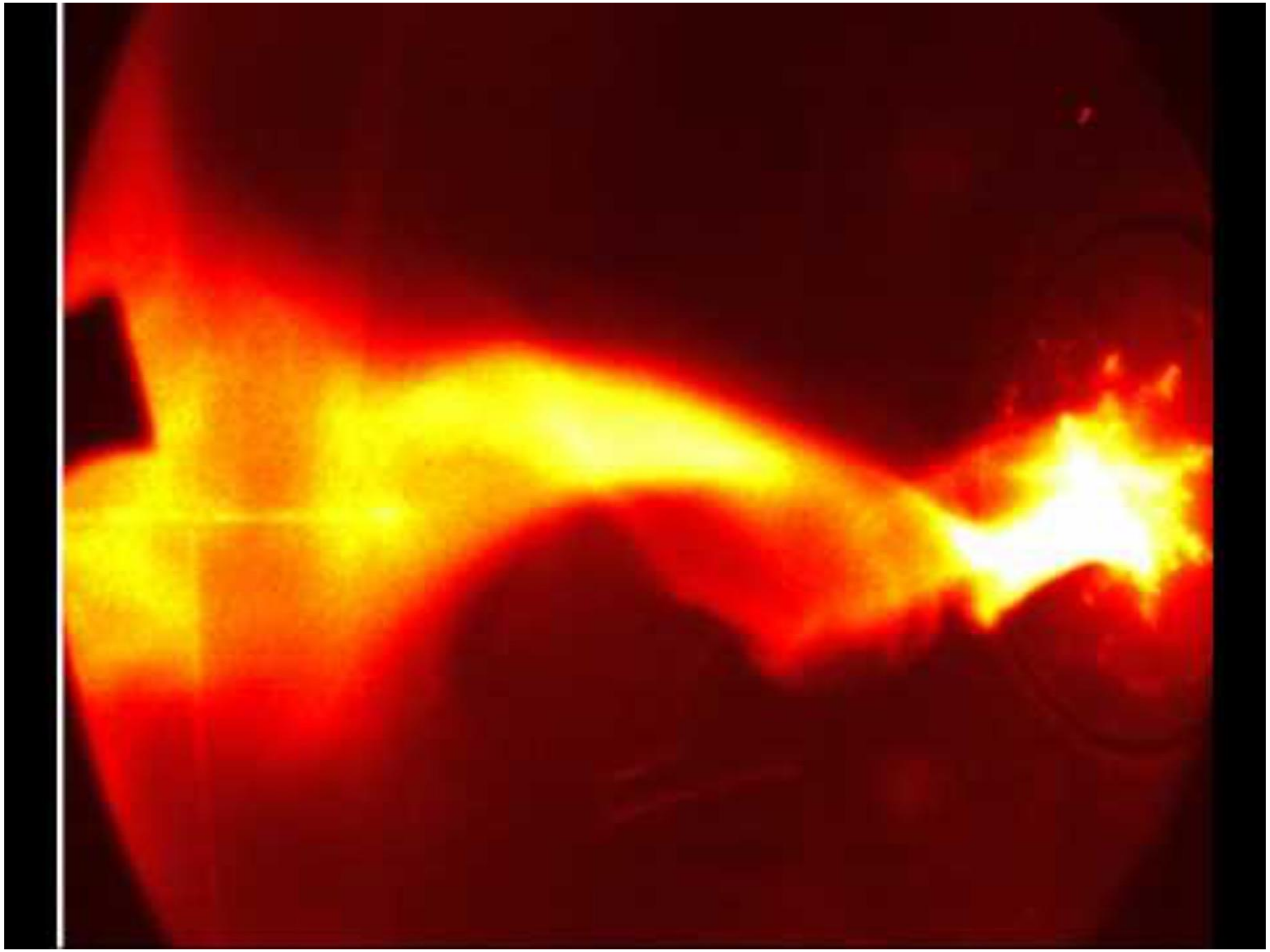

TOKAMAK

OBSERVATIONAL COMPARISONS & SYNTHETIC IMAGING

Run the simulations, and now what?

SYNTHETIC JET IMAGES - GRRT

Relativistic jets emit primarily via synchrotron and inverse Compton processes.

Radiative transfer codes account for:

- **Emission**: Synchrotron from relativistic electrons spiralling in magnetic fields.
- **Scattering**: Inverse Compton upscattering of photons by high-energy electrons.
- **Faraday Effects**: Rotation and polarisation due to magnetised plasma.

GRRT (General Relativistic Radiative Transfer) codes such as **RAPTOR, GRTRANS, BHOSS, IPOLE**

Used to compare simulated jet emission with VLBI, EHT, Chandra, and ALMA observations.

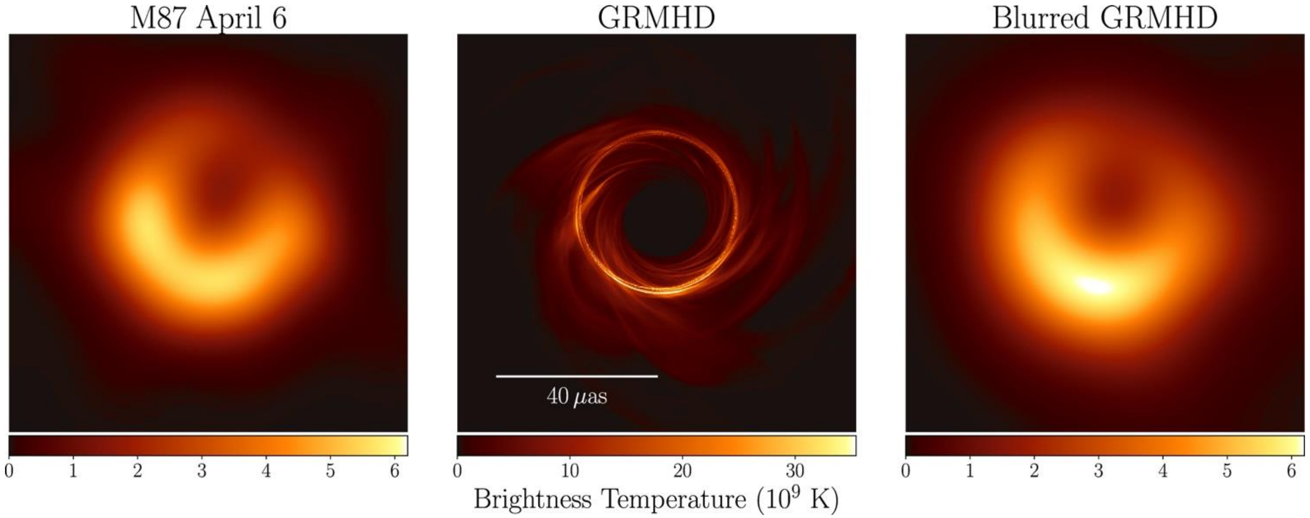

EHT Collaboration

SYNTHETIC DATA VS OBSERVATIONS

EHT M87 image - great agreement with MAD simulations

Low resolution of the image

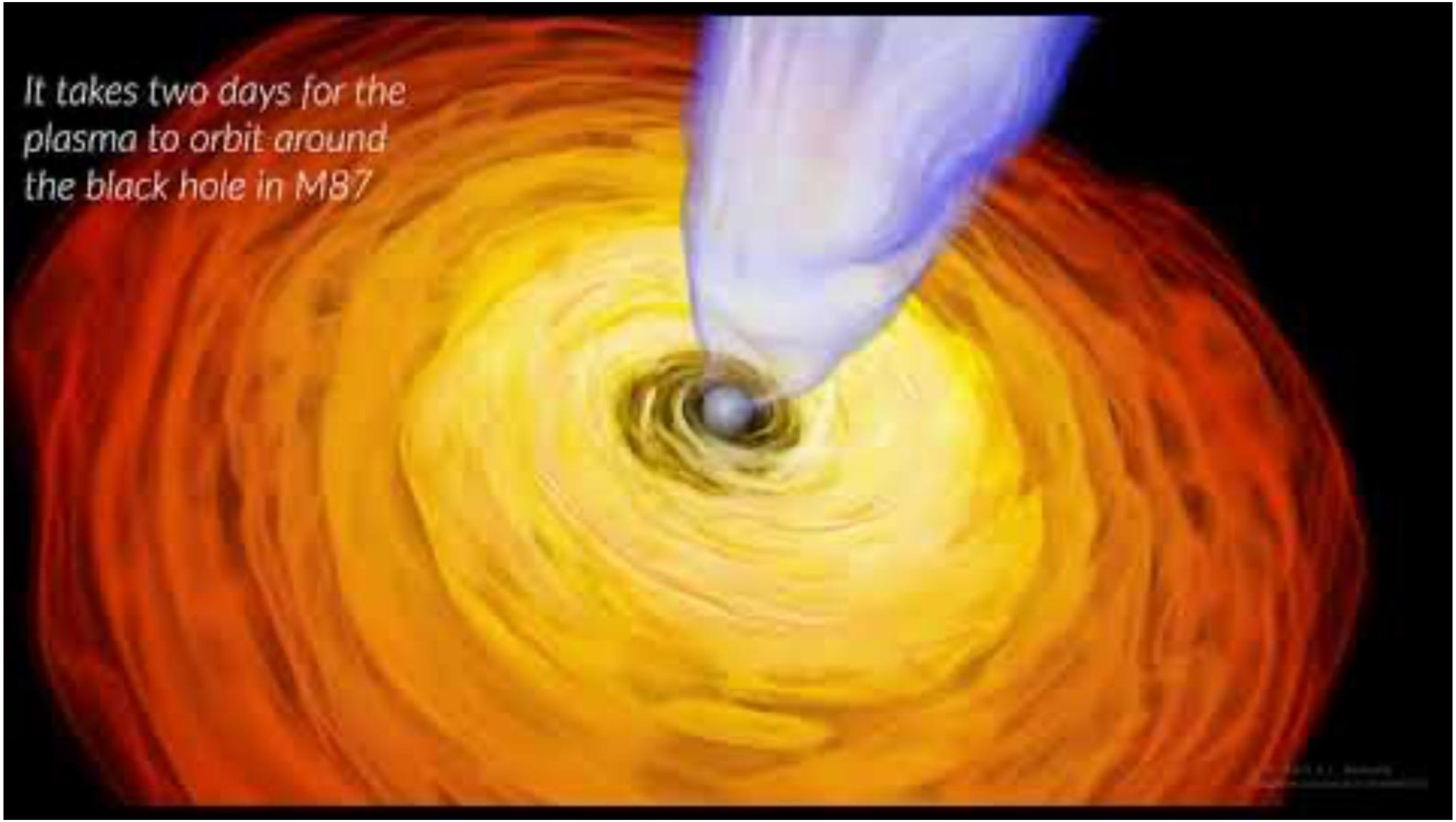

EHT Collaboration

POLARIZATION

Strong MF strongly influence the polarized image

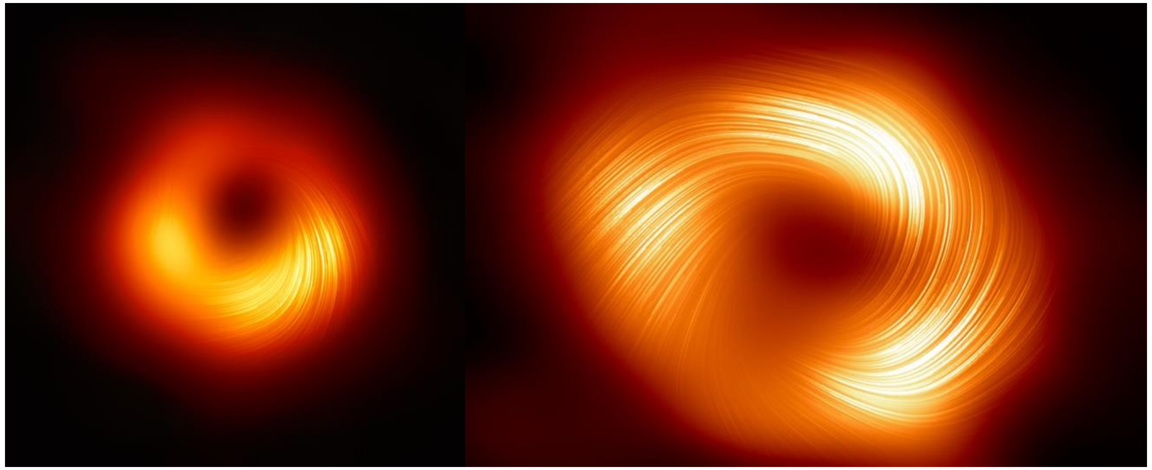

EHT Collaboration

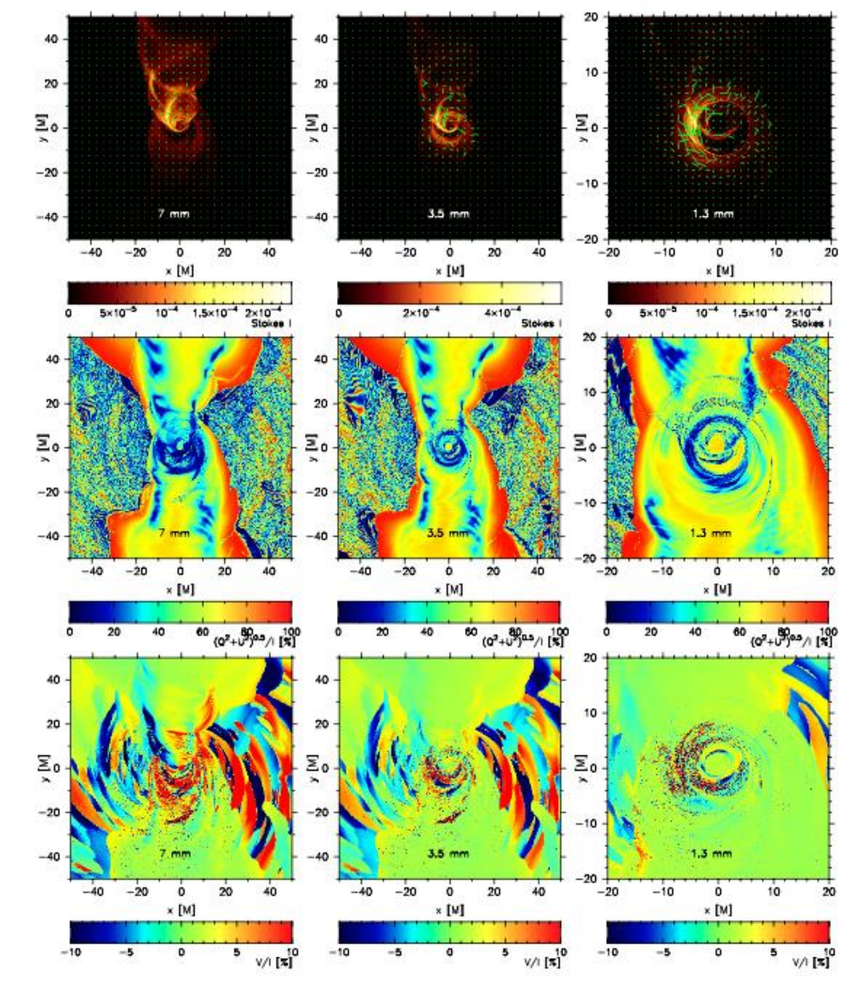

Moscibrodzka+ 2017

THE MAGIC R IN GRRMHD

GRRMHD course, CAMK

Debora Lančová

What to do with radiation

Dynamical influence – radiation pressure and cooling affect the structure and behaviour of the plasma

Usually frequency-integrated, maybe some sub-grid opacities or Comptonisation to capture energy *and* momentum exchanges

A radiation closure scheme is needed – good enough to solve both optically thin and thick regimes

Dynamical influence can be approximated using artificial cooling

Full radiative transfer is needed to model observables

Solve radiation transfer equations, follow paths of photons through plasma

Resolve energy changes to the photons

Post-processing of the time-averaged data from simulations

Full MC radiation within GRMHD – so computationally expensive it is imposible in optically thick regime

See, however bhlight by Ryan+2015

What to do with the heat

- When the radiation strongly couples with the gas, its dynamical influence has to be included
- Thin disc regime – radiation efficiently cools the disc fluid

$$Q_{visc}^{+} \sim Q_{rad}^{-}$$

- Disc – optically thick
- Funnel – optically thin
- Observable spectra emerge from $\tau \sim 1$
- We need to model both thin and thick regimes correctly!
- Correct modelling of radiation
    - Artificial cooling function
    - Evolve radiation together with gas (and magnetic field)

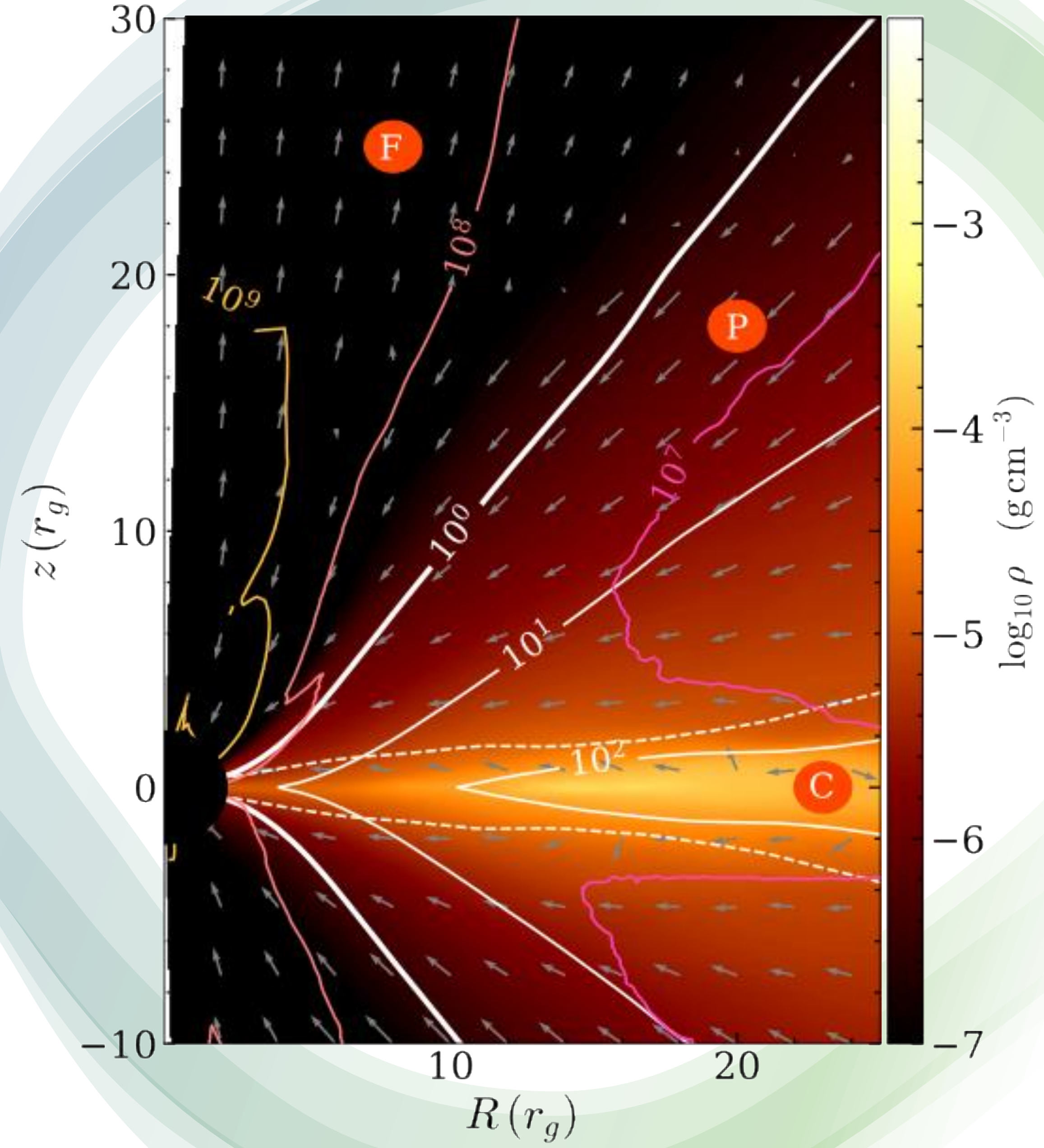

Artificial cooling in Global simulations

- Noble+ 2009 – implemented in HARM

$$\nabla_\mu T^\mu{}_\nu = -\mathcal{F}_\nu, \qquad \mathcal{F}_\nu = \mathcal{L} u_\nu$$

- Cooling towards target disk temperature and thickness

$$T_* = \frac{\pi}{2}\left[\frac{H}{r} r \Omega(r)\right]^2 .$$

- Needs to coll fast enough where $T > T_*$

$$\mathcal{L} = s\Omega\rho\epsilon\left[\frac{(\Gamma-1)\epsilon}{T_*} - 1 + \left|\frac{(\Gamma-1)\epsilon}{T_*} - 1\right|\right]^q .$$

β-cooling

- Gammie 2001

$$Q^- = -\frac{P}{t_{\rm cool}}, \quad t_{\rm cool} = \beta\Omega^{-1}$$

$$\frac{du}{dt} = -\frac{u}{\beta\Omega^{-1}}$$

- t_{cool} cooling timescale
- β usually constant
- Variation with β function of local disc properties or another heating/cooling mechanism (irradiation of the disc, heating via other than viscous heating,…) (e. g. Johnson&Gammie 2003, Vorobyov+ 2020)

Or, solve the interplay between gas and radiation directly in each cell

GRRMHD

GENERAL RELATIVISTIC RADIATIVE MAGNETOHYDRODYNAMIC

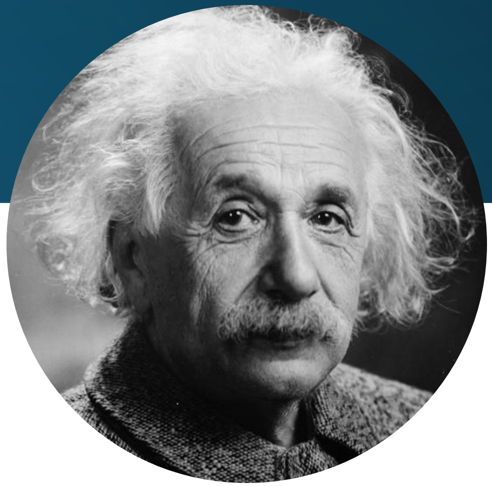

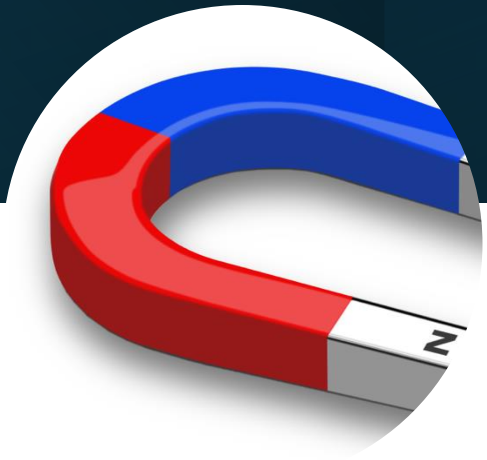

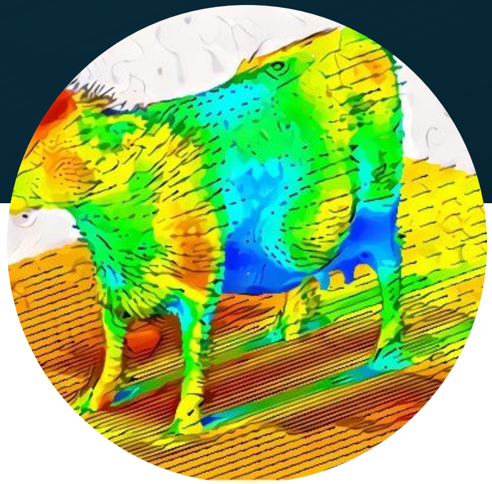

KORAL

- Sądowski+ 2013a,b, 2015, 2017, Chael+ 2019, 2024
- Global 3D two-temperature GRRMHD code with force-free solver in highly magnetized regimes
- Godunov finite-difference code with semi-implicit radiation-gas coupling solver
- Using M1 radiation closure
- Arbitrary metric (analytical and numerical)
- Logarithmic grid
- 2D dynamo – imitates 3D magnetic field – enables longer simulations with MRI
- MPI paralised

- https://github.com/achael/koral_lite

Radiation as a "fluid"

$$\begin{aligned}(\rho u^\mu)_{;\mu} &= 0,\\ \cancel{(T^\mu_\nu)_{;\mu}} &\cancel{= 0,}\end{aligned}$$

MHD stress-energy tensor

$$T^\mu_\nu = (\rho + u + p + b^2)u^\mu u_\nu + (p + \frac{1}{2}b^2)\delta^\mu_\nu - b^\mu b_\nu.$$

RADIATION

$$(T^\mu_\nu + R^\mu_\nu)_{;\mu} = 0.$$

$$\begin{aligned}(T^\mu_\nu)_{;\mu} &= G_\nu,\\ (R^\mu_\nu)_{;\mu} &= -G_\nu,\end{aligned}$$

RADIATION
4-FORCE
DENSITY

$$\widehat{G} = \begin{bmatrix} \kappa(\widehat{E} - 4\pi\widehat{B}) \\ \chi\widehat{F^i} \end{bmatrix}.$$

In the fluid-frame

Sądowski+ 2013a,b, Mihalas+Mihalas 1984

Radiation tensor

- Consists of moments of frequency-integrated specific intensity $I = \int_\nu I_\nu \mathrm{d}\nu$
  - Energy density $\widehat{E} = \int \widehat{I}_\nu \mathrm{d}\nu \mathrm{d}\Omega,$
  - Radiation fluxes $\widehat{F}^i = \int \widehat{I}_\nu \mathrm{d}\nu \mathrm{d}\Omega N^i$
  - Rad. pressure tensor $\widehat{P}^{ij} = \int \widehat{I}_\nu \mathrm{d}\nu \mathrm{d}\Omega N^i N^j.$
- In arbitrary frame

$$\widehat{R} = \begin{bmatrix} \widehat{E} & \widehat{F}^i \\ \widehat{F}^j & \widehat{P}^{ij} \end{bmatrix}$$

Closure

- How to find the whole $R^{\mu\nu}$ in an arbitrary frame
- We know only energy and fluxes
- Eddington closure
  - Assuming almost isotropic radiation field
  - Works in optically thick regimes

$$\widehat{P}^{ij} = \frac{1}{3}\widehat{E}\delta^{ij}.$$

M1 closure

- Radiation "rest-frame" – where it is isotropic and metric locally Minkowski

$$\tilde{R}^{\mu\nu} = \begin{pmatrix} \tilde{E} & \tilde{E}/3 \\ \tilde{E}/3 & 0 \end{pmatrix} = \frac{4}{3}\tilde{E}\tilde{u}_R^{\mu}\tilde{u}_R^{\nu} + \frac{1}{3}\tilde{E}\eta^{\mu\nu},$$

- Is covariant. Thus, we can find (with u_R^{μ} - rad. frame 4velocity)

$$R^{\mu\nu} = \frac{4}{3}\tilde{E}u_R^{\mu}u_R^{\nu} + \frac{1}{3}\tilde{E}g^{\mu\nu}.$$

Sądowski+ 2013a,b, Levermore 1984

M1

$$\widehat{P}^{ij}_{\tau \gg 1} = \begin{bmatrix} 1/3 & 0 & 0 \\ 0 & 1/3 & 0 \\ 0 & 0 & 1/3 \end{bmatrix} \widehat{E}.$$

Optically thick

$$\widehat{P}^{ij}_{\tau \ll 1} = \begin{bmatrix} 1 & 0 & 0 \\ 0 & 0 & 0 \\ 0 & 0 & 0 \end{bmatrix} \widehat{E},$$

Optically thin

- Specific intensity is always symmetric with respect to the mean flux
- Only approximative with multiple source of light

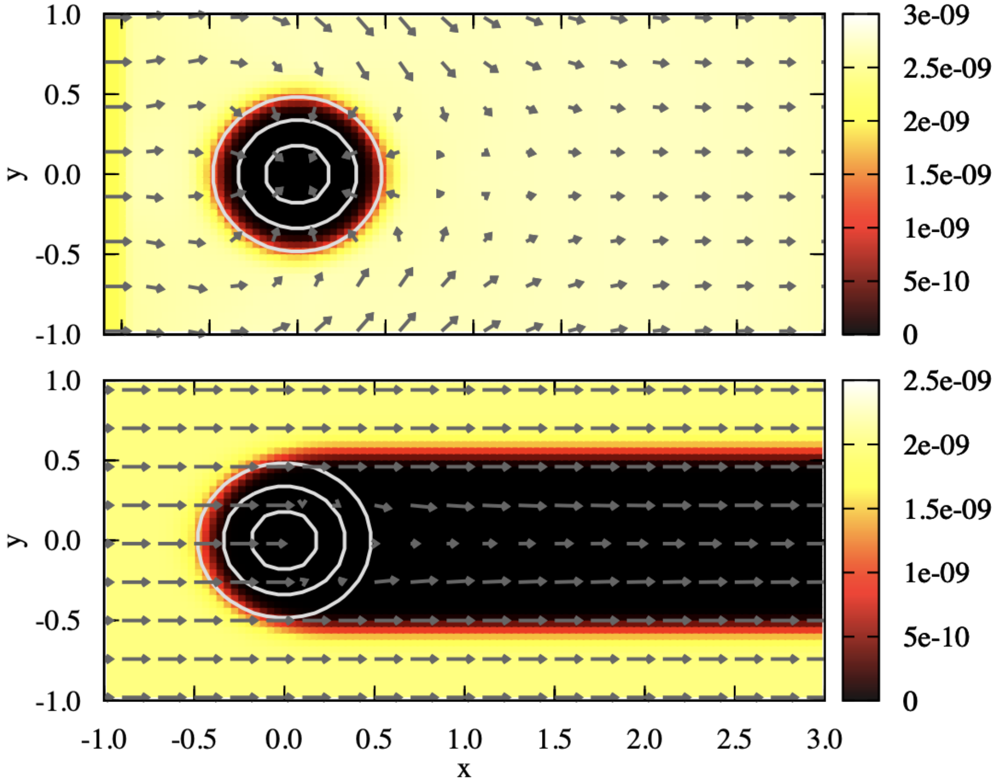

Eddington

M1

- M1 can resolve shadows, but not multiple sources of radiation
- Not a case of accretion disks simulations

Tests

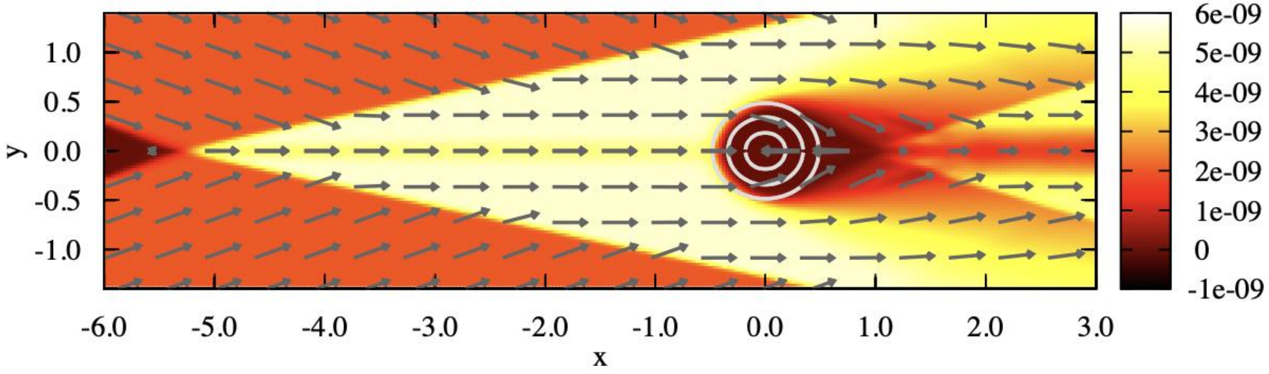

Sądowski+ 2013a

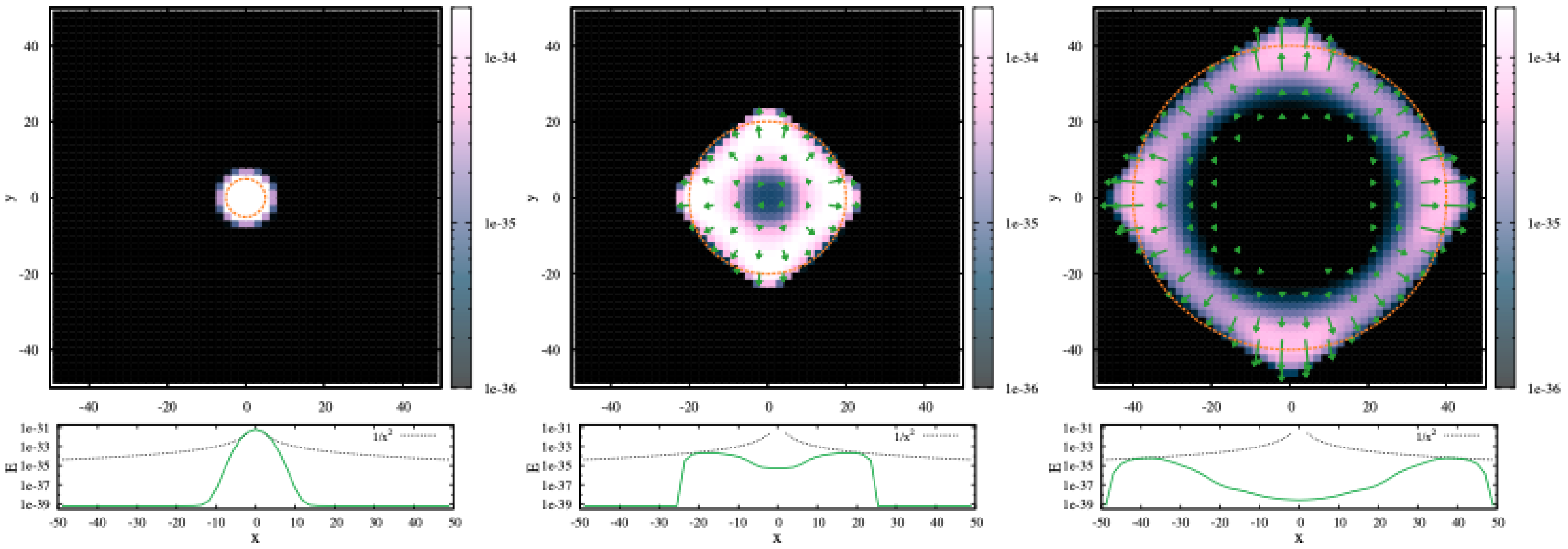

Figure 8. Profiles of the radiative energy density (E) for the optically thin radiative pulse test described in Section 4.4. The top panels show its distribution in the xy plane at (from left to right) $t = 0$, 15 and 35. The orange circle in the first plot denotes the initial width and expands at the speed of light to provide the expected pulse front location in the other two plots. The bottom panels show the corresponding profiles measured along $y = z = 0$ line and the $1/x^2$ dependence

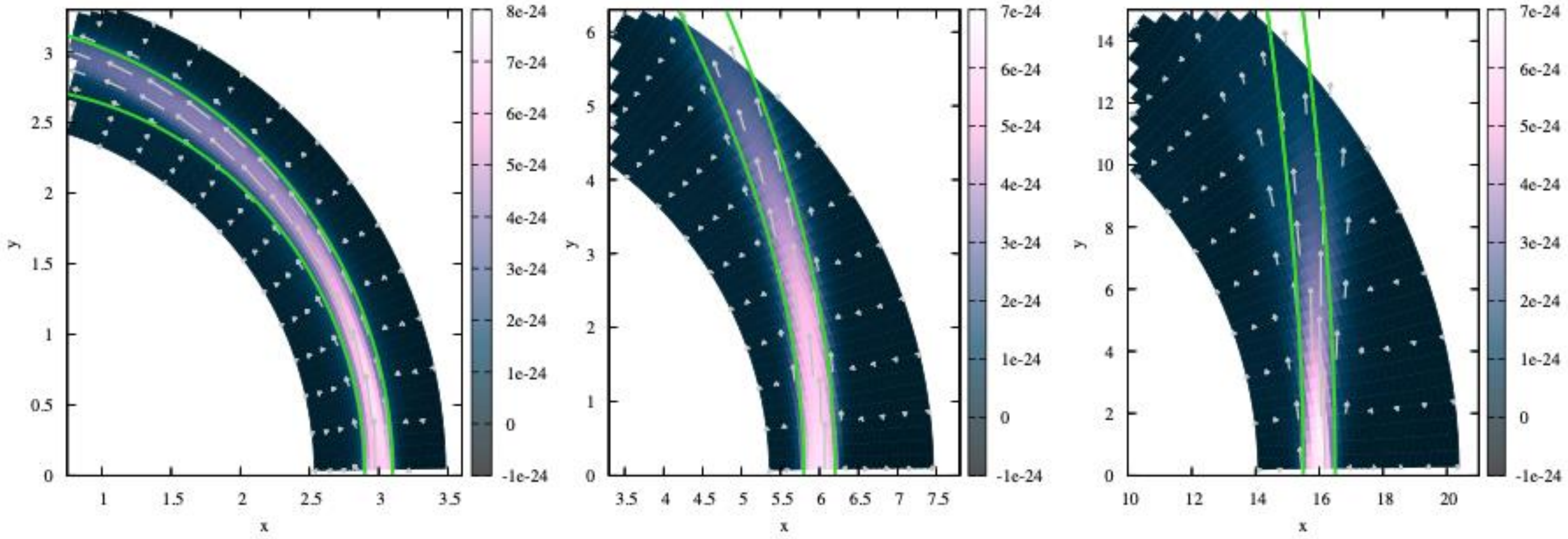

Figure 13. Results for Model 1 (left panel), Model 2 (middle), Model 3 (right), involving light beams propagating near a Schwarzschild BH (see Table 4 for model details). The BH is at $r = 0$ (i.e., $x = y = 0$). The beams are introduced via a boundary condition on the x-axis. The beams initially move vertically, i.e., in the azimuthal direction. Color indicates the radiation energy density and arrows show the radiative flux as measured by a ZAMO. The solid green lines indicate true geodescis of photons at the beam boundaries. They were calculated using the ray-tracing code GYOTO (Vincent et al. 2011).

Fluid-radiation interactions

$$
\begin{aligned}
(T^{\mu}_{\nu})_{;\mu} &= G_{\nu}, \\
(R^{\mu}_{\nu})_{;\mu} &= -G_{\nu},
\end{aligned}
$$

- Exchange of energy (scattering and absorption)
- Exchange of momentum (inverse Compton)
- Conservative - all included in radiation 4force
- For frequency-integrated radiation

$$
\widehat{G}^{\mu} = \begin{pmatrix} \kappa_a \rho \left(\widehat{E} - 4\pi \widehat{B} \right) \\ (\kappa_a + \kappa_{es})\, \rho \widehat{F}^i \end{pmatrix}
$$

$$
\widehat{B} = a T_g^4 / 4\pi,
$$

$$
\chi = \kappa_a + \kappa_{es}
$$

- Covariant form (Sądowski+ 2014):

$$
G^{\mu} = -\rho \left[\chi R^{\mu\nu} u_{\nu} + \left(\kappa_{es} R^{\alpha\beta} u_{\alpha} u_{\beta} + 4\pi \kappa_a B \right) u^{\mu} \right]
$$

- G^0 → LTE everywhere $$\widehat{G}^0 = \kappa_a \rho a \left(T_R^4 - T_g^4\right),$$
- G^i → zero rad. flux everywhere (symmetric absroption and emmision)

- Comptonisation – exchange of energy *and* momentum (Sadowski&Narayan 2015) – assumes BB radiation everywhere

$$\widehat{G}^\mu = \widehat{G}^\mu_{\mathrm{BB}} - \widehat{G}^\mu_{\mathrm{Compt}},$$

$$\widehat{G}^0_{\mathrm{Compt}} = \rho \widehat{E} \kappa_{es} \left[\frac{4k_B\left(T_g - T_R\right)}{m_e}\right] \left(1 + 3.683\frac{k_B T_g}{m_e} + \frac{4k_B T_g}{m_e}\right)\left(1 + \frac{4k_B T_g}{m_e}\right)^{-1}$$

Photon number conserving scheme for Comptonisation

- Sądowski&Narayan 2015
- Bose-Einstein distribution of photons in fluid frame
- Higher gas and radiation temperature

$$kT_{\rm r} = \frac{\widehat{E}/\widehat{n}}{[3 - 2.449724(\widehat{n}^4/C\widehat{E}^3)]}. \qquad C \equiv \frac{8\pi}{c^3 h^3}.$$

- Photon number evolved

$$(n u_r^\mu)_{;\mu} = \dot{\widehat{n}},$$

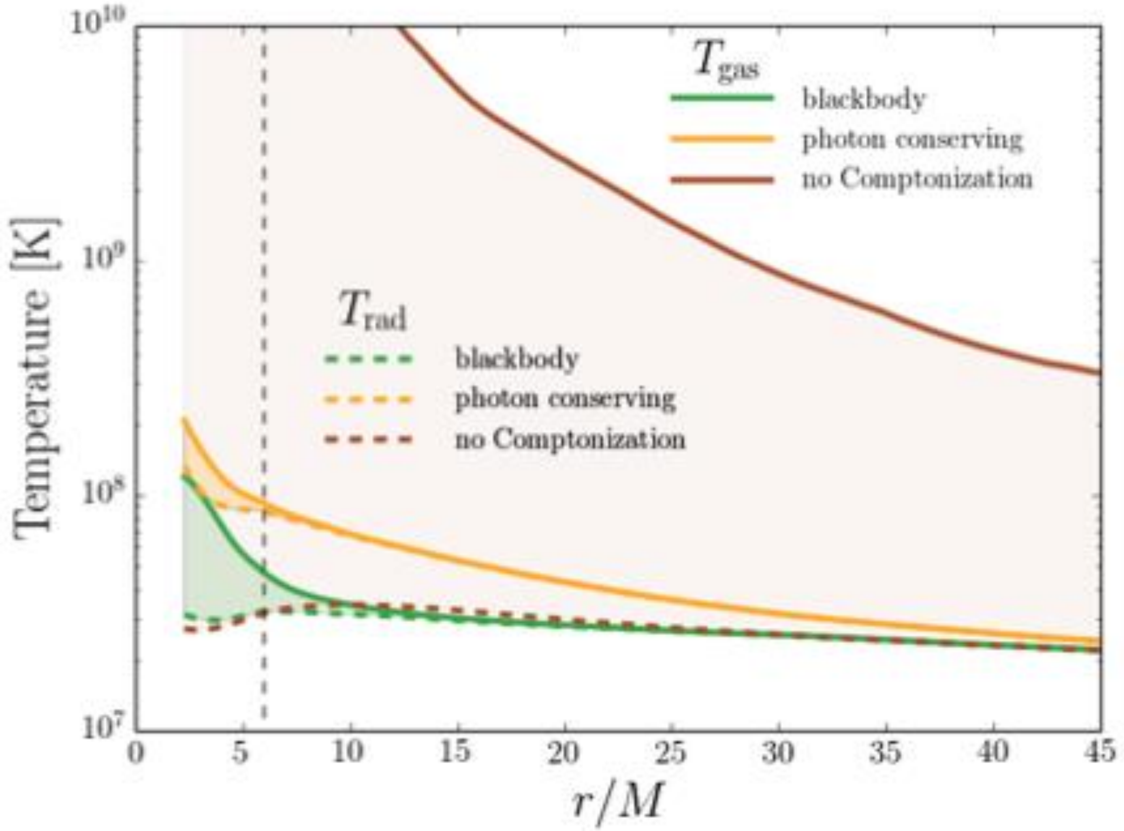

Compton cooling

Without comptonisation, the radiation temperature is a function of rad. energy density only

Semi-implicit scheme

- Explicit scheme works well until we get into very optically thick regions - G_ν becomes too big and the solver numerically unstable

$$T^t_{\nu,(n+1)} - T^t_{\nu,(n)} = \Delta t \, G_{\nu,(n)},$$
$$R^t_{\nu,(n+1)} - R^t_{\nu,(n)} = -\Delta t \, G_{\nu,(n)},$$

- `KORAL` implements semi-implicit scheme and approximative analytical method if this scheme fails
- Radiation shocks in optically thin regime – `KORAL` includes shock-capturing mechanism

Other closures

- FLD – Flux-limited diffusion (Levermore+ 1981)
- Non-LTE methods – implemented in PLUTO (Colombo+ 2019)
- OTVET – time-dependent radiation transfer equations (Jiang+2014) – ATHENA code

GRMCRMHD

- Fill the domain with sample photons and see how they interact with matter
- Can be used for modelling optically thin accretion flows (eg. `bhlight` by Ryan+2015)
- Photons can propagate in any direction – multiple light sources
- Can be used for frequency-dependent radiative transport
- In optically thick regions, the mean free path of the photons is too short – billions of particles would be needed